ISOLATION AND PURIFICATION OF GLUTATHIONE S-TRANSFERASES (GSTs) FROM *Orbicularia orbiculata*.

MARINI BINTI IBRAHIM

FACULTY OF SCIENCE
UNIVERSITY OF MALAYA
KUALA LUMPUR

2012

ISOLATION AND PURIFICATION OF GLUTATHIONE S-TRANSFERASES (GSTs) FROM *Orbicularia orbiculata*.

MARINI BINTI IBRAHIM

DISSERTATION SUBMITTED IN FULFILMENT OF THE REQUIREMENTS FOR THE DEGREE OF MASTER OF BIOTECHNOLOGY

INSTITUTE OF BIOLOGICAL SCIENCES
FACULTY OF SCIENCE
UNIVERSITY OF MALAYA
KUALA LUMPUR

2012

ABSTRACT

Glutathione S-transferases (GSTs) in bivalves which belong to the phase II detoxification metabolism, have an advantage to be used as biomarkers of aquatic pollution. The preliminary study was to isolate and purify the GSTs from Malaysian bivalve, *Orbicularia orbiculata* or locally known as Siput Lala. The GST enzyme was purified by using two different matrices of affinity chromatography which were GSTrap^{TM} HP and GSH-agarose (C_3). Total proteins attained from both eluates were 0.24±0.003mg and 0.12±0.07mg for GSTrap^{TM} HP column and GSH-agarose (C_3) column, respectively. Of the enzyme activity, 18% was retained on the GSTrap^{TM} HP column and gave purification factor of 60.2-fold. Meanwhile 16% was retained on the GSH-agarose (C_3) column and gave purification factor of 89.4-fold. SDS-PAGE analysis suggested the isolated GSTs from GSTrap^{TM} HP have two subunits molecular weight of 27 kDa and 26 kDa, while GSH-agarose (C_3) eluted GSTs resulted in a band (26kDa). 2D gel analysis indicated the both matrices bound different isoforms of GST. GSTrap^{TM} HP resolved into ten spots while GSH-agarose (C_3) resolved into six spots, suggesting the variation of bound GSTs using different matrices with different length of spacer. There were six similar spots from both columns at lower molecular weight (26 kDa), meanwhile four extra spots from GSTrap^{TM} HP appeared at higher molecular weight (27 kDa). Substrate specificities indicated that both bound GST isoforms active towards 1-chloro-2, 4-dinitrobenzene (CDNB), 3, 4-dichloronitrobenzene (DCNB) and ethacrynic acid (EA). This study had not shown the extra spots gained in GSTrap^{TM} HP active towards other GST substrates such as 4-nitrocinnamaldehyde (NCA), trans-4-phenyl-3-butene-2-one (PBO), p-nitrobenzyl chloride (NBC) and sulfobromophthalein (BSP).

ABSTRAK

Enzim Glutathione S-transferases (GSTs) daripada dwicangkerang adalah dalam kategori metabolism penyahtoksikan fasa II, didapati mempunyai kelebihan sebagai penanda aras biologi bagi pencemaran akuatik. Kajian awal adalah untuk memencilkan dan mengasingkan enzim GSTs dwicangkerang Malaysia, *Orbicularia orbiculata* atau nama tempatan Siput Lala. Enzim GSTs diasingkan dan ditulenkan menggunakan dua matrik kromatografi affiniti berbeza iaitu GSTrap^{TM} HP kolum dan GSH-agarose (C_3) kolum. Jumlah protein elute yang diperolehi daripada kolum GSTrap^{TM} HP adalah 0.24±0.003mg dan jumlah protein elute daripada kolum GSH-agarose (C_3) adalah 0.12±0.07mg. Dengan faktor penulenan 60.2 sebanyak 18% aktiviti enzim dikesan melekat pada kolum GSTrap^{TM} HP. Manakala dengan faktor penulenan 89.4 sebanyak 16% aktiviti enzim dikesan melekat pada kolum GSH-agarose (C_3). Analisis SDS-PAGE menunjukkan GSTs yang dipencilkan daripada kolum GSTrap^{TM} HP kelihatan pada saiz 26 kDa dan 27 kDa manakala GSTs yang dipencilkan daripada kolum GSH-agarose (C_3) kelihatan pada saiz 26 kDa sahaja. Analisis gel 2D menunjukkan kedua-dua kolum mengikat bentuk isomer GSTs yang berbeza. Terdapat sepuluh isoenzim yang dipencilkan dan ditulenkan menggunakan kolum GSTrap^{TM} HP , manakala hanya enam isoenzim kelihatan pada kolum GSH-agarose (C_3), mencadangkan bahawa kepelbagaian isomer GSTs terperangkap dengan penggunaan matrik berbeza pada panjang ikatan. Terdapat enam isomer sama kelihatan pada saiz lebih kecil, 26 kDa dipurifikasi daripada kedua-dua kolum. Manakala, empat isomer lain kelihatan pada saiz lebih besar 27 kDa. Kespesifikan substrat menunjukkan isoenzim-isoenzim GSTs terikat pada kedua-dua kolum mempunyai aktiviti terhadap 1-kloro-2,4-dinitrobenzene (CDNB), 3,4-dikloronitrobenzene (DCNB) dan asid ethacrynic (EA). Walaubagaimanapun, kehadiran isomer lain daripada GSTrap^{TM} HP kolum tidak

menunjukkan sebarang aktiviti terhadap substrat lain seperti 4-nitrocinnamaldehyde (NCA), trans-4-phenyl-3-butene-2-one (PBO), p-nitrobenzyl chloride (NBC) dan sulfobromophthalein (BSP).

ACKNOWLEDGEMENT

In the name of ALLAH, Most Gracious, Most Merciful. Alhamdulillah, with the will of Almighty Allah s.w.t, finally this thesis is completed.

First and foremost, I would like to express my deepest gratitude and appreciation to my supervisor, Dr. Zazali Alias, who has supported me throughout my thesis with his patience, knowledge and motivations. I attribute the completion of this thesis due to his encouragement and effort to guide me all the time.

Special and grateful thanks to my beloved husband and daughter for their love, support and motivation that gives me strength and passion to work hard to fulfill my goal. This piece of work is a token of dedication to my beloved who have always be a good friend, a good critic and a good supporter and also encouraged me a lot throughout my study. Thank you for their endless love and always be by my side**.** I also would like to thank both of my parents and all my family members who have been so cooperative and understanding throughout this thesis completion.

Last but not least, my heartfelt thanks to all lab members, my project mates and friends for their cooperation, technical assistance and their helping hand. Thank you very much. May Allah bless all of you.

TABLE OF CONTENT

LIST OF FIGURES

LIST OF TABLES

LIST OF ABBREVIATIONS

GSTs	Glutathione S-transferases
GSH	reduced glutathione
EDTA	Ethylenediamine tetra-acetic acid, tetrasodium salt
SDS	Sodium dodecyl sulphate
CBB	Coomassie Brilliant Blue G-250
DCNB	3, 4-Dichloronitrobenzene
NCA	4-Nitrocinnamaldehyde
CDNB	1-chloro-2, 4-dinitrobenzene
EA	Ethacrynic Acid
PBO	*Trans*-4-phenyl-3-butene-2-one
NBC	*p*-Nitrobenzyl chloride
BSP	Sulfobromophthalein
TEMED	N,N,N',N'-tetramethylenediamine
CHAPS	(3-[(3-cholamidopropyl)dimethylammonio]-1-propanesulfonate)
BSA	Albumin, bovine serum
TCA	Trichloroacetic acid
DTT	Dithiothreitol
IAA	Iodoacetamide
pI	Isoelectric point
MW	Molecular Weight
SDS-PAGE	Sodium Dodecyl Sulfate – Polyacrylamide Gel Electrophoresis
IEF	Isoelectric Focusing
mM	milimolar
2-DE	Two-Dimensional Electrophoresis
dH_2O	Distilled water
h	hour
MALDI-TOF	Matrix-Assisted Laser Desorption Ionisation-Time of Flight
Mins	minutes

IPG	Immobilised pH gradient
ATP	Adenosine triphosphate

CHAPTER 1

INTRODUCTION

In recent years, marine pollution becomes a major threat to human and environmental health due to the increasing level of contaminants in the marine environment. This phenomenon will lead to the depletion of natural resources as a result of the diminishing of water and sediment quality. Thus, an effective method for identification, estimation, comparative assessment, management of risks including deleterious effects of contaminants need to be developed without solely dependent on chemical analysis of environmental samples. Therefore, the use of biological markers at the molecular or cellular level have been proposed as sensitive 'early warning' tools for biological effect measurement in environmental quality assessment (Cajaraville et al., 2000). There are some advantages of biomarkers such as biomarker responses may indicate the presence of a biologically existence contaminant, rather than a biologically inert form of contamination. As suitable biomarker implemented, it may reveal the presence of contaminants that were not suspected initially (Handy et al., 2003).

Bivalves have been widely used in the biomonitoring of chemical pollution in the aquatic environment. Their capability to filter large amounts of water for nutrition and respiratory needs, enable bivalves to bioaccumulate pollutants in their tissues. In order to identify the level of pollutants, a complementary approach based on responses of biological parameters need to be developed with appropriate organisms. Bivalves are commonly preferred as biomarkers due to several attributes such as wide geographical distribution, sedentary, abundant, tolerance to environmental changes or contaminants, reasonably long-lived, reasonable size and study enough to survive in laboratory and field studies (Zhou et al., 2008). The means of organic pollutants detoxification engage

a group of enzymes mainly enclosed in functional reaction (phase I) and in conjugative reaction (phase II) of biotransformation (Porte et al., 2001). In the phase II, GST isoforms are involved in the metabolism of organochlorine compounds (Alias and Clark, 2007). GST facilitates the glutathione conjugation to foreign compounds and aids in the excretion of ROS from the organism. The enzymes are able to catalyse the conjugation of organic electrophiles with the thiol group of gluthathione produce a hydrophobic, easily excreted product (Winterbourn, 2008). The increase of enzyme activity signify that the organism is fighting against the toxic environment while lower enzyme activity could be an indication of less toxic present in the surrounding area or it could also possibly due to the elevated environmental stress that overwhelming the cells' defense system (Cossu et al., 2000). Thus, GSTs are expected to respond to changes in levels of contaminants in the marine environment studied (Manduzio et al., 2004). The expression of GSTs is induced under a defined condition as same as another protein. The respond of GSTs are associated with the presented number of substrates thus substrate accretion will increase GSTs expression to the optimum level.

More importantly, bivalve GSTs has high potential to be used as biomarker because their expression are not affected by abiotic and biotic factors such as temperature, season, sex, or age (Vidal et al., 2002). The survival of bivalves in continous toxic exposure showed that bivalves have a very effective detoxification system, where GSTs are most likely take part in this process. Therefore, GSTs activity in bivalve could be a good starting point for marine quality assessment bioindicator.

Due to the detoxification role played by GST superfamily in the most of cells, the implementation of local bivalves GSTs as tool of biomonitoring is expected to be very attractive. However more comprehensive research needs to be carried out to get

better understanding about the correlation between pollutants and GSTs expression. There are many species of bivalves in Malaysian waters can be used as biomarker; one of them is *Orbicularia orbiculata*, or locally known as Siput Lala (Figure 1.1). The main objectives of the study are:-

1. To isolate and purify GSTs from bivalve, *Orbicularia orbiculata.*
2. To determine the substrate specificity of purified GSTs from *Orbicularia orbiculata.*

Figure 1.1 *Orbicularia orbiculata* (short-necked clam)

CHAPTER 2

LITERATURE REVIEW

2.1 Glutathione S-Transferases (GSTs)

Glutathione S-transferases (GSTs) are a prime family of detoxification enzymes discovered in most organisms. They are multifunctional intracellular enzymes which catalyse the conjugation of reduced glutathione (GSH) with a broad range of compounds bearing electrophilic centre, indicate a vital role of GSTs in phase II detoxification and excretion of endogenous compounds, xenobiotics and products of oxidative stress (Sheehan et al.,2001). GSTs can also bind hydrophobic compounds that are not their substrates. This non-substrate binding is possibly associated with the sequestration, storage and transportation of drugs, hormones and other metabolites, such as bilirubin, fatty acid and heme (Lo Bello et al., 2001).

GSH or tripeptide, L-γ-glutamyl-L-cysteinyl-glycine is the major low molecular weight thiol compound involving in cellular redox reactions and thioether formation (Sies, 1999). GSH is discovered in the intracellular space of plants, animals and microorganism served two main roles, which remove toxic metabolites from cell and maintain cellular sulfhydryl group in reduced form (Pal, 2010). There are a series of various steps in the cell detoxification mechanism of xenobiotic and endobiotic compounds. Firstly, conversion of toxic compounds into strong electrophiles with present of cytochrome P-450's oxidation activity. The electrophiles are seb sequently transformed into more soluble and less toxic substrates which are recognized by ATP-dependent transmembrane pumps then expelled from the cell (Frova, 2006).

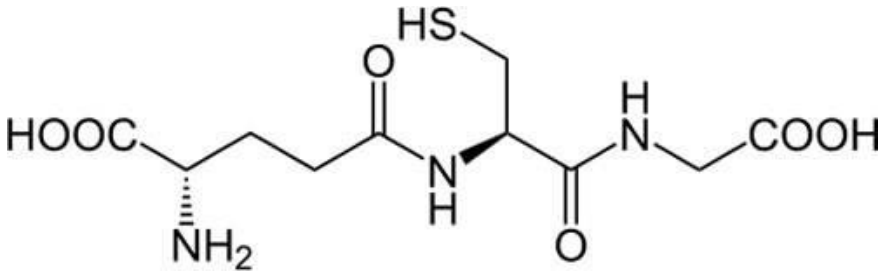

Figure 2.1: Gluthathione structure (adapted from Pal, 2010)

The diverse family of GSTs found ubiquitously distributed in aerobic organisms such as mammals (Johansson and Mannervik, 2001), plants (Dixon et al., 2002), microorganisms (Sheehan et al., 2001) and insects (Enayati et al., 2005). Furthermore, GSTs from these organisms are well studied and characterized compare to GSTs from marine organism especially bivalve mollusks. Its importance to establish the patterns of the cytosolic glutathione S-transferases such as the dimeric structures, specific activities, pI value, molecular weight and substrate specificity in the bivalve due to some of GST isoenzymes show selective response towards pollutants and high activity towards certain substrates (Manduzio et al., 2004). Thus, this may be useful for better understanding of the enzyme as an effective tool in environmental monitoring.

2.2 Structure of Glutathione S-Transferase

The family of GSTs is classified based on their location within the cell, microsomal and cytosolic. The microsomal GSTs are trimeric and membrane bound proteins meanwhile the cytosolic GSTs are hetero or homo-dimeric proteins (Enayati et al., 2005). The catalysis reactions of microsomal GSTs are similar to the cytosolic GSTs even though they are different in structure and origin (Gakuta and Toshiro, 2000). The identification and characterization of GSTs classes mainly cytosolic, according to their amino acid sequence, immunological, kinetic and structural properties (Alias and Clark, 2007). Cytosolic GSTs are approximately 25 kDa in subunit size; assemble to hetero- or homo-

dimeric proteins. The feature of the GST superfamily is the occurrence of multiple enzymes forms based on sequence similarities and subcellular distribution of the mammalian enzymes, which divided to their classes as Alpha, Mu, Pi and Theta (Dirr et al.,1994; Sheehan et al.,2001) and recently Zeta, Sigma, Kappa and Omega (Agianian et al., 2003).

Sheehan et al. (2001) representatived and mentioned the crystal structure of all the cytosolic GSTs classes. Monomer of subunits consist two domains linked by a variable linker region. The N-terminal domain (residues 1–80) consists of four beta sheets and three flanking alpha helices, adopts a conformation similar to the thioredoxin domain (Enayati et al., 2005). This domain highly conserved and provides majority of residues involved in the binding of glutathione. The C-terminal domain is larger, which contains a variable number of alpha helices, thus provide the variable hydrophobic H-site for electrophilic substrates interactions. The C-terminal domain is quite difference between three classes of mammalian Alpha/Mu/Pi and this contribute to the differences of substrate specificity (Sheehan et al., 2001). Structural elements from both subunits are needed for fully functioning dimeric GSTs although their active site catalytically independent. G-site has a great specificity for GSH and only completed on dimerization, is observed in a cleft between the N and C-terminal domains.

Availability of high intracellular concentration GSH leads to high affinity of GSTs towards GSH. The interaction between GSH and active side residue in the N-terminal domain activates the sulphydryl group. Most of the mammalian classes Alpha/Mu/Pi active site residue is a tyrosine, but different in Theta class GSTs which have a catalytically essential serine, while active site residue for Omega and Beta is cysteine (Sheehan et al., 2001). Generally GSTs that sharing greater than 60% identity

of sequence similarity are in the same class while those with less than 30% identity are clustered to separate classes (Sheehan et al.,2001). Besides, each class of GST genes differ in size, in intron or exon structure and their chromosomal localizations supporting the hypothesis which the classes represent separate families of GSTs (Sheehan et al., 2001).

Three dimensional structures of alpha GSTs classes showed a subunit molecular weight approximately 26 kDa (Dirr et al., 1994). The subunit interface is a ball-and-socket type joint with Phe52 serving as the ball and the hydrophobic socket residing between helices of domain II (Amstrong, 1997). The C-terminal of the alpha class GSTs is longer by some 4 to 8 amino acid residues (Salinas and Wong, 1999) compared to the pi and mu GSTs lead to positive effect on catalytic activity by not blocking access to the G-site and forming a portion of the H-site.

Dirr et al. (1994) had presented the mu GSTs are 26 kDa in subunit molecular mass and ball-and-socket type interface for subunit interaction of dimer. A highly distinguishable feature of the mu class GSTs is the so-called mu loop, which is the result of an insertion in domain I. A subunit molecular mass of pi class GSTs are slightly smaller 23 kDa (Dirr et al., 1994) and have the ball-and-socket style interface, which seems to be closest in structural relation to the mu class. Both of mu and pi classes GSTs share similarities in C-terminal structural and share an H-site form that is larger and more open to solvent entry than the alpha class GSTs (Dourado, 2008).

Meanwhile the theta class GSTs is very different from alpha, mu or pi class GSTs. The main subunit interface for theta class lacks a ball-and-socket style and with average at 27 kDa in subunit molecular mass. Generally the G-site of the theta class

GSTs much deeper than that of alpha, mu and pi class GSTs (Wilce et al., 1995). Sigma class GSTs are lacking in both components of the ball-and-socket interface present in the alpha, mu and pi class GSTs (Armstrong, 1997). The subunit molecular mass of the sigma class GSTs show with the average at 23 kDa. The hydrogen bonding interaction between the glutathione and the class sigma GST is quite similar to the alpha and pi class GSTs but differ from the mu class (Sheehan et al., 2001).

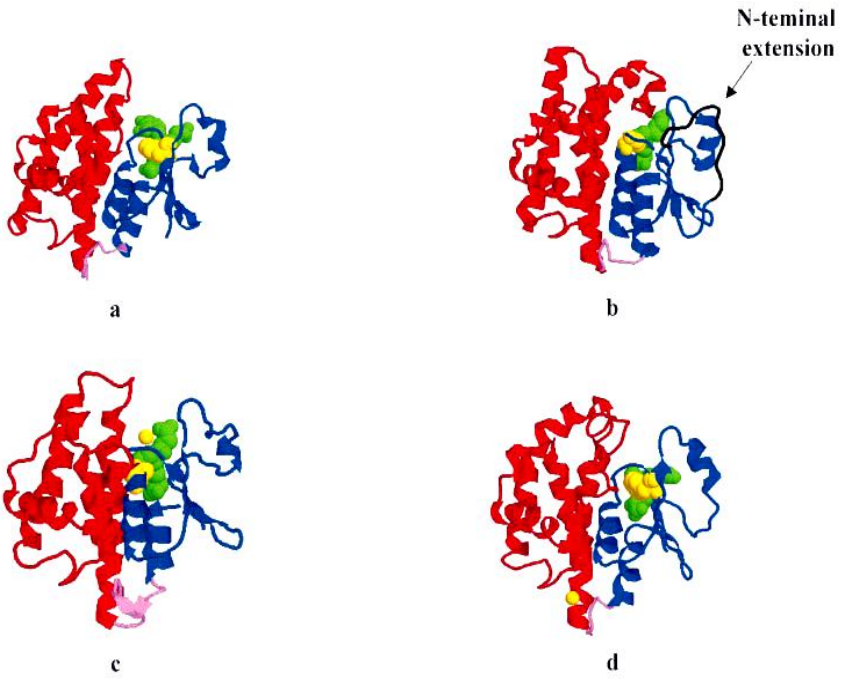

Figure 2.2: Domain structure of GST subunits (adapted from Sheehan et al., 2001).

Three-dimensional structures of individuals GST subunits are shown. The N-terminal domain is coloured blue, while the C-terminal domain is red. Catalytically essential residues (tyrosine in a and d; cysteine in b and c) are coloured yellow and presented in space-filling mode, while ligands with which the protein was co-crystallized are shown in green. Linker strands connecting the two domains are shown in violet. Protein database codes and references are given in parentheses: (*a*) squid Sigma class (1GSQ); (*b*) human Omega class (1EEM) [the C-terminal extension (residues 1±19) unique to this class is shown in black]; (*c*) bacterial (*Proteus mirabilis*) Beta class (1PM7); (*d*) *Fasciola hepatica* Mu class (1FHE).

2.3 Function of GSTs

The crucial function of GSTs is the detoxification of both endogenous and exogenous compounds directly or indirectly by reacting with the oxidised metabolites produced by the cytochrome P450 family. The ability of all GSTs to conjugate GSH with compounds consists of electrophilic centre lead to the reactions on electrophilic carbon sites (Jakoby, 1978) which contributed from saturated carbon atoms or unsaturated carbon atoms including aromatic carbon. Other sites of GSTs reactivity are nitrogen, electrophilic oxygen and electrophilic sulphur in disulphide exchanges (Pal, 2010).

Besides, GSTs catalyze reactions that activate certain chemical substances including toxic and carcinogenic substance. In addition to their catalytic function, GSTs also been demonstrated to have binding capacity towards specific substances. GSTs bind to a broad range of lipophilic substances at the non catalytic binding site thus facilitate the transport of those lipophilic substances. The quantity of GSTs and their broad specificity for binding large amounts of ligands suggested the existence of similarities with serum albumin functions in blood plasma, and is the reason for the term "ligandin". Large amounts of chemical substances including xenobiotics and products of oxidative stress may serve as a GST substrate.

2.4 GST Classification

The most frequently used standard substrate for almost all GSTs is l-chloro-2,4-dinitrobenze (CDNB). Conjugation CDNB-GSH gives S-(2,4-dinitrophenyl) glutathione, which possesses an absorbance spectrum adequately dissimilar from that of CDNB to permit a simple spectrophotometric assay at 340 nm (Clark et al., 1973). An

increased activity towards CDNB represents a total activity of various GST isoforms, and for that reason it is not possible to differentiate between effects of substances on individual GST isoforms. And so while the total specific GST activity may show little or no variation following pollution exposure, greater variations may be found in individual samples of each of the isoenzymes provided a good environmental biomarker is used.

Determination of GSTs classes is upon on efficiency of cytosolic GSTs towards substrates and their sensitivity to some inhibitors. Amongst the reactions catalysed by GSTs are substitution of halogens in halogenohydrocarbon, addition to double bonds, cleavage of epoxides and organic peroxides reduction. GSTs have broad and overlapping substrate specificity, thus lead to complicated GST classification. However, this knowledge remains valuable as a mode of understanding their properties. The compounds such as bromosulphothalein (BSP, Mu class), 1,2-dichloro-4-nitrobenzene (DCNB, Mu class), *trans*-4-phenyl-3-buten-2-one (PBO, Mu class), ethacrynic acid (EA, Pi class), 1,2-epoxy-3-(*p*-nitrophenoxy)propane (EPNP, Theta class) and cumene hydroperoxides (CuH_2O_2, Alpha class) are still used as class markers (Hayes et al., 2005; Kim et al., 2006; Mannervik, 1985). Some of the substrates used for the study of GSTs are shown in Figure 2.3.

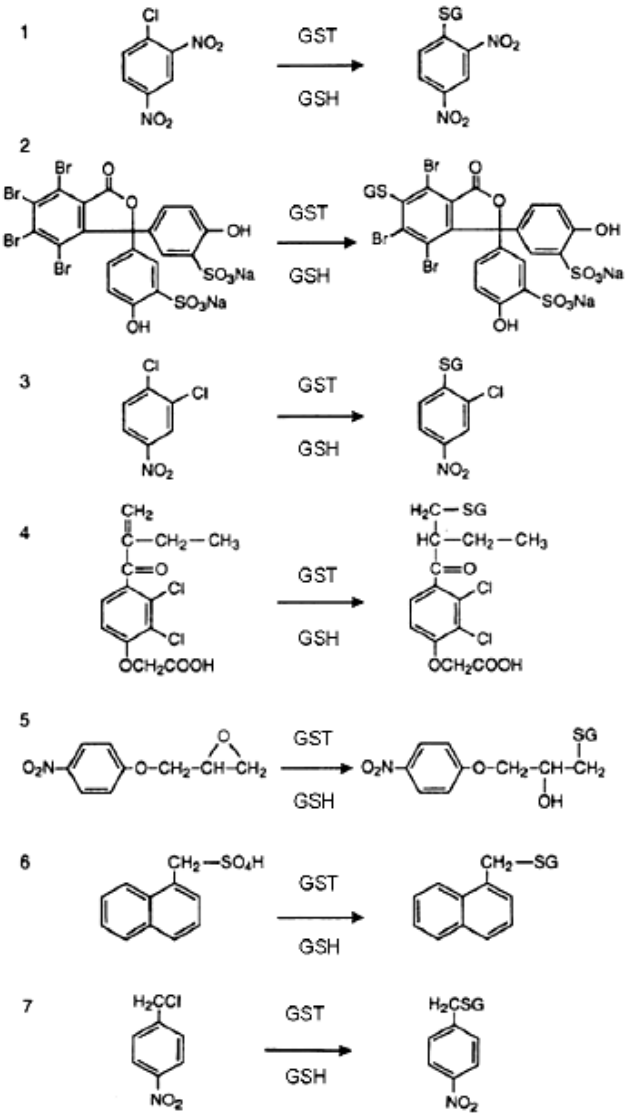

Figure 2.3: Model substrate used in the study of GST (Adapted from Alias, 2006)

(1)1-chloro-2,4-dinitrobenzene; (2)Bromosulfophthalein; (3) 1,2-dichloro-4-nitrobenzene; (4) Ethacrynic acid; (5) 1,2-epoxy-3-(p-nitrophenoxy)propane; (6) 1-menaphthyl sulphate; (7) 4-nitrobenzyl chloride

2.5 Bivalve species, *Orbicularia orbiculata*

Orbicularia orbiculata is one of bivalves' species under the class Bivalvia in the phylum Mollusks. *Orbicularia orbiculata*, the short-necked clam is locally known as Siput Lala and discovered by Wood, 1828. Instead of they are classified by shell which is separated from front to back into left and right valves and often have well-developed byssus apparatus permitting them to attach to rocky substrates (Bayne, 1976). The bivalve mollusks have properties such as high distribution worldwide, sedentary and filter-feeding habits lead to accumulation of bacteria and chemical pollutants, both are known as source of nourishment and immune challenge (Bernal-Hernandez et al., 2010). Besides, they are capable of withstanding baseline levels of pollution and are abundant in estuaries where much human contact with the aquatic environment occurs (Sheehan et al., 1995).

Bivalves are appropriate organisms to use when measuring antioxidant enzymes as biomarkers of diminished health because the existence a wide range of antioxidant defenses (Verlecar et al., 2007). One of the antioxidant enzymes is Glutathione S-Transferases (GSTs). Since these enzymes are inducible by a wide range of chemicals, it has been suggested that the levels of GST in mussels might be a useful index indicative of conjugating activities and exposure to chemical pollution (Fitzpatrick and Sheehan, 1993).

However, information about marine invertebrate GSTs is poorly understood especially bivalve mollusks (Blanchette et al., 2007). Most of the previous studies are focused on purification and biochemical measurement of total GSTs or different isoforms by using in vivo organisms.

There are a few of the aquatic invertebrates in which GST has been studied including blue mussels (*Mytilus edulis*) (Fitzpatrick et al., 1995; Yang et al., 2004), marine gastropod (*Cyphoma gibbosum*) (Whalen et al., 2008), mangrove oyster (*Crassostrea rhizophorae*) (Zanette et al., 2006), brown mussels (*Perna perna*) (Saenz et al., 2010), clam (*Venerupis philippinarum*) (Xu et al., 2010) and bivalve mollusks (*Mytilus galloprovincialis)* (Fitzpatrick et al., 1995).

2.6 Affinity Chromatography Matrices for GST Purification

Purification of GSTs' bivalves had been done by separation of chromatography techniques. One of techniques is by using affinity chromatography. Affinity chromatography rely on proteins biological functions which depend on the specificity and high adsorptive features towards substances. The purified protein is specifically and reversibly bound onto the stationary phase, which contains a ligand bound to a matrix or supporting phase with the help of spacer arms. The bound target protein is recovered by eluting the protein-ligand binding in column with salt and chemical or by changing the pH of the solution.

There are many types of matrix employed to purify GSTs by using affinity chromatography separation. The different matrices used in the GST purification were GSH-Sepharose 4B affinity column followed by reverse-phase HPLC (Yang et al., 2002; 2003), glutathione-Sepharose affinity column, anion-exchange chromatography and reverse-phase HPLC (Vidal et al., 2002), GSH-Sepharose column followed by FPLC analysis on a Mono-Q anion exchange column (Fitzpatrick et al.,1995), GSH-agarose column and S-hexyl GSH-agarose column followed by anion exchange chromatography (Hoarau et al., 2002). The form of affinity matrix employed widely is

the immobilized GSH-agarose matrix. The bound enzymes are best eluted from this support with GSH solution. Another form of affinity column is the immobilized S-hexylglutathione.

The chemical structure of the different matrices for agarose-affinity chromatography was showed in Figure 2.4. A number of affinity matrices have been constructed to fulfill the need of rapid, simple and efficient GST purification methods. Selective or isotype specific of isolated GSTs might be achieved by using different affinity matrices in mounted series in order to analyse properties of GSTs from different species. The ligands that have been used for purification of GSTs are BSP-GSH (Clark et al., 1977), GSH (Simons and Vanderjagt, 1977), S-hexyl-GSH (Guthenberg and Mannervik, 1979). Different classes of mammals GSTs tend to produce different conjugates due to matrices preferable. A matrix with long linker arm (C12) of GSTrap column gives easier access of the GSTs to the ligand and yield higher GST activity in the affinity eluents due to its higher substitution (Alias and Clark, 2007).

Investigation of multiple forms of GSTs with different isoelectric points could be performed by using isoelectric focusing (IEF) gel according to the method described by Robertson et al. (1987). The presences of multiple isoenzymes of GSTs have also reported in most of bivalve's species. Blanchette and Singh (1999) purified and characterized GST from quahog (*Mercinaria mercinaria*), resulted multiple forms of GSTs with subunit molecular masses of 22, 24 25 and 27 kDa, while the isoelectric point (pI) values for three isozymes of 5.1, 4.9 and 4.6.

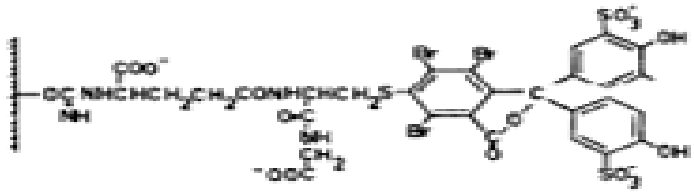

Sulfobromophthalein-gluthathione linked to agarose (Clark et al., 1977)

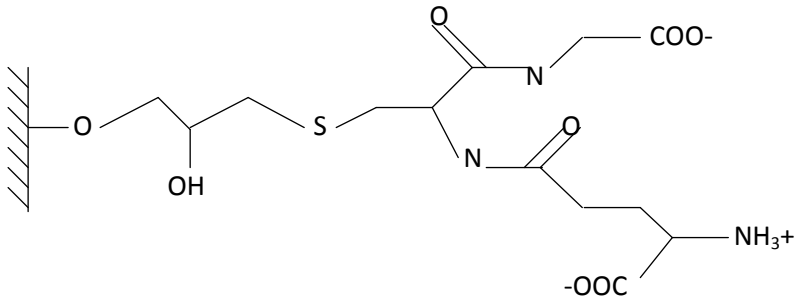

Gluthathione with C_3 spacer linked to agarose (Clark et al., 1990)

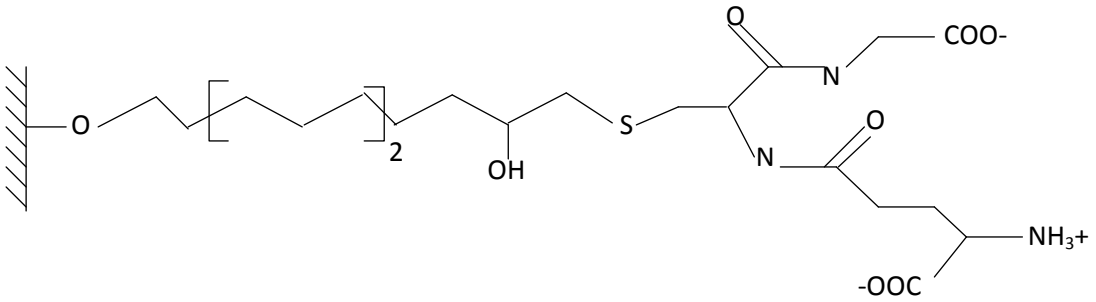

Gluthathione with C_{12} spacer linked to agarose (Simons and van der Jagt, 1977)

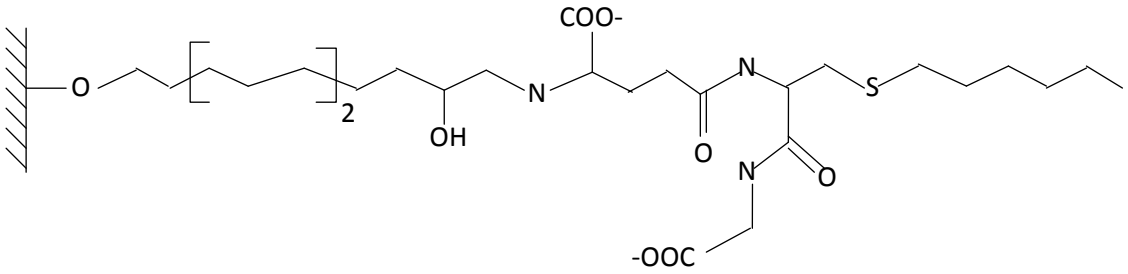

S-Hexylgluthathione with C_{12} spacer linked to agarose (Mannervik and Guttenberg, 1981)

Figure 2.4: Structures of different types of affinity matrix used for GST purification.

2.7 Bivalve GSTs

GSTs in aquatic organisms are capable to detoxify the environmental pollutants, such as heavy metals, polychlorinated biphenyls (PCBs), dichlorodiphenyltrichloroethane (DDT) and polycyclic aromatic hydrocarbons (PAHs) (Fitzpatrick et al., 1997; Pérez et al., 2004; Hoarau et al., 2006). Although they have potential as a biomarker to monitor the pollution in the aquatic environment, but often results obtained with GST activity in environmental studies are conflicting. The differential observation obtained in GST activity which exposed to pollutants due to induction or repression of GST subunit classes in a differential manner depending on the contaminant. Besides, the measurement of a total GST activity may not be representative of the actual molecular events. Thus, the study of the isoenzyme or subunit pattern following exposure of the bioindicator species to pollutants has been performed in mussels (Fitzpatrick et al., 1997). In bivalves, some differences in GST responses were observed depending on the species. More knowledge about the possible novel GST isoenzymes in some habitual bivalve seashells is needed and meaningful. The previous studies have used different approach of total GST purification via chromatography techniques associated with treatment and optimized methods for getting maximum purified GSTs.

The purified GSTs from the digestive gland of *Cyphoma gibbosum* were identified as putative mu-class GSTs while one minor subunit was identified as a putative theta-class GSTs (Whalen et al., 2008). Fitzpatrick et al. (1995) purified major isoenzyme GSTs (GST1) from cytosolic extracts of *Mytilus edulis* gill tissue at molecular mass of 24.5kDa, was identified as Pi class GSTs due to immublotting, amino acid sequencing and particularly active with 1-chloro-2, 4-dinitrobenzene and ethacrynic acid as substrate.

Table 2.1: Summary of the affinity purification schemes for bivalve GSTs.

Affinity matrix	Condition of elution	Apparent molecular mass of eluted GSTs (kDa); pI value	Source	Reference
GSH-Sepharose 4B	10mM GSH, 10mM Tris–HCl, 1mM EDTA, 3mM DTT and pH 8.0	24 kDa; 5.5	hepatopancreas (*Atactodea striata)*	Yang et al., 2003
GSH-Sepharose 4B	10mM GSH, 10mM Tris–HCl, 1mM EDTA, 3mM DTT and pH 8.0	23 kDa; 4.6	liver intestine (*Asaphis dichotoma)*	Yang et al., 2002
GSH-Sepharose	10 mM GSH, 50mM Tris–HCl, pH 8.6	30.2, 29.2, 28.5 and 27.2 kDa; 5.1, 4.7, 4.8 and 4.45	clam (*Corbicula fluminea)*	Vidal et al., 2002
GSH–agarose and S-hexyl GSH–agarose	0.2mM GSH,200 mM Tris/HCl, pH 9 5 mM GSH, 200 mM Tris/HCl, pH 9.	22 to 26 kDa	clam *(Ruditapes decussates)*	Hoarau et al., 2002
GSH-agarose	10 mM GSH, pH 7.2	24 and 25 kDa	gill *(Mytilus edulis)*	Fitzpatric et al., 1995
GSTrap FF	10 mM GSH, 50mM Tris–HCl, pH 8	22 kDa	scallop *(Chlamys islandica)*	Myrnes and Nilsen, 2007
GSH-agarose	10 mM GSH, 50 mM Tris–HCl, pH 8	22, 24, 25, and 27 kDa; 5.1, 4.9 and 4.6	Quahog *(Mercenaria mercenaria)*	Blanchette and Singh, 2002

In the *U. tumidus* and *C. fluminea*, freshwater bivalves, GSTs that belong to the pi class which revealed the GSTs are expressed at the same level in the digestive gland, gills and the excretory system (Doyen et al., 2005). The deduced amino acid sequences GST of clam (*Venerupis philippinarum*) indicated the enzymes belong to pi class GSTs, molecular mass of 23.9 kDa at the pI value of 7.9 (Xu et al., 2010). The rho class GSTs of *Laternula elliptica* have 41% and 40% identity from *Ctenopharyngodon idella* and *Pleuronectes platessa*, respectively, while the sigma class share only 22% identity with sigma class from *Xenopus laevis* (Park et al., 2009). However Kim et al. (2009) identified the pi class GSTs from the Antartic bivalve, *Laternulla elliptica* with an estimated molecular mass of 23.9 kDa and predicted isoelectric point 8.3.

GST gene from *Mytilus edulis* encodes a protein with molecular mass of 23.68 kDa and deduced amino acid sequence showed similarity with the pi class GST. This GST have high activity towards the substrates ethacrynic acid (EA) and 1-chloro-2, 4-dinitrobenzene (CDNB) (Yang et al., 2004). A novel GST isoenzyme was purified from *Atactodea striata* with molecular weight 24 kDa, pI value of 5.5, exhibited high activity towards CDNB and NBD-Cl (Yang et al., 2003). Meanwhile two subunits of GSTs were purified from liver intestine *Asaphis dichotoma*, revealed at 23 kDa and have pI value of 4.6 (Yang et al., 2002).

Classification of GSTs from aquatic organisms especially bivalve mollusks have not been well studied and investigated to date. The limited structure and properties information of marine GSTs poses problem to categorize the marine GSTs. It is crucial to develop a suitable classification system for marine GSTs which corresponding to recent studies and focusing on GSTs as biomarker traits of the enzyme.

2.8 Proteomics

Proteomics is an emerging field of protein biochemistry that performs large-scale studies of diverse protein mixtures. Proteomics is the study of the proteome, the protein complement expressed in a given biological system under a defined set of condition. Most proteomics research is directed towards investigating protein expression, quantitation, localizations, functions and interactions of proteomes under specified physiological conditions. Proteomics uses a combination of techniques to resolve (two-dimensional polyacrylamide gel electrophoresis, 2D page), quantitate (scanning) and identify (mass spectrometry) proteins produced by an organism under defined circumstances (Lee, 2001; Patterson, 2000).

Protein identification in gel-based proteomics requires five steps: sample preparation, separation, digestion, mass spectrometry and informatics. The sample preparation involves the extraction of the proteins from cells, and then followed by separation by 2D gel electrophoresis. The separated proteins on the gel are commonly visualized by coomassie blue staining. The next step usually involve proteins digestion since it is easier to identify peptides rather than proteins and peptide also contain more mass information compared to the the intact proteins. Mass spectrometry is used to detect peptides and peptides fragments. Finally, the sequence of the protein is determined by interpreting all the data obtained by matching the generated peptide masses with known proteins in a variety of databases or through sequence comparison if tandem mass spectrometric methods are applied.

The 2DE technology was originally described by O'Farrell (1975) and reviewed by Gorg et al. (2004). In the first dimension the proteins are separated according to their

charge by isoelectric focusing and in the second dimension proteins are separated by molecular weight using SDS-PAGE. Such analysis generally begins with solubilising a protein sample in zwitterionic detergents such as CHAPS and Triton X100. Ampholytes are added to further enhance the effect of the detergents and dithiothreital (DTT) is added as a reducing agent for any disulphide bonds. Thiourea is added to enhance the solubility of hydrophobic proteins. The function of each denaturant, surfactant and reductant and the rationale of solubilisation have been reviewed by Shaw and Reiderer (2003).

In the first dimension technique, an IPG strip gel needs rehydration prior to use. The sample is applied by cup loading on to hydrated strip or during the gel rehydration process. After focusing the strips are equilibrated in the presence of detergent (eg SDS), reducing agents (eg DTT) and denaturing agent (eg urea). During the equilibration, the proteins are first reduced and alkylated by including dithiothreiol (DTT) and iodoacetamide (IAA) respectively. The purpose is to break both inter and intra chain disulfide bonds of protein molecules and to ensure that cysteine residues are fully alkylated. Reduction and alkylation are normally carried out in a buffer pH 6.8. The efficiency of cysteine alkylation of IPG strips can be increased by equilibrating in a buffer with higher pH, higher concentration of reducing and alkylating reagents and prolong incubation time (Yan et al., 1999). Both reduction and alkylation are less efficient at low pH as the optimal pH for these reactions is usually at pH 8.5–8.9. Complete alkylation is important in order to improve the efficiency of protein digestion, carried out later in the analysis. Accidental alkylation of proteins by cross linker (Hamdan et al., 2001) and immobiline monomers (Bordini et al., 2000) is well documented. In order to minimize the unnecessary alkylation of the protein interest, the

reduction and alkylation of the protein should be done prior to isoelectric focusing step (Herbert et al., 2001; Galvani et al., 2001a and Galvani et al, 2001b).

In the second dimension step, the isoelectrofocused protein on the IPG strip was separated based on molecular mass. The typical Laemmli sodium dodecyl sulfate (SDS) buffer system (Laemmli, 1970) is used with percentage of acrylamide of 10 or 12% for MW ranges of 20 to 200kDa. The pre-equilibrated IPG strip with its plastic backing on the glass plate is pushed down on to the gel surface. Bubbles in between the IPG strip and solving gel interface are eliminated to ensure complete protein transfer. The strip is normally sealed with 1% agarose to prevent movement during electrophoresis.

2.9 Peptide Mass Fingerprinting

Peptide Mass Fingerprinting is a protein identification technique, in which mass spectrometry (MS) is used to identify a protein of interest by measuring the mass of proteolytic peptide fragments obtained by specific cleavage (Liebler and Yates, 2002). Mass spectrometers are analytical instruments used primarily to measure the masses of molecules, determine chemical formulas and molecular structure and identify unknown substances.

The instrument has three essential parts, first, the source which produces ions from the sample. The second is the mass analyser, which resolves ions based on their mass/charge (*m/z*) ratio. The third part is the detector that detects the ions resolved by the mass analyser. There are two different types of instruments used in proteomics MS work. These are matrix-assisted laser desorption, ionization time-of-flight (MALDI-TOF) instruments (Kaufman, 1995) and electrospray ionization-tandem (ESI) (Fenn et

al., 1990) mass spectrometry instruments. In MALDI, the protein sample is applied as part of crystalline matrix, which is irradiated by a laser pulse. The energy of the laser excites the matrix and the absorbed energy converts the peptides into gaseous ions.

Sample which needs to be analysed with MALDI-TOF is mixed with a chemical matrix. Typical matrix compounds include 2,5-hydroxybenzoic acid (DHB), 3,5-dimethoxy-4-hydroxycinnamic acid (sinapinic acid) and a-cyano-4-hydroxycinnamic acid (a-CHCA). The α-CHCA is a good choice of matric for peptide analysis as it has relatively low proton affinity as compared to other matrices. There is several sample preparation techniques such as dried-droplet, thin layer and sandwich (Alias, 2006).

First part (MALDI) refers to the source. The mixture of sample and matrix is spotted onto target plate and allowed to evaporate. The evaporation of residual water and organic solvent allows the formation of crystals in which the peptides are incorporated. A laser fires a beam of light onto the matrix. The matrix chemical absorbs photons from the beam and become electronically excited. The excess energy is then transferred to the peptides or proteins in the sample, which are then ejected from the target surface. The ionization process produces both positive and negative ions. The positive ions are the species of interest. They are formed when accepting a proton as they are ejected from the matrix. Each peptide molecule tends to pick up a single proton. For proton transfer to occur, the proton affinity of the acceptor must be greater than that of the donor. The presence of the amide bond with high proton affinity suggests a ready route for formation of the protonated peptide by proton transfer from ground state [matrix + H^+] ion (Alias, 2006)

Thus, most of the resulting peptide ions are single charged. The ions are resolved based on their mass/charge (m/z) ratio. The measured values of peptide ions are compared to the expected values to identify the protein of interest. The introduction of a permanent positive charge in a peptide by trimethylation of a α or ε-amino group can lead to enhance detection by MALDI MS (Stewart et al., 2002).

The TOF analyser measures the time it takes for the ions to travel from one end of the analyser to the other end and strike the detector. The speed with which the ions fly through the analyser is proportional to their m/z values. For TOF analyser that operates in linear mode, the ions that are generated from the MALDI source are continually extracted and sent down the flight tube to the detector. The resolution of the instruments running in the linear mode with continuous extraction of ions may be relatively poor. This is due to the fact that in linear mode instruments there is variation in the velocities of ions of the same m/z as they travel down the flight tube.

There are two ways to improve resolution of TOF analyser from that found in 'linear mode'. First is the use of the reflection. It focuses ions of the same m/z values and allows them to reach the detector at the same time. Another approach is the use of pulsed-laser ionization with delayed extraction. This technique creates a slight delay between the laser pulse (ionization) and the propulsion of ions down the flight tube. This allows the ions all to get a 'fair start' so that all species of the same m/z hit the detector at the same time. All in all, the key feature of the MS analysis is the ability of the technique to generate different types of structural information about any particular digested protein or peptide of interest.

In MALDI-TOF when ions are singly charged, the molecular weights of the peptides are reported as monoisotopic $(M+H)^+$ form. The most important consideration in the use of MALDI-TOF analyses is the accuracy of the molecular weight measurement so that the mass difference between the calculated mass of particular peptide sequence and its measured mass is minimal. This is achieved by proper calibration of the spectrum. An external calibration requires placing the standard in close proximity to the analyte sample. The standard spectrum is then acquired either immediately prior to or immediately after acquisition of the analyte spectrum. One way of internal calibration is to use combination of matrix ions or/and trypsin autolysis peptide ions that are observed in the spectrum. The second way is to use a peptide or peptides specifically added to the sample as standard.

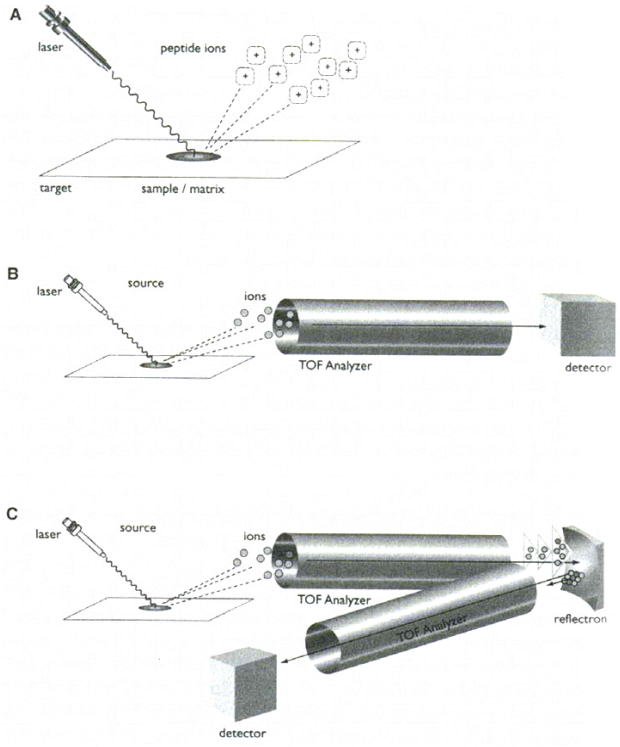

Figure 2.5: Schematic representation of a MALDI-TOF mass spectrometer. **(**A) The MALDI ionization process (B) A MALDI-TOF instrument operating in linear mode. (C) A MALDI-TOF instrument equipped with reflection (Adapted from Liebler and Yates, 2002).

2.10 Protein Identification

There are various databases available to be searched for protein identification. The most popular and broadly used protein sequence databases are the SWISS-PROT (http://www.expasy.cb/sprot/) and NCBI's (National Centre for Biotechnology Information) at (http://www.ncbi.nlm.nih.gov/blast/db/nr.Z) for non redundant database. TrEMBL (Translation of EMBL nucleotide databases at http://www.expasy.cb/srs5t/), is another protein sequence database supplementing SWISS-PROT. It consists of entries in SWISS-PROT- like format derived from the translation of all coding sequences (CDSs) in the EMBL (European Molecular Biology Laboratory Nucleotide Sequence Database (http://www.ebi.ac.uk/embl/index/html. Beside protein and nucleotide sequence databases, there are also genomic databases that are useful for protein identification. These databases contain information on the genetic organization of species of interest such as gene names, gene localization, description of function of gene products and cross-references to nucleotide and protein sequence databases.

Protein identification need a software tool equipped with a sophisticated scoring logarithm to determine the best match between the experimental data and a sequence that is in database. These algorithms correct for scoring bias due to protein size, the tendency of smaller peptides in databases to have greater number of matches with search m/z values and apply probability-based statistics to better define the significance of a putative protein identification (Liebler and Yates, 2002). The software tools available on the internet are PepIdent (http://www.expasy.cb/tols/peptident.html), MOWSE (http://www.srs.hgmp.mrc.ac.uk/cgi-bin/mowse), MS-Fit (http://www.prospector.ucsf.edu/), XProteo (http://xproteo.com:26981) and Profound (http://www.prowl.rockefellar.edu/cgi-bin/Profound).

CHAPTER 3

MATERIALS

3.1 Chemicals and Disposables

Systerm

Ethanol

Glacial acetic acid

Methanol

Orthophosphoric acid

Sodium thiosulfate

Glycerol

Sodium Chloride

Silver nitrate

Sodium carbonate

Sigma Chemical Company, St.Louis,USA

Ethylenediamine tetra-acetic acid, tetrasodium salt (EDTA)

Sodium dodecyl sulphate (SDS)

Thiourea

Coomassie Brilliant Blue G-250

Sodium Phosphate Monobasic

GSH L-Glutathione Reduced

3,4-Dichloronitrobenzene (DCNB)

4-Nitrocinnamaldehyde (NCA)

1-chloro-2,4-dinitrobenzene (CDNB)

Ethacrynic Acid (EA)

Trans-4-phenyl-3-butene-2-one (PBO)

p-Nitrobenzyl chloride (NBC)

Protease Inhibitor cocktail for general use

Sulfobromophthalein (BSP)

Phenylthiourea (PTU)

Bio Rad Laboratories, Richmond,USA

30% Acrylamide/ Bis solution, 19:1 (5% C)

1.5M Tris-HCl pH 8.8

0.5M Tris-HCl pH 6.8

N,N,N',N'-tetramethylenediamine (TEMED)

(3-[(3-cholamidopropyl)dimethylammonio]-1-propanesulfonate) (CHAPS)

Albumin, bovine serum (BSA)

R & M Chemicals

Ammonium Persulfate

Ammonium sulfate

Sodium carbonate

Urea

Trichloroacetic acid (TCA)

Sulfosalicylic acid

Merck

Dithiothreitol (DTT)

B-mercaptoethanol

Iodoacetamide (IAA)

Invitrogen

2% Biolyte/ Pharmalyte/ Ampholyte

BENCHMARK™ Protein Ladder

SDS Running Buffer

Novex® IEF Anode buffer

Novex® IEF Cathode buffer

Sample buffer

Novex® IEF Gels pH 3-10

Ammersham Biosciences

Immobiline® DryStrip, pH 3.0 – 10.0 L, 7cm

Glutathione-agarose matrix

Immobiline Phase DryStrip Cover Fluid, mineral oils

Promega

Agarose

Tris base

Sartorius Stedim Biotech GmbH

Vivaspin 20ml concentrators (MWCO: 10,000)

Minisart Cellulose acetate (CA) Syringe Filter

SERVA

SERVA Liquid Mix IEF Markers 3-10

BDH Laboratory Supplies Poole, England

Bromophenol blue

3.2 Equipments

Waterbath –Memmort Co.

Sonicator – Hwashin Technology Co.

Homogenizer – WiseTis Homogenizer HG-15D

Vortex – Labnet International,Inc

pH meter – Hanna Instruments

Weight – Supreme Lab Supplies

Bio rad Mini PROTEAN® Tetra Cell

Multiphor II Electrophoresis Unit, GE Healthcare Bioscience

XCell *SureLock*™ Mini-Cell

AKTAprime Plus (Ammersham Scientific)

Jasco V-630 Spectrophotometer

CHAPTER 4

METHODOLOGY

4.1 Sample Preparation

Orbicularia orbiculata, bivalve species were collected at Jeram, Kuala Selangor, Malaysia (Figure 1.1). The fleshes of bivalves were stored at -20°C after removal of the shell. About 10 gram of *O. orbiculata* was homogenized in ice cold prepared eluting buffer containing 1.0 mM ethylenediamine tetra-acetic acid or tetrasodium salt (EDTA), 0.1 mM dithiothreitol (DTT), 0.1 mM phenylthiourea (PTU) and protease inhibitor cocktails as in Appendix A using WiseTis homogenizer. The eluting buffer was a 25 mM phosphate buffer, pH 7.4 which usually used in chromatography analysis. The homogenized sample was centrifuged at 10000 rpm for an hour. The supernatant or crude preparation was collected and then filtered using minisart syringe filter before subjected to affinity chromatography. All the procedures were carried out at 4 °C to avoid protein degradation.

4.2 Isolation and Purification of GSTs

GSTs were isolated and purified from supernatant using GSH-agarose affinity chromatography which was connected to automated AKTA Prime Plus equipped with Prime View^{TM} software and a fraction collector. This purification process has used two different types of GSH matrix which each type of matrices differed by the carbon number in the linker and the way of the glutathione was attached to the agarose. The affinity matrices were GSTrap^{TM} HP and GSH-agarose (C_3). GSTrap^{TM} HP was purchased from GE Healthcare, meanwhile the GSH-agarose (C_3) was provided by Dr. Zazali Alias. The column was washed and equilibrated with eluting buffer (Appendix

A). 2 ml of crude sample was kept for activity measurement before loading into superloop (50 ml) and the flow rate was fixed at 0.3 ml/min.

The volume of loaded sample was measured and then injected into the instrument, permitting the sample to flow through the column, in which specific protein bound to the matrices meanwhile non-specifically protein was washed out with eluting buffer. The first peak consisted bulk of unbound protein was collected and known as void. The column was re-equilibrated with eluting buffer prior to elution with 10 mM GSH. The volume of the void and elute fractions were measured before proceeding to activity assay and total protein content determination. The active fraction of elution was then concentrated using 20 ml vivaspin concentrator (MWCO: 10000) and kept under -20°C for further analysis.

4.3 Enzyme Assays and Substrates Specificities

GST activity of the crude, void and elute of samples from both affinity matrices were determined by the method of Habig et al (1974) using 1-chloro-2, 4-dinitrobenzene (CDNB) as substrate at the presence of reduced gluthathione (GSH). The reaction mixture was prepared by mixing 2.85 ml 0.1 M sodium phosphate buffer pH 6.5, 0.05 ml of the sample, 0.05 ml 60 mM GSH and 0.05 ml 60 mM CDNB. The change of absorbance at 340 nm was recorded for 6 minutes. The reaction solution without the samples was used as blank. The active fraction of elution purified from both affinity matrices were then subjected to substrate specificities assay.

Several substrates such as 3,4-dichloronitrobenzene (DCNB), 4-nitrocinnamaldehyde (NCA), ethacrynic acid (EA), *trans*-4-phenyl-3-butene-2-one

(PBO), *p*-nitrobenzyl chloride (NBC) and sulfobromophthalein (BSP) in Appendix F were used in these assays were dissolved primarily in 95% ethanol. Enzyme activities were performed at 25°C in Jasco V-630 spectrophotometer equipped with Spectra Manager Version 2.0 software. Each assay was carried out in triplicate and a control which constituted a complete assay mixture exclude enzyme in total volume of reaction 3 ml. For all assays, buffer, GSH were added in the cuvette orderly and then put in the spectrophotometer followed by addition of substrate to initiate the reaction. The assay condition and parameters used for each substrate were listed in Appendix F.

4.4 Quantitative Protein Determination

Total protein content of sample was estimated via Bradford assay using bovine serum albumin BSA (Biorad) as a standard (Spector, 1978). Bradford reagent was prepared as in Appendix B. This assay was measured using Jasco V-630 spectrophotometer at absorbance wavelength of 595 nm.

4.4.1 BSA Standard Curve

Bovine serum albumin (BSA) stock (2 mg/ml) was dissolved into a series of solutions of known concentration. The BSA concentration was diluted into a serial of known concentration in final volume of 100 µl. Aliquots of BSA were pipetted into test tubes in range of 5 µl, 10 µl, 15 µl, 20 µl, 25 µl, 30 µl, 35 µl, 40 µl, 45 µl and 50 µl corresponded to 10 µg, 20 µg, 30 µg, 40 µg, 50 µg, 60 µg, 70 µg, 80 µg, 90 µg and 100 µg of BSA. Buffer was added to each test tube to bring the total volume of 100 µl. Reagent blank was prepared by addition of 100 µl appropriate buffer solution. Unknown samples were prepared in dilutions of 2 fold. 5 ml of Bradford reagent was added into

each tube of BSA standard and unknown sample followed by vortexing. Then both were incubated at room temperature for at least 5 minutes and less than 1 hour before the absorbance was measured. The BSA standard and unknown samples were assayed in duplicate. The standard curve of absorbance at 595 nm versus BSA concentration was plotted (Appendix G). The protein content of the unknown sample was estimated from the BSA standard curve.

4.5 Electrophoresis Technique

4.5.1 Laemmli Discontinous Sodium Dodecyl Sulfate – Polyacrylamide Gel Electrophoresis (SDS-PAGE)

SDS-PAGE was performed using a MINI-PROTEAN® Tetra Cell electrophoresis unit. The assembly and preparation of the electrophoresis apparatus was as according to the instruction manual. The concentrated protein (elution) from GSTrap™ HP and GSH-agarose (C_3) were resolved by SDS-PAGE using 12% (w/v) resolving gel and 4% (w/v) stacking gel according to Laemmli (1970). Both resolving and stacking gel were prepared as in Appendix C. The resolving gel was prepared first. TEMED and ammonium persulfate (APS) were added into the mixture after degassing. The resolving gel solution was swirl gently for well mixing and pipetted into the gel casting form by leaving some space for the stacking gel approximately 2.0 cm below the top of the short plate. Then, the top gel was layered with overlay solution, 0.1% (w/v) of SDS to prevent air from entering the gel solution and disrupted gel polymerization. The resolving gel was allowed to polymerize in more than an hour. The 4% (w/v) stacking gel was prepared in the same manner as the resolving gel. The overlay solution was removed after resolving gel was completely polymerized, and then the stacking gel was pipetted and loaded on top of resolving gel.

The comb with 10 wells was inserted slowly to avoid bubble stuck underneath. The gel was allowed to polymerize for overnight. Samples were diluted with sample buffer at least at 1:4 ratios. The sample buffer was prepared as in Appendix C. Then the diluted samples were heated at 95°C for 4 minutes before electrophoresis. The comb was removed carefully before loading the samples into the wells. A protein marker (BENCHMARK™ Protein Ladder) approximately 4 µl was loaded into well beside the samples for molecular weight estimation. The buffer chamber was filled with 1X SDS running buffer and the electrophoresis was run at 150 V for 1.5 hours or until the blue dye front reaches the bottom. The gel was removed from the glass plates into staining solution.

4.5.2 Subunit Molecular Weight Determination

The protein subunit were dissociated and separated by 12% (w/v) SDS-PAGE as described. The subunit of molecular mass was estimated from the linear plot of $\log_{10}$ MW versus mobilities of protein marker. Bands of the protein marker (BENCHMARK™ Protein Ladder) which represent the size of 10, 15, 20, 25, 30, 40, 50, 60, 70 and 80 kDa were used to construct the calibration plot (Appendix H).

4.6 Two-Dimensional (2D) Gel Electrophoresis

4.6.1 Sample Application by In-Gel Rehydration

The concentrated sample was applied directly to the rehydration buffer which containing 8 M urea, 0.15% (w/v) Dithiothreitol (DTT), 30 mM Thiourea, 2% (v/v) Biolyte/ Pharmalyte/Ampholyte, 2% (w/v) CHAPS and traces of bromophenol blue (BPB). The rehydration buffer was prepared as in Appendix D. The Immobiline®

DryStrip gels, pH 3-10 linear from GE Healthcare were used in this procedure. The Drystrip contained a performed pH gradient immobilized in homogenous polyacrylamide gel. The gel was casted on a plastic backing and delivered dried. The gel was rehydrated with an appropriate rehydration buffer containing sample prior to use. The 7 cm DryStrip gels used required rehydration solution in total volume of 125 µl. The total amount of the concentrated protein sample to load per Drystrip was varied depending on the sample. The rehydration solution consisting sample was pipetted into a graduated plastic pipette, which used as rehydration device. One end of the pipette was sealed with parafilm.

The Immobiline® Drystrip was slid (gel side down) and rehydration solution was loaded underneath. The rehydration solution was distributed evenly under the strip. Precautions were taken to minimize the existence of bubbles between the solution and the gel. Then the other side of the pipette was sealed and the gel was allowed to rehydrate overnight at room temperature.

4.6.2 First Dimension – Isoelectric Focusing (IEF) Technique

The components such as Immobiline® Drystrip tray, Immobiline® Drystrip aligner and electrodes were cleaned with detergent, rinsed thoroughly with distilled water and then allowed to dry. The red bridging cable in Multiphor II unit was ensured connected. The temperature on MultiTemp III Thermostatic Circular was fixed to 18°C. The cooling plate was placed on the Multiphor II unit by ensuring that the surface was level.

Approximately 3-4 ml of Immobiline Drystrip Cover Fluid was pipetted onto the cooling plate. The Immobiline Drystrip tray was positioned on the cooling plate so the

red (anodic) electrode connection of the tray was positioned at the top of the plate near the cooling tubes. Any large bubbles between the tray and the cooling plate were removed meanwhile small bubbles was ignored. The Immobiline Drystrip Cover Fluid was used as an insulating fluid to ensure good thermal contact between the cooling plate and the tray. The red and black electrode leads were connected on the tray to the Multiphor II unit. Approximately 5 ml of Immobiline Drystrip Cover Fluid was poured into the Immobiline Drystrip tray. The Immobiline Drystrip aligner was placed, 12-groove side up into the tray on top of the Immobiline Drystrip Cover Fluid. The presence of air bubbles between the strips positions under the aligner would not affected the experiment.

The IEF electrode strips were prepared by cutting into two, lengths of 110 mm each. The electrode strips were placed on a clean, flat surface such as a glass plate and each electrode strip was soaked with 0.5 ml distilled water. Excess water was removed by blotting with tissue paper. The Immobiline® Drystrip gel in the rehydration device was pulled out using forceps. The Immobiline® Drystrip was placed with gel side up on a sheet of damp filter paper and then was blotted with clean tissue paper to remove excess rehydration solution. The rehydrated Immobiline® Drystrip gel (gel side up) was transferred onto grooves of the aligner in the Immobiline® Drystrip tray. The Immobiline® Drystrip with the acidic ends was placed at the top of the tray near the red electrode (anode) meanwhile the other ends was at the bottom of the tray near the black electrode (cathode). If several Immobiline® Drystrip gels were aligned in the grooves, the anodic gel edges were made to line up.

The prepared moistened electrode strips were placed laterally across the cathodic and anodic ends of the aligned Immobiline® Drystrip gels. The electrode strips were

positioned in partial contact with the gel surface of each Immobiline® Drystrip gel. Each electrode was aligned over an electrode strip and the marked side was ensured corresponding to the side of the tray giving electrical contact. The electrode was pressed down to contact the electrode strip once it's properly aligned. Each Immobiline® Drystrip gel was overlaid with 3 ml of Immobiline Drystrip Cover Fluid to minimize evaporation and urea crystallization. The IEF was run using an EPS 3501 XL power supply. The running condition was programmed in gradient mode modified from manufacturer guideline. The setting for the programme was; 1st stage was 200V: 2mA : 5W : 0:01 hour, 2nd stage was 3500V : 2mA : 5W : 1:30 hours and 3rd stage was 3500V: 2mA : 5W : 1:30 hours. After the IEF was completely run, the Immobiline Drystrip gel was removed and subjected to the second dimension.

4.6.3 Second Dimension (SDS-PAGE) Technique

The Immobiline® Drystrip gels from the first dimension were equilibrated twice, each time for 15 minutes. Each 7 cm Immobiline® Drystrip required 2.5 ml equilibration buffer (1.5 M Tris-HCl pH 8.8, 6 M urea, 30% (v/v) glycerol and 2% (w/v) sodium dodecyl sulfate (SDS)). The first equilibration (equilibration solution I) was prepared by dissolving 0.25% (w/v) of dithiothreitol (DTT) into the equilibration buffer. Approximately 2.5 ml of the equilibration solution I was poured into the falcon centrifuge tube and the Immobiline® Drystrip was soaked into with the gel side down. The falcon tube was capped tightly and then put on a shaker for 15 minutes. In meantime, the second equilibration (equilibration solution II) was prepared by dissolving 4.5% (w/v) of iodoacetamide (IAA) and traces of bromophenol blue (BPB) into the equilibration buffer. The equilibration buffer, equilibration solution I and II were prepared as in Appendix D.

The equilibration solution I was discarded after 15 minutes and then substituted with the equilibration solution II. The Immobiline® Drystrip was soaked and equilibrated for another 15 minutes. After that, the Immobiline® Drystrip was placed on a piece of moistened filter paper and was stood on its edge to remove the remaining buffer. The second-dimension (SDS-PAGE) was performed using Mini-PROTEAN™ II electrophoresis unit. The equilibrated Immobiline® Drystrip gel was positioned in between the plates with the gel edge touching the surface of the SDS-PAGE gel. No bubbles were allowed between the two gels. The BENCHMARK protein ladder was loaded on small filter paper and this marker used to be inserted at one end (acidic) of the strip. Agarose sealing solution (0.5% (w/v) agarose and traces of BPB into SDS Electrophoresis Buffer) was then loaded and overlaid onto to ensure the strip was not moving during the electrophoresis. The electrophoresis was run at a constant 120 V using Bio-Rad Model 1000/5000 Constant Voltage power supply.

4.7 Isoelectric Focusing (IEF)

Isoelectric Focusing (IEF) electrophoresis was performed using XCell *SureLock*™ Mini-Cell and a power supply with Novex® IEF Pre-Cast gels from Invitrogen. This electrophoretic technique was applied to separate proteins based on their pI value using the Novex® IEF gels pH 3-10 which consisted of 5% (w/v) polyacrylamide with a fixed pH gradient. The pI means the pH at which a protein has not net charge and thus does not migrate further in an electric field. Individual proteins from protein sample were immobilized in the pH gradient as they approached their pI.

Gloves and safety glasses were used when handling the Novex® IEF gels. The Novex® Pre-Cast Gel was removed from the pouch. The gel cassette was rinsed with

deionized water and the tape from the bottom of the cassette was peeled off. The comb of the cassette was pulled out gently in one smooth motion. Then the sample wells were rinsed with appropriate 1X IEF Cathode Buffer. The gel was inverted and shaken to remove the buffer. This step was repeated two more times. The buffer core was lowered into the Lower Buffer Chamber to ensure the negative electrode fitted into the opening in the gold plate on the Lower Buffer Chamber. The Gel Tension Wedge was inserted into the XCell *SureLock*™ behind the buffer core. The Gel Tension Wedge was ensured in its unlocked position, allowing the wedge to slip easily into the XCell *SureLock*™ unit and was rested on the bottom of the Lower Buffer Chamber.

The two gels were oriented in the Mini-Cell such that the notched 'well' side of the cassette faced inwards toward the Buffer Core. The gels were seated on the bottom of the Mini-Cell. The Gel Tension Lever was pulled forward in a direction towards the front of the XCell *SureLock*™ unit until came to a firm stop and the gel was appeared snug against the buffer core. The cassette and buffer core were in place and the Gel Tension Wedge was locked into position when fully assembled. The plastic Buffer Dam was used in place of the second gel cassette when running just one gel to form the Upper Buffer Chamber. The Upper Buffer Chamber was filled with a small amount of the 1X IEF Cathode Buffer to check for tightness of seal. The buffer was discarded and the chamber was resealed if a leak was detected from Upper to the Lower Buffer Chamber. Then the seal was checked again.

The Upper Buffer Chamber (Inner) was filled with 200 ml of the appropriate 1X IEF Cathode Buffer once the seal was tightened. The buffer level was ensured to exceed the level of the wells. The 1X IEF Cathode Buffer was prepared using 10X Novex® IEF Cathode Buffer pH 3 -10 by adding 20 ml of the buffer into 180 ml of deionized water.

The samples for IEF Gels were prepared without SDS or reducing agents to avoid affecting the protein. The sample was prepared in 1:1 ratio with 2X Novex® IEF Sample Buffer, pH 3-10. The 2X IEF Sample Buffer, pH 3-10 was prepared by mixing 2 ml of 10X IEF Cathode Buffer, pH 3-10 with 3 ml of glycerol, then was mixed well and the volume was adjusted to 10 ml with ultrapure water. The buffer was stored at 4°C to maintain its stability for 6 months. An appropriate volume of sample at the desired protein concentration and appropriate protein molecular weight markers were loaded onto the gel. SERVA Liquid Mix, IEF Markers 3-10 was used as a protein marker.

The Lower Buffer Chamber was filled with 600 ml of the 1X IEF Anode Buffer. The 1X IEF Anode Buffer was prepared using 50X Novex® IEF Anode Buffer by adding 20 ml of the buffer into 980 ml of deionized water. After that, the XCell *SureLock*™ Mini-Cell was placed on the Buffer Core. The electrode cords were connected to the power supply. The gel was run at 100 V constant for 1 hour, followed by 200 V constant for 1 hour, and finished with 500 V constant for 30 minutes. After the electrophoresis was completed, the power was shut off and electrodes were disconnected. The lid was removed and the Gel Tension Lever was unlocked by not removing it. The gel cassette was removed from the XCell *SureLock*™ Mini-Cell and was handled by their edges only. The gel cassette was laid on a flat surface such as the bench top. One edge was allowed to hang ~1 cm over the side of the bench top. The notched ‘well’ side of the cassette was faced up. Each of the three bonded sides of the cassette was separated by inserting the Gel Knife into the gap between the two plastic plates that made up the cassette. The knife handle was pushed down gently to separate the plates. This step was repeated on each side of the cassette until the plates were completely separated. The bonds which held the plates together were broke when a

cracking sound heard. The top plate was removed carefully and discarded, allowing the gel to rest on the bottom (slotted) plate.

The gel was removed from the cassette plate by one of the two methods. Firstly, if the gel was on the shorter (notched) plate, the sharp edge of the Gel Knife was used to remove the bottom foot of the gel. The Gel Knife was held at a 90°C angle to the gel and the slotted cassette plate. The knife was pushed straight down and then the motion across the gel was repeated to cut off the entire foot. The cassette plate and gel were held over a container with the gel facing downward. The knife was used to carefully loosen one lower corner of the gel and the gel was allowed to peel away from the plate. Secondly, if the gel remained on the longer (slotted) plate, the cassette plate and gel were held over a container with the gel facing downward. The gel knife was pushed gently through the slot in the cassette, until the gel peeled away from the plate. The foot was cut off the gel after fixing and staining but before drying.

The gel was fixed immediately in fixing solution which consisted of 12% trichloroacetic acid (TCA), or 12% (w/v) TCA with 3.5% (w/v) sulfosalicylic acid. The fixing step was recommended after electrophoresis to remove carrier ampholytes from the gel, resulting in lower background after staining. The fixing solution was prepared by dissolving 60 g TCA and 17.5 g sulfosalicylic acid into 500 ml deionized water, and then was mixed thoroughly. The gel was fixed for 30 minutes before proceeding to silver staining.

4.8 Gel Staining

4.8.1 Colloidal Coomassie Blue Staining

Colloidal Coomassie Blue Staining was used for the visualization of proteins due to its simplicity technique, sensitivity and compatibility with mass spectrometric protein identification. The procedure was implemented from Neuhoff (1988). Coomassie Brilliant Blue (CBB) G-250 was used as dye and prepared separately. The 5% (w/v) CBB solution was prepared by dissolving 1 g of CBB G-250 into 20 ml deionized water. On the other hand, the stock solution was prepared by adding 100 g of ammonium sulfate into 500 ml deionized water and dissolved completely. Then 11.8 ml of 85% (v/v) orthophosphoric acid solution was added into ammonium sulfate solution. Lastly, 20 ml of aqueous 5% (w/v) Coomassie Brilliant Blue (CBB) was added gradually. The volume of stock solution was made up to 1 liter. This solution was shaken vigorously before use for even distribution of the colloidal particles.

For actual staining, the staining solution was prepared by mixing one part of methanol approximately 20 ml with four parts of stock stain solution approximately 80 ml. The staining solution was prepared fresh and discarded after use. The staining was done in sealed container and put on a shaker overnight for a gentle shaking. The staining solution was substituted with new staining solution after overnight for next cycle of staining to enhance dye deposition of low abundance proteins. After completely staining, the gel was briefly washed in 20% (v/v) methanol in 80 ml deionized water, to wash off the colloidal dye particles. This step was repeated until a clearer background was achieved.

4.8.2 Silver Staining

Silver staining was applied for protein visualization with a detection level down to the 0.3 to 10 ng level. The silver staining technique was introduced by Switzer et al. (1979) and can be categorized into two, silver amine or alkaline methods and silver nitrate or acidic methods. The silver nitrate or acidic protocol by Merril (1990) was faster than alkaline method but slightly less sensitive. In this instance, the procedure was adopted from Gromova and Celis (2006) which was slightly modified from Shevchenko et al (1996) and Yan et al. (2000). This silver staining was conducted into several steps by using the appropriate solutions. The solutions for this staining were fixation solution, washing solution, sensitizing solution, staining solution, developing solution, terminating solution and preserving solution. All of solutions were prepared as in Appendix E.

Gel was removed from cassette after electrophoresis and placed into a tray containing the appropriate volume of fixing solution. The gel was immersed in fixing solution, which consisted 50% (v/v) methanol, 12% (v/v) acetic acid and 0.05% (v/v) formalin for 2 hours or overnight. The fixation step restricted protein movement from the gel matrix and removed interfering ions and detergent from the gel. Then, the fixation solution was discarded and the gel was washed in 35% (v/v) ethanol for 20 minutes. The solution was changed three times to remove remaining detergent ions as well as fixation acid from the gel.

After that, the ethanol solution was discarded and the sensitizing solution, 0.02% (w/v) sodium thiosulfate dissolved in deionized water, was added. The gel in the sensitizing solution was incubated for 2 to 3 minutes with gentle rotation. This step will

increase the sensitivity and the contrast of the staining. The sensitizing solution was discarded and the gel was washed in deionized water three times, 3 to 5 minutes each time. The water was then discarded. The silver staining solution was added and shaken for 20 minutes to allow the silver ions to bind to proteins. This solution consisting 0.2% (w/v) silver nitrate and 0.076% (v/v) formalin, was not poured directly on the gel as it may result in unequal background, despite added to the corner of the tray.

After staining was completed, the staining solution was poured off and the gel was rinsed with a large volume of deionized water twice for 20 – 60 s to remove excess unbound silver ions. However the gel was washed for more than 1 min will remove silver ions from the gel, resulting in decreased sensitivity. The developing solution was added after washing and the protein image was developed by incubating the gel for 2 to 5 minutes. The developing solution was prepared by mixing 6% (w/v) sodium carbonate, 0.0004% (w/v) sodium thiosulfate and 0.05% (v/v) formalin into deionized water. The reaction was stopped as soon as the desired intensity of the bands was reached. The reaction was terminated using 50% (v/v) methanol and 12% (v/v) acetic acid with gentle agitation for 5 minutes. Development was stopped as soon as 'bubbling' was over. Lastly the moist gel was kept into preserving solution, 1% (v/v) of acetic acid at 4°C in sealed plastic bags.

4.9 Gel Visualisation

The stained gels were scanned using Ammersham scanner equipped with Lab Image software for gel image visualization and analysis.

4.10 MALDI-TOF Analysis

Protein spots of interest were excised from the stained 2D gel using a clean, sharp scalpel and transferred into 1.5 ml capped Eppendorf tubes. The spots in each tube were labeled correctly according to the information requirements. Samples were dried and sent to Proteomics International (Perth, Australia) for MALDI-TOFF analysis. A standard technique of Bringans et al. (2008) was applied to the protein samples during the process and peptides generated were analyzed by MALDI TOF-TOF mass spectrometer using a 5800 Proteomics Analyzer (AB Sciex). Bovine serum albumin was used as a standard. Generated mass spectra of the peptides were analyzed using ProFound software, a tool for searching a protein sequence collections with peptide mass maps (http://prowl.rockefeller.edu/prowl-cgi/profound.exe).

ProFound was developed based on Bayesian algorithm to rank the protein sequences in the database according to their probability of producing the peptide map. The Z score was calculated for each candidate sequence indicating the probability of that candidate belongs to a random match population which value of 1.65 or lower signifies that the candidate is likely to be random match with 95 % confidence. ProFound included several informations, such as the type of digestion, links to the appropriate database and taxa, and range of *p*I and molecular masses of the samples. One missed cleavage *per* peptide was allowed and an initial mass tolerance of 0.05 Dalton was set up in all searches. Partial carbamidomethylation of cysteine and partial modification of methionine (methionine oxidation) were assumed. Another software tools available on the internet used were PepIdent (http://www.expasy.cb/tols/peptident.html), MOWSE (http://www.srs.hgmp.

mrc.ac.uk/cgi-bin/mowse), MS-Fit (http://www.prospector.ucsf.edu/), XProteo (http://xproteo.com:26981).

CHAPTER 5

RESULTS

5.1 Affinity Chromatography

Purification of GST expressed in the *Orbicularia orbiculata* was carried out using AKTA Prime Plus system. In order to get effective purification of GSTs, two different GSH matrices were used. The chromatograms in Figure 5.1 and Figure 5.2 showed the purification of GSTs using GSTrap^{TM} HP and GSH-agarose (C_3) columns, respectively. The bound GSTs were eluted with concentration of 10mM GSH in 25mM sodium phosphate buffer, at pH 7.4. The presence of peaks which highlighted in the red box beside the chromatograms (Figure 5.1 and Figure 5.2) indicated that the bound GSTs on both affinity matrices were successfully eluted.

The GST activity was tested in crude preparation, void and eluant fraction by using general substrate which was CDNB. Table 5.1 summarized the results of GSTs purification from *O. orbiculata* using two different matrices of affinity chromatography. The bound GSTs from both matrices resulted low percentage yield, 18% and 16% compared to the unbound GST which constituted about 82% and 80% from GSTrap^{TM} HP column and GSH-agarose (C_3) column, respectively. The amount of GSTs eluted from GSTrap^{TM} HP column and GSH-agarose (C_3) column were 0.24±0.003mg and 0.12±0.07mg, respectively. The degree of purification measured for isolation of GSTs using GSH-agarose (C_3) column higher than obtained with GSTrap^{TM} HP column. The GSTs fraction from the GSTrap^{TM} HP column purified was 60.2-fold but with 2% lower recovery, while GSH-agarose (C_3) eluted GSTs showed better purification fold, 89.4X.

The bound GSTs on GSTrap™ HP matrix was shown to have greater total activity than the bound GSTs on GSH-agarose (C_3) column. Total activity of GSTrap™ HP eluted GSTs was 0.49±0.004 μmol/min, meanwhile 0.41±0.003 μmol/min for GSH-agarose (C_3) eluted GSTs. On the other hand, total activities of the unbound GSTs or in void fraction from both columns were detected, which 2.18±0.02 μmol/min from GSTrap™ HP matrix and 2.0±0.01 μmol/min from GSH-agarose (C_3) column, but specific activities of unbound fractions were very low. Specific activity of GSH-agarose (C_3) eluted GSTs was 3.43±0.02 μmol/min/mg meanwhile specific activity of GSTrap™ HP eluted GSTs was 2.01±0.02 μmol/min/mg.

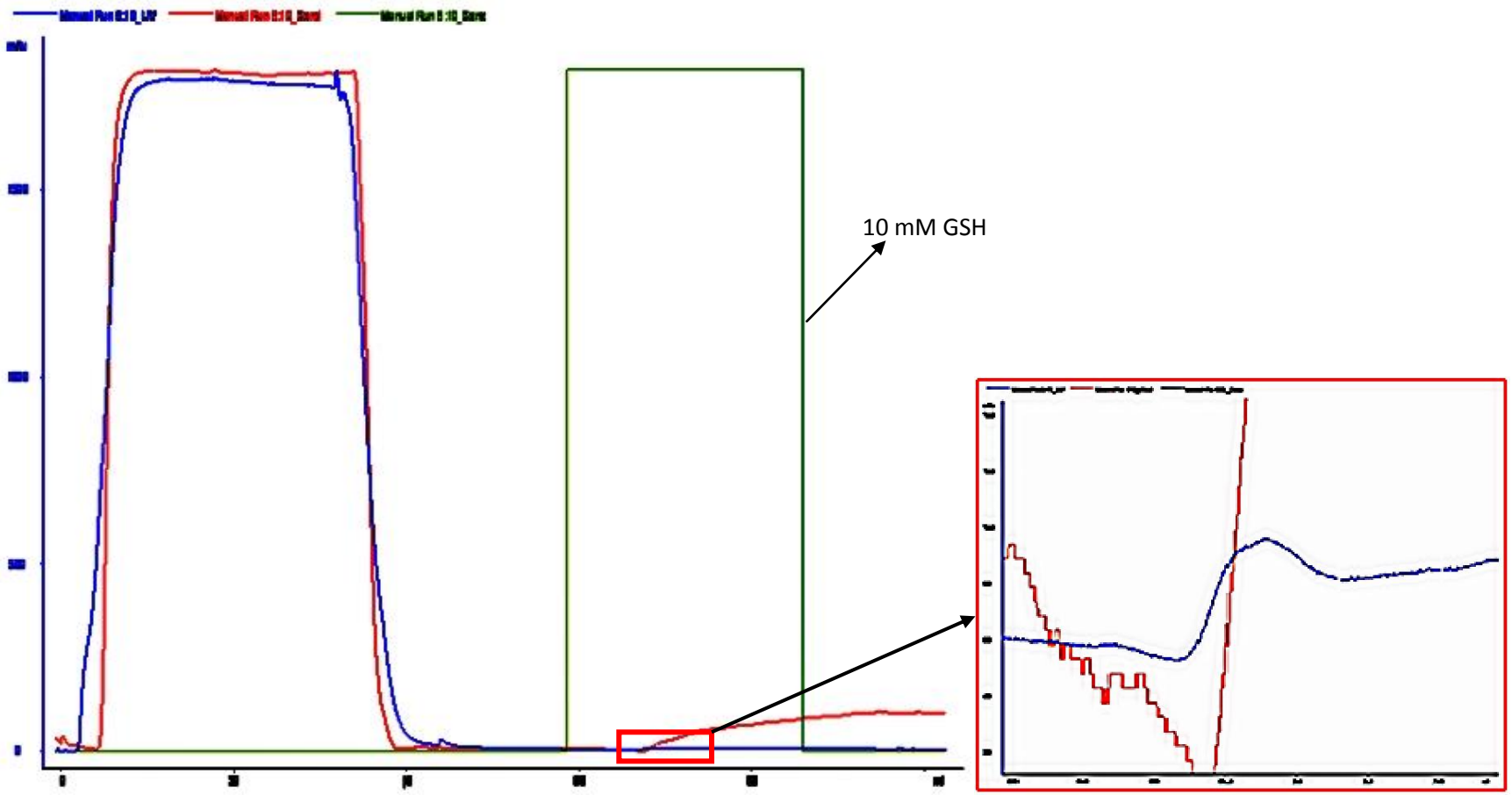

Figure 5.1: Chromatogram of *Orbicularia orbiculata sp.* homogenate purified using GSTrap^{TM} HP column. The GST captured in affinity column was eluted by using 10mM GSH (highlighted in the red box). (——) the % of GSH concentration (10mM), (——) conductivity and the protein measurement at A280 nm (——) were continuously monitored.

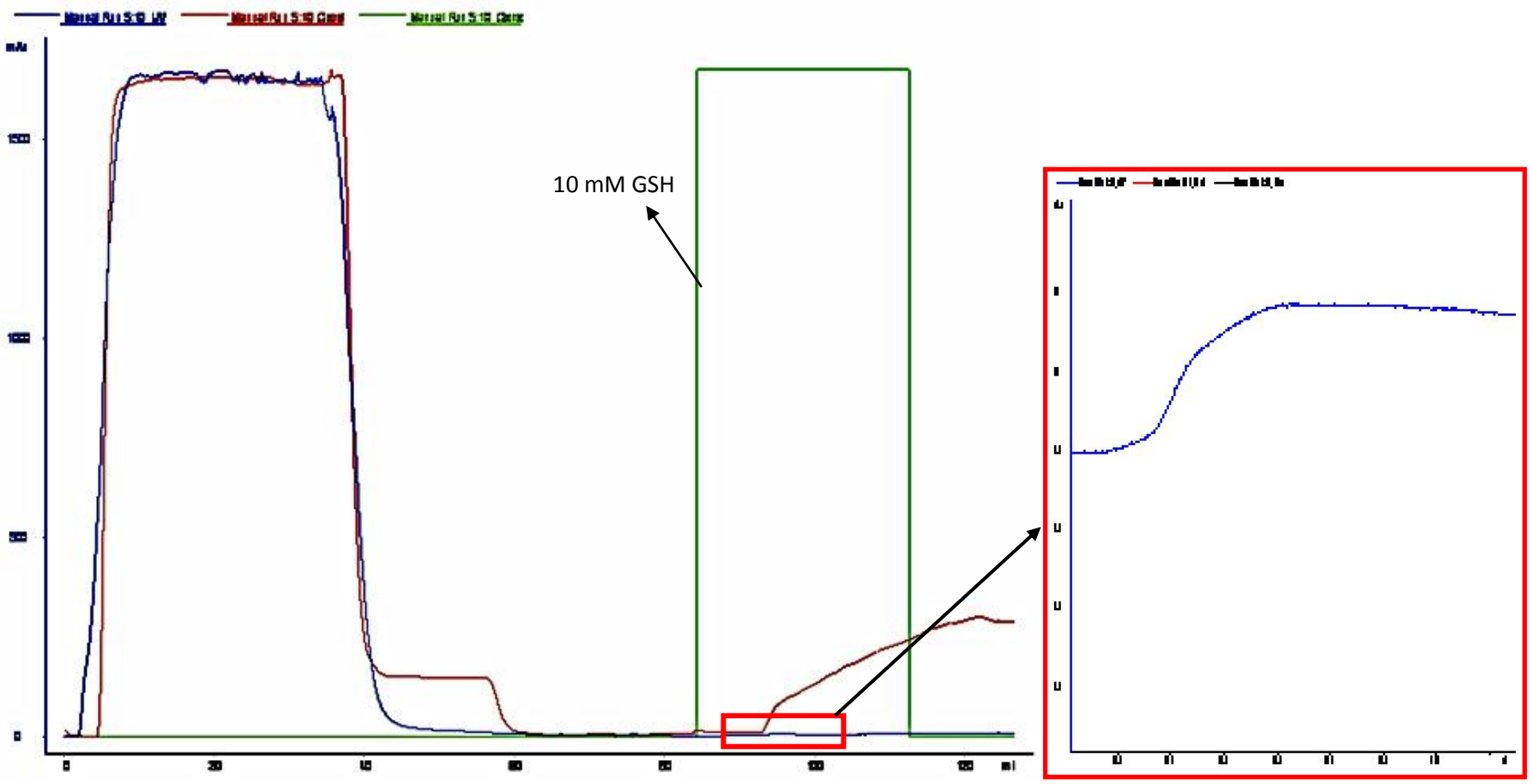

Figure 5.2: Chromatogram of *Orbicularia orbiculata sp.* homogenate purified using GSH-agarose (C_3) column. The GST captured in affinity column was eluted by using 10mM GSH (highlighted in the red box). (——) the % of GSH concentration (10mM), (——) conductivity and the protein measurement at A280 nm (——) were continuously monitored.

Table 5.1: Purification of gluthatione S-transferases from *Orbicularia orbiculata sp.* using affinity chromatography, GSTrap^{TM} HP (I) and GSH-agarose (C_3) (II) columns. Values are means ± SD taken from three independent replications.

	total protein (mg)	**total activity (µmol/min)**	**specific activity (µmol/min/mg)**	**purification factor (X)**	**Yield (%)**
			CDNB		
I GSTrap^{TM} HP					
10 000 rpm supernatant	78.99±1.68	2.64±0.006	0.033±0.001	1	100
Affinity eluate	0.24±0.003	0.49±0.004	2.01±0.02	60.2	18
Void	76.94±0.67	2.18±0.02	0.028±0.0002	0.84	82
II GSH-Agarose (C_3)					
10 000 rpm supernatant	65.08±0.49	2.50±0.02	0.038±0.0003	1	100
Affinity eluate	0.12±0.07	0.41±0.003	3.43±0.02	89.4	16
Void	62.71±0.45	2.0±0.01	0.032±0.0002	0.83	80

5.2 Substrate Specificities Assay

The active eluant fractions from both affinity matrices then tested with a range of substrates which listed in Table 5.2. Interestingly, both purified GSTs showed strong specific activity towards EA, but had little enzymatic activity towards DCNB, which were 0.005±0.002 μmol/min/mg for GSTrap^{TM} HP eluted GSTs and 0.004±0.001 μmol/min/mg for GSH-agarose (C_3) eluted GSTs. The specific activity of GSH-agarose (C_3) eluted GSTs towards EA and CDNB were 12.66±1.09μmol/min/mg and 3.43±0.02μmol/min/mg, respectively. Meanwhile specific activity of GSTrap^{TM} HP eluted GSTs towards both substrates, EA and CDNB were 9.97±1.06 μmol/min/mg and 2.01±0.02 μmol/min/mg, respectively. However both purified GSTs did not show any activity towards other substrates; NBC, PBO, BSP and NCA.

Table 5.2: Substrate specificities of elution purified from affinity chromatography GSTrap^{TM} HP and GSH-Agarose (C_3). The activities were monitored under conditions shown in Appendix F.

*n.d, activity was not detected. The data are the means ±SD for three replicate determinations of independent experiments.

	Specific activity μmol/min/mg	
Substrates	**GSTrap^{TM} HP**	**GSH-Agarose (C_3)**
1-chloro-2,4-dinitrobenzene (CDNB)	2.01±0.02	3.43±0.02
3,4-dichloronitrobenzene (DCNB)	0.005±0.002	0.004±0.001
ethacrynic acid (EA)	9.97±1.06	12.66±1.09
p-nitrobenzyl chloride (NBC)	n.d	n.d
trans-4-phenyl-3-butene-2-one (PBO)	n.d	n.d
sulfobromophthalein (BSP)	n.d	n.d
4-nitrocinnamaldehyde (NCA)	n.d	n.d

5.3 Electrophoresis Results

5.3.1 SDS-PAGE Analysis

Due to detectable activity with several substrates employed, the eluted GSTs from both matrices were concentrated prior to check the purity and present of GSTs protein. The purity of the bound GSTs from GSTrap™ HP and GSH-agarose (C_3) columns were analysed with SDS-PAGE. Concentrated elution from the GSTrap™ HP column had resulted in the isolation of two intense bands at molecular weight (MW) of 27 kDa and 26 kDa respectively (Figure 5.3). Meanwhile, the concentrated GSH-agarose (C_3) eluted GSTs had resulted in the isolation of a propable single faint band at molecular weight (MW) of 26 kDa (Figure 5.4).

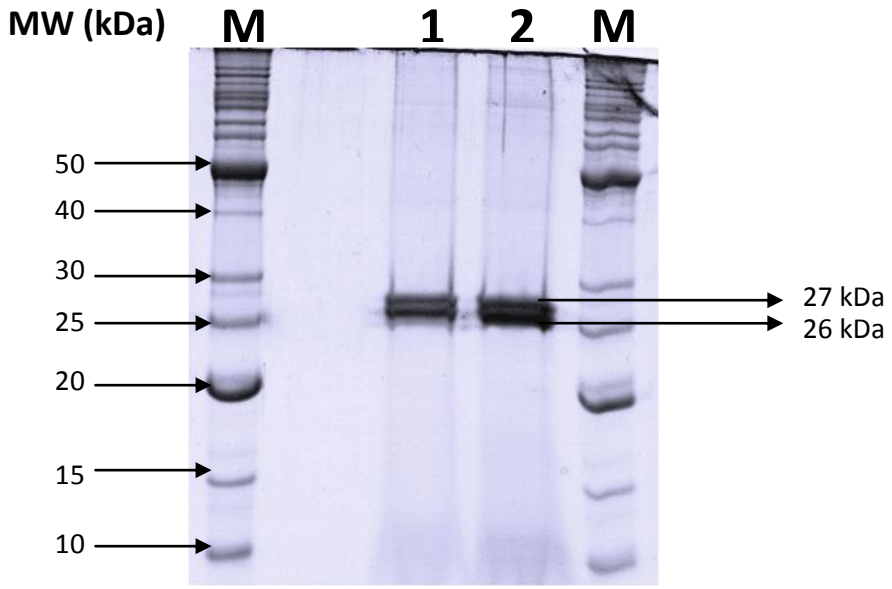

Figure 5.3: SDS-PAGE 12% (w/v) of GSTs purified from affinity chromatography using GSTrap™ HP column. The gel was stained with coomassie blue and BENCHMARK protein ladder was used as marker. Lane 1 and 2 are replicate samples of GSTrap™ HP eluted GSTs. Concentration of the loaded sample was 15µg. M = BENCHMARK protein ladder.

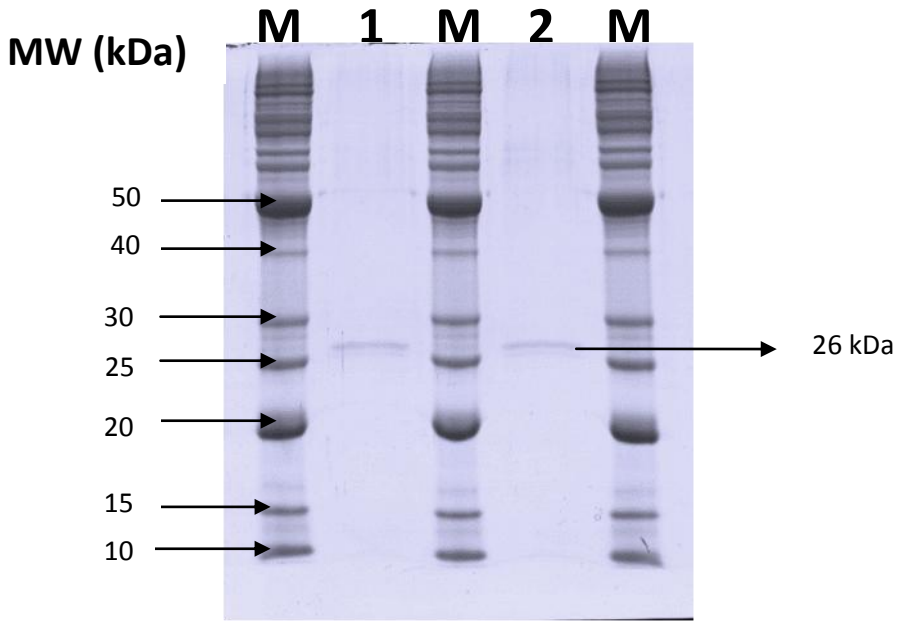

Figure 5.4: SDS-PAGE 12% (w/v) of GSTs purified from affinity chromatography using GSH-agarose (C_3) column. The gel was stained with coomassie blue and BENCHMARK protein ladder was used as marker. Lane 1 and 2 are replicate samples of GSH-agarose (C_3) eluted GSTs. Concentration of the loaded sample was 7.5µg. M = BENCHMARK protein ladder.

5.3.2 Two-dimensional electrophoresis (2-DE)

The 2-DE gel analysis was utilized to separate GSTs from eluate fractions according to their isoelectric points (pI) and molecular weight (MW). The use of immobilize pH gradient enables separation of complex protein mixture into single protein species represent by series of spot on the SDS-PAGE gel. This is important as complex protein mixtures might lead to a higher chance of spots overlapping and co-migration when analysed on a 1D gel. Thus, a possible co-migration of GST isoforms on 1D SDS-PAGE could not be ruled out. In order to identify the GST isoforms, the 2D gels of the GSTs isolated from both matrices were compared (Figure 5.5). The 2D gel analysis indicated that both matrices captured different isoforms of GST. GSTrap^{TM} HP resolved into ten spots which designated as spots # 1, 2, 3, 4, 5, 6, 7, 8, 9, and 10

(Figure 5.5 [B]) while GSH-agarose (C_3) resolved into six spots which designated as spots # 1, 2, 3, 4, 5 and 6 (Figure 5.5 [A]).

The 2D gel analysis revealed six similar spots resolved in both matrices, spots # 1, 2, 3, 4, 5 and 6 were in a line (Figure 5.5 [C]), meanwhile four extra spots appeared in GSTrap™ HP column. GSTrap™ HP column had bound four extra spots at higher molecular weight compared to the six similar spots. The extra spots were designated as spots # 7, 8, 9 and 10 in Figure 5.5 [B]. The apparent spots from both matrices were proceeding to IEF for pI value determination.

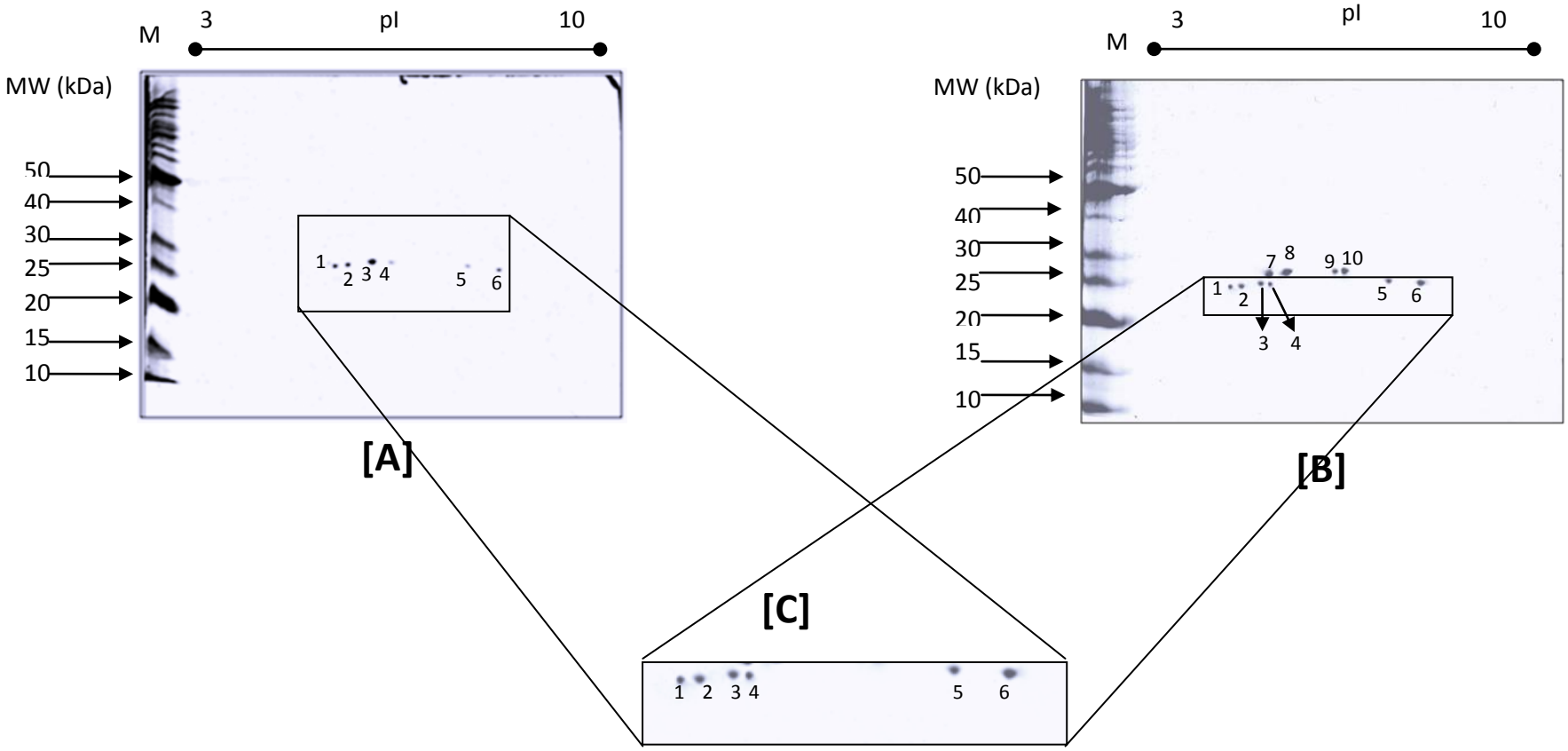

Figure 5.5: The comparison of 2D gels of GST isolated from [A] GSH-agarose (C_3), and [B] GSTrap^{TM} HP column. It shows that both matrices captured the same spots labeled #1, 2, 3, 4, 5 and 6 in box C. The GSTrap^{TM} HP column captured four extra spots labelled #7, 8, 9, 10 as in box B.

5.3.3 Isoelectric Focusing Analysis

Figure 5.6 showed the IEF analysis from both matrices. Lane 1 was GSTrap™ HP eluted GSTs, while Lane 2 was GSH-agarose (C_3) eluted GSTs. There were ten apparent bands in the Lane 1, while only six bands appeared in Lane 2. The IEF analysis showed there were six bands have same pI value from the both matrices. Four out of six bands were appeared on the bottom of the both IEF gel had shown the pI values in range of 4.5 to 5.3. This indicated the four bands were acidic protein. Another two bands were appeared on top of gel and the pI values were 8.3 and 9.5 respectively. Both matrices had bound GSTs at acidic pI protein (bands 1, 2, 3 and 4) exclude two bands, 5 and 6 were basic protein.

However, there were four bands only appeared on the gel of GSTrap™ HP eluted GSTs, illustrated as band 7, 8, 9 and 10 in Figure 5.6 (Lane I). The IEF image had shown the pI value of bands 7 and 8 in between 6.0 to 6.9 while bands 9 and 10 have 6.9 and 7.0 of pI value, respectively. The extra bands 7, 8, 9 and 10 bound on the GSTrap™ HP matrix were neutral protein.

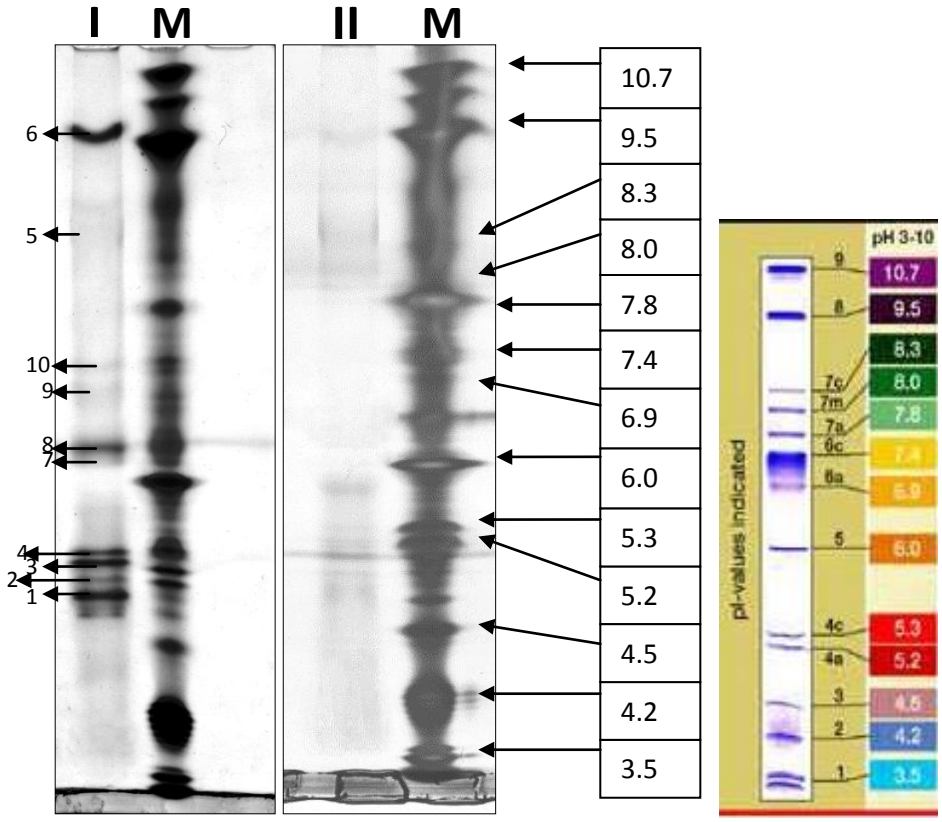

Adapted from SERVA Electrophoresis GmbH Manual

Figure 5.6: Isoelectric focusing (IEF) of active proteins fraction eluted from GSH-agarose affinity chromatography by using two different GSH based matrices. IEF SERVA marker was used as indicator for prediction of pI value of eluted GSTs. The gel was stained with silver. Lane 1 was GSTrap^{TM} HP eluted GSTs and lane 2 was GSH-agarose (C_3) eluted GSTs.

5.4 Protein Identification

Protein identification of each spots was performed using MALDI-TOFF analysis to determine to which class the subunit belongs to. Ten spots obtained from GSTrap^{TM} HP column and six spots obtained from GSH-agarose (C_3) column were sent for amino acid determination. The generated peptides were analyzed by MALDI TOF mass spectrometer had resulted in good readings. Then, the generated mass spectra of the peptides (Appendix I) were analyzed using several software which were ProFound software, PepIdent (http://www.expasy.cb/tols/peptident.html), MOWSE (http://www.srs.hgmp.mrc.ac.uk/cgi-bin/mowse), MS-Fit (http://www.prospector.ucsf.edu/) and XProteo (http://xproteo.com:26981) for searching a protein sequence collections with peptide mass maps. Unfortunately, none of the spots were identified using the available databases. There were some factors influenced to the unidentified GSTs such as lack of information of bivalves GSTs in the current databases.

CHAPTER 6

DISCUSSION

Purification of GSTs from *O. orbiculata* employed two different matrices of affinity chromatography which connected to AKTA prime. Affinity chromatography was the preferred isolation and purification tool due to its high selectivity towards target, simple, efficient and rapid process. There were two different affinity matrices used to purify GSTs. This is to compare the proteome of GST binding to both matrices. The reduced GSH was used as affinity matrix competitor for both columns because all described GST isoforms have good affinity for free GSH. Moreover, the GSH is non inhibitory and may stabilize the enzyme (Hoarau et al., 2002), allowing further purification and assays test. In this study, a 10mM GSH solution that has higher affinity towards bound GSTs compared to immobilize GSH was used to pull the enzymes from matrix. The application of 10mM GSH was sufficient to collect bound proteins from both matrices, indicated by total yield percentage of eluate and void that gave almost 100% recovery.

From the study, the purification Table 5.1 it is indicated that only 18% and 16% of GSTs bound to the GSTrap^{TM} HP and GSH-agarose (C_3) column, respectively. This suggests a lot of CDNB active GSTs were not bound to GSH-agarose. The low yields which obtained after the affinity purification step are commonly observed other invertebrate such as about 12% for *Mercinaria mercinaria* (Blanchette and Singh, 1999). However, GST purification reports that were performed using GSH-agarose column alone had showed moderate recovery of ~50% of the initial CDNB activity (Yuen and Ho, 2002) and 46% for *Octopus vulgaris* (Tang et al., 1994).

There are activities detectable within the flowthrough collected from matrices (Table 5.1), suggesting the presence of other unbound GSTs which either does not bind or weakly bind to GSH-agarose matrices. The discovery was in line with Alias (2006), who noted the detectable in the flow-through fraction of *D. melanogaster* when GSH-agarose (C_3) and (C_{12}) were used. Since *O. orbiculata* flesh was used, it is likely that total GSTs consisted of wider classes while GSH-agarose matrices were discriminating towards specific group of GSTs (Clark et al., 1990). Clark et al. (1990) also reported GSH-agarose (C_3) capability to capture CDNB-active *Musca domestica* GSTs but not to the other isozymes group. So there is possibility that the unbound *O. orbiculata* GSTs remain in the void fraction. Therefore, it is suggested that next purification schemes should be emphasized to capture the unbound GSTs by using wide range of specific affinity matrices or different types of chromatography.

This study also revealed GSTrap^{TM} HP capability to recover more *O. orbiculata* enzyme compared to GSH-agarose (C_3), which count about 2 times higher (Table 5.1). This result is in line with Alias (2006) who succeeds to isolate fruit fly GSTs from GSH-agarose (C_{12}) as much as 2-fold than GSH-agarose (C_3). This indicated GSTrap^{TM} HP capability to capture GSTs in larger aptitude than GSH-agarose (C_3). In this case both matrices use the same ligand which is GSH to capture GST molecules and seem very look alike but different in arrangement of their linker arm. Both matrices will behave similarly due to the same ligand attachment and have capability to bind the same active site of GSTs molecule but it did not happen. This dissimilar result is believed contributed by the different length of linker arm that hold GSH. Results obtained from this study and Alias (2006) clarify the ability of GSH-agarose (C_{12}) to capture more GSTs compared to GSH-agarose (C_3). Therefore, this indicated that GSH-agarose (C_{12}) may have better sample exposure during the purification process. It is logical that the

nature of GSH-agarose (C_{12}) longer arm contributed to this better exposure from GSH-agarose (C_3).

Enzyme activity was calculated to measure the quantity of active enzyme present per volume of solution in a specified condition or can be simplified as moles of substrates converted per unit time. In this study, the total activity i.e total number of enzyme units showed that purification of *O.orbiculata* GST from both matrices was not much different although total protein recovered from GSTrap^{TM} HP was more than GSTs obtained from GSH-agarose (C_3). This condition was contributed by the present of inactive enzymes in GSTrap^{TM} HP column. In theory, the rate of the enzymatic reaction is related to the concentration of enzyme-substrate complex. The formation of enzyme-substrate complex takes place within the active site of the enzymes or normally known as key and lock model. According to this law, enzyme activity or the rate of the reaction will be increased if the sample contain larger amount of enzymes which mean more active site are available. However there was exemption in this study as shown in Table 5.1 which the total activity for both was quite similar. The reason was due to enzymes present in GSTrap^{TM} HP have different active site which is some are specific towards CDNB substrate and some are not specific towards CDNB substrate.

As shown in Table 5.1, the use of GSH-agarose (C_3) gave 3.43±0.02 μmol/min/mg of specific activity compared to 2.01±0.02 μmol/min/mg in GSTrap^{TM} HP. This showed that the formation of enzyme-substrate complex in GSH-agarose (C_3) is more specific and gave better purification fold which was 89.4%.

One D gel analysis has shown that GSTs purified from GSTrap^{TM} HP having the possible molecular weights of 27 kDa and 26 kDa (Figure 5.3). In contrary, GSH-

agarose (C_3) had bound GST only at single molecular weight of 26 kDa (Figure 5.4). The presence of two bands in GSTrap^{TM} HP and a band in GSH-agarose (C_3) suggested high possibility of at least two different GST classes were successfully isolated from these purification schemes. The number of carbon atoms on the linker has been demonstrated to affect the binding capability of the matrix. The GSH-agarose (C_3) was linked by 3 carbon atom linkers; meanwhile the GSTrap^{TM} HP was linked by 12 carbon atom linkers, which has the ability to bind GST more tightly than the GSH-agarose (C_3) column. The fact was supported by Alias (2006) who reported that the purified fruit fly GSTs was 2 fold higher from GSH-agarose (C12) than GSH-agarose (C3). Result showed that less subunit was obtained when GSH-agarose (C_3) used in this study which was consistent with Alias (2006) and Clark et al. (1990) where they purified GSTs from *D. melanogaster* and *M. domestica.* Most of the reported bivalves GSTs were expected to be in range of 20 kDa to 30 kDa in their subunit molecular weights as indicated in the literature review. Thus, it is suggested both purified GSTs were inhibitors free due to unbound protein at higher than 30 kDa of molecular weight.

Referring to table 5.1, the purification factor for GSTrap^{TM} HP is less than GSH-agarose (C_3). With apparent of two bands on GSTrap^{TM} HP, the purification fold is less with 60.2X, meanwhile a band at 26 kDa on GSH-agarose (C_3) resulted in 89.4X of purification fold, and this suggesting the non-active presence of GST-molecule, which at 27 kDa. This is supported by the substrate specificities in Table 5.2, showing no differences of activity between GSTrap^{TM} HP and GSH-agarose (C_3), only exhibiting the specificities towards EA, CDNB and DCNB, but not active towards other substrates such as PBO, BSP, NBC and NCA. GSTs purified from both columns showed similar pattern of activity towards all tested substrates; 1) both purified GSTs were active towards EA, CDNB, and DCNB and 2) both purified GSTs were not active towards

PBO, BSP, NBC, and NCA. These substrates with differential specificity are commonly used for identification of the GST multigene family, such as DCNB, PBO and BSP are specific substrate for GST mu class and NBC for GST theta class.

Interestingly, both have captured a band of EA-active GSTs which at 26 kDa. EA was found to be the best substrate with the specific activity of 12.66±1.09 μmol/min/mg and 9.97±1.06 μmol/min/mg for GSH-agarose (C_3) and GSTrap^{TM} HP, respectively. The band at 26 kDa resolved into six similar spots on 2DE gel electrophoresis for both GSTrap^{TM} HP and GSH-agarose (C_3) columns, which indicated as spot # 1, 2, 3, 4, 5 and 6 in Figure 5.5 [C]. Four isoforms of GSTs, spots 1, 2, 3 and 4 were separated at almost equal distance on the 2DE gel, with estimated isoelectric points in range of 4.5 to 6.0. These indicated that purified GSTs from both column (spots # 1, 2, 3, and 4) probably belong to class pi since EA is specific substrate for GST class Pi. These isoforms seemed to be similar to those from *M. edulis* GST1 (Fitzpatrick et al., 1995) and GSTs from *A. striata* (Yang et al., 2004) in certain aspects such as at lower molecular weight, strong enzymatic activity for EA but very little activity towards DCNB and at acidic pI protein. The above-mentioned features were encountered in pi-class GSTs which was in accordance with the acidic pI of the Pi class isoenzymes and the relatively low MW of identified subunits. As mentioned in literature review, most of the GSTs isolated from marine organisms were encountered in Pi-class GSTs which in good agreement with this study. The evidence for Pi-class GSTs has been obtained in clam, *Venerupis philippinarum* (Xu et al., 2010), freshwater bivalves, *U. tumidus* and *C. fluminea,* (Doyen et al., 2005) and freshwater clam *Corbicula fluminea* (Vidal et al, 2002). Morever, the GST related Pi class not only discovered in most aquatic invertebrates but also in aquatic vertebrates such as fish (Pe´rez-Lo´pez et al., 2000).

However, there are exemption for two isoforms which were migrated at basic pI protein, spot 5 and spot 6 at pI value of 8.3 and 9.5, respectively (Figure 5.6). This finding was inconsistent with previous study which most of the purified GSTs from bivalve were found in acidic pI protein via direct purification method. But interestingly, Kim et al. (2009) who used molecular approach discovered GSTs from specific tissues of the Antartic bivalve, *Laternulla elliptica* was Pi class and basic pI protein with the predicted isoelectric point 8.3.

The additional band appeared on GSTrap^{TM} HP at 27 kDa displayed no activity towards other substrates such as PBO, NBC, NCA and BSP. This indicates that those GSTs are not participating in direct detoxification catalysis. This band comprised of four additional isoforms (spot # 7, 8, 9 and 10 on Figure 5.5[B]) which were neutral protein in range of pI value 6.0 to 7.0 (Figure 5.6). The extra isoforms at higher molecular weight presumably act as structural GSTs with non catalytic function or GSH-binding protein which possessing only GSH binding properties. This discovery is in line with Fitzpatrick et al., 1995, who succeeded to purify GST-like protein at higher molecular weight of subunit than GST. Apart from enzymatic functions, the structural GSTs serve as intracellular carrier proteins or ligandins. Due to their abundance in cells and binding properties, they mediate the intracellular storage and transport of hormones, metabolites, drugs and a great variety of other hydrophobic non-substrate compounds (Dirr et al., 1994). Another possible reason is that the proteins have GSH conjugation activity with other substrates that were not utilised in this study. Therefore, it is suggested that the extra isoforms should be tested with other substrates such as 3-(ρ-nitophenoxy) propane (EPNP) for GST theta, 7-chloro-4-nitrobenzo-2-oxa-1,3-diazole (NBD-Cl) for GST alpha and others in future studies.

Confirmation of the predicted Pi class GSTs and GSH binding protein can be identified using MALDI TOF-TOF mass spectrometer. Generated mass spectra of the peptides from MALDI TOF-TOF mass spectrometer were used for searching in a non-redundant NCBI database. Several databases were referred to identify the purified GSTs from both affinity matrices. The prime database utilized in this study was Profound which uses the Bayesian theory for protein identification as the search engine due to the fact Profound is established for its reliability to identify proteins compared to any other Peptide Mass Fingerprinting (PMF) search algorithms. Besides, it can provide the best discrimination between random matches and correct identification (Chamrad et al., 2004).

Unfortunately, none of the protein spots matched with the Profound databases. All of the unmatched monoisotopic peptides genenerated from MALDI-TOF were submitted to FindPept, PepIdent, MOWSE, MS-Fit and XProteo softwares. However, the generated monoisotopic peptides did not match with all databases mentioned. Sheehan and McDonagh (2008) highlighted the difficulty in bivalve proteins identification thus may be the main reason behind the failure in generating a significant score for peptide mapping and identification even though all spots obtained in this study produced good MALDI-TOF spectra result.

There may be several reasons contributing to this occurrence. First, information concerning marine invertebrate GSTs is relatively less documented and is very limited in the current databases. This is contrast with GSTs subunits of vertebrate species which is well studied and documented. There are very few aquatic GSTs have been fully characterized as the full complement of GSTs has not been studied in marine organisms

up to date. Thus, the results from partially characterized GSTs only bring additional confusion to the classification attempts.

In fact, it is challenging to assign classes of marine GSTs because the ambiguous and contradictory data are often obtained using the existing standard classification procedure (Blanchette et al., 2007). Hence, there is urgency to study and document a fully characterized marine GST. In order to develop a new classification for marine organism GSTs, several aspects should be considered, such as a set of complete sequence data to support results from other important properties such as substrate specificities test, immunological analysis, three dimensional structures prediction and biological functions studies.

Furthermore, the expression of mussel GST activity was reported to be different among varied tissues, which was explained by the tissue-specific expression of different GST isoenzymes (Yang et al., 2004). Therefore, present investigation of purified GSTs from the global GST activity may not represent the actual molecular events. Other than that, previous studies showed that there were different GSTs in different species. The *in vitro* study on bivalve GSTs in molecular genetics level expanded the classification of GSTs which were encountered into mu and theta GST (Whalen et al, 2008), rho and sigma class GST (Park et al., 2009).

Therefore, based on our current findings and data supported with previous literatures made by other scholars, it is assumed that unidentified proteins obtained in this study are Pi-class GSTs and GSH-binding proteins. Six isoforms labeled as spot 1, 2, 3, 4, 5 and 6 while the remaining four labeled as spot 7, 8, 9 and 10 are predicted belongs to Pi-class GSTs and GSH-binding proteins, respectively.

The results presented probably unraveled the classification and characterization of GSTs present in the *O. orbiculata*. The study has a big potential to be extended and further analysed through different approach to overcome the drawbacks. The purified GSTs can be further investigated by using immunological analysis, which is widely applied in addition for fully characterized GSTs (Vidal et al., 2002; Hoarau et al., 2002). This technique use antibodies which are very specific to one class of GST and are utilized to distinguish GSTs from a wide range of organisms. The immunological cross reactivity may produce helpful information for the classification of marine GSTs eventhough antibodies made against mammalian GSTs may not cross react toward marine GSTs. In fact, despite the characterisation of marine GSTs based on the mammalian GSTs criterion with consideration of divergent properties, certain marine GSTs may belong to different classes.

In the moment, there is no doubt that whole genome sequence of *O. orbiculata* will assist in better characterization, revealing the range of GST genes existing in the genome and perhaps providing the information about gene expression regulation. Thus, the N-terminal amino acid sequence analysis is the best choice. GSTs are well conserved at their N-termini, but are diverse at their C-termini (Blanchette et al., 2007). The deduced N-terminal amino acid sequencing of expressed GSTs would provide important information in the search for homology with other aquatic GSTs. The conserved N-terminal region can be used to obtain DNA sequences for different classes of GSTs from the *O. orbiculata*. This approach has been used to study individual GSTs from *Laternula elliptica* (Park et al., 2009). More extensive and successful *de novo* sequencing of individual *O. orbiculata* isoforms would be useful to support the characterisation presented in this work. The complete development of genetic database

will lead to GST transcriptome analysis which useful to understand gene expression pattern and gene functions.

Hopefully that current finding will be beneficial for the future study to get more comprehension on *O. orbiculata* GSTs. Implementation of local bivalves GSTs as biomarker is expected to be very attractive but more detailed research must be carried out to get better comprehension, especially on interaction between pollutants and GSTs expression as an attempt to for future promising application. Chronopoulou and Labrou (2009) reported the patents related GSTs and their application in plant biotechnology, medicine and analytical biotechnology. Recently, the selected isoenzymes of GSTs originated from mammalian, bacteria, plant, fungi and insects have successfully applied in the production of biosensors for direct monitoring of environmental pollutants, such as herbicides and insecticides. Thus the potential applications are very significant to be extensively studied and investigated on GSTs from bivalves' species.

CHAPTER 7

CONCLUSION

The aim of this study to isolate and purify GSTs from *Orbicularia orbiculata* has been achieved successfully using two different agarose matrices, GSTrap^{TM} HP and GSH-agarose (C_3) column. This study discovered *O. orbiculata* GSTs have enzymatic activity towards CDNB, DCNB and EA, but not active towards BSP, PBO, NBC and NCA. Even though no significant score for peptide mapping, it is assumed that GSTs obtained in this study are belonging to pi-class which has been recorded in other bivalves' species previously. Several exciting results obtained during this study are worthy of note. It is interesting that *O. orbiculata* GSTs behave differently towards GSTrap^{TM} HP and GSH-agarose (C3), which more classes were recovered on GSTrap^{TM} HP, in consistent with previous studies that obtained more specific classes by using GSH-agarose (C3). Based on the overall results, it can be concluded that there are six isoforms GSTs and four isoform of GSH binding protein in *O. orbiculata*. There is high possiblity that the six isoforms appeared on both 2-DE gels at the size of 26kDa are belonged to pi-class GSTs due to an extensive EA activity. Meanwhile the four additional spots at 27kDa on GSTrap^{TM} HP are belonged to GSH-binding protein due to no differences in substrate specificities assay. This assumption is based on the current result obtained from SDS-PAGE, 2-DE, IEF gel, and substrate specificity assays studies. However, further analysis need to be carried out in order to strengthen and validate the current findings.

APPENDICES

APPENDIX A - Buffer Solution Preparation

Homogenising Buffer

To prepare 50 ml homogenizing buffer, 0.019 g of EDTA, 0.0008 g DTT, 500 µl Protease Inhibitor Cocktail and a half a spatula of PTU were added in a beaker and dissolved in 50 ml eluting buffer.

Eluting Buffer – 25 mM Sodium Phosphate Buffer, pH 7.4

3 g of NaH_2PO_4 was dissolved in approximately 900 ml of dH_2O. The pH of the solution was adjusted to 7.35 at 20°C and the volume was made up to 1000 ml.

Buffer A – 0.1 M Sodium Phosphate Buffer, pH 6.5

12 g of NaH_2PO_4 was dissolved in approximately 900 ml of dH_2O. The pH was adjusted to 6.5 at 20°C and the volume was made up to 1000 ml.

Buffer B – 0.1 M Tris Buffer, pH 9.0

12.114 g Tris base was dissolved in approximately 900 ml dH_2O. The pH was adjusted to 9.0 at 20°C and the volume was made up to 1000 ml.

Buffer C – 0.1 M Sodium Phosphate Buffer, pH 7.5

12 g of NaH_2PO_4 was dissolved in approximately 900 ml of dH_2O. The pH of the solution was adjusted to 7.5 at 20°C and the volume was made up to 1000 ml.

APPENDIX B – Bradford Reagent for Protein Determination

Bradford Reagent (Spector, 1978)

Coomassie Brilliant Blue G-250 (100 mg) was dissolved in 50 ml 95% ethanol. To this solution 100 ml 85% (w/v) phosphoric acid was added. The resulting solution was diluted to a final volume of 1 liter with dH_2O. The solution was stirred overnight and filtered (Whatman No.1) before used.

APPENDIX C- Laemmli Discontinous SDS Polyacrylamide Gel Electrophoresis

10% (w/v) SDS.

100 g SDS was dissolved in 50 ml deionized water with gentle shaking. Then the volume was made 100 ml.

Resolving Gel (0.375 M Tris-HCl, pH 8.8

To prepare 10 ml of 12% gel : 4.0 ml 30% Acrylamide/Bis, 2.5 ml 1.5 M Tris-HCl, pH 8.8, 0.1 ml 10% SDS, 3.35 ml deionized water, 0.005 ml TEMED and 0.05 ml 10% APS was mixed gently and poured into the electrophoresis plates. All the ingredients except TEMED and APS were combined and degassed using sonicator for at least 3 minutes. The polymerization was initiated by addition of TEMED and APS followed by gentle swirling for complete mixing.

Stacking Gel (0.125 M Tris-HCl, pH 6.8)

To prepare 10 ml of 4 % gel : 1.33 ml 30% Acrylamide/Bis, 2.5 ml 0.5 M Tris-HCl, pH 6.8, 0.1 ml 10% SDS, 6.1 ml deionized water, 0.01 ml TEMED and 0.05 ml 10% APS was mixed gently and poured into the electrophoresis plates. All the ingredients except TEMED and APS were combined and degassed using sonicator for at least 3 minutes. The polymerization was initiated by addition of TEMED and APS followed by gentle swirling for complete mixing.

Overlay solution

The solution was 200 µl of 0.1% (w/v) SDS solution, 100 µl of 10% (w/v) SDS was mixed with 900 µl dH_2O.

Electrophoresis (Running) Buffer

Stock of Invitrogen 10X Tris/Glycine/SDS buffer was used and diluted to the final concentration of 1X.

SDS Sample Buffer

To prepare a buffer solution of 10 ml, 1.25 ml of 0.5 M Tris-HCl, pH 6.8, 2.5 ml glycerol, 2.0 ml 10% (w/v) SDS, 0.5 ml 0.5% (w/v) bromophenol blue and 3.55 ml deionized water were mixed. 0.5 ml β-mercapthoethanol was added 9.5 ml sample buffer prior to use. The protein sample was prepared by diluting the sample at least 1:4 ratios with sample buffer and then heated at 95°C for 4 minutes.

APPENDIX D – Reagents for Proteome Analysis

DryStrip Rehydration Solution

The solution consisted of 8M urea, 0.15% Dithiothreitol (DTT), 30 mM Thiourea, 2% Biolyte/ Pharmalyte/Ampholyte, pH 3-10, 2% (w/v) CHAPS and traces of bromophenol blue (BPB). To prepare 1 ml of the solution; 0.48 g of urea was dissolved in 400 µl dH_2O completely. Then 0.02 g of CHAPS, 0.0015 g DTT, 0.0017 g thiourea and 20 µl Biolyte were added and vortexed to dissolve. The solution was level 1 ml with deionized water. The rehydration solution was prepared freshly once needed.

Equilibration Solution

The equilibration buffer consisted 1.5 M Tris-HCl pH 8.8, 6 M urea, 30% (v/v) glycerol and 2% (w/v) sodium dodecyl sulfate (SDS). To prepare 20 ml of the buffer, 7.2 g of urea was dissolved in 7 ml dH_2O. Then 0.67 ml Tris-HCl, 6.9 ml of glycerol and 0.4 g SDS were dissolved and the solution was then made up to 20 ml with dH_2O. The equilibration buffer was divided into two, 10 ml for each tube and known as equilibration solution I and II. 25 mg of DTT was added into the equilibration solution I, meanwhile 0.45 g of iodoacetamide and traces of BPB was added into equilibration solution II.

Agarose Sealing Solution.

0.5 g agarose and traces of bromophenol blue were added into 100 ml of SDS electrophoresis buffer and swirled to disperse. The mixture was heated in a microwave until agarose was completely melted.

APPENDIX E – Reagent for Gel Staining

Silver Staining

Fixation solution in 100 ml: 12 ml of acetic acid was added into 50 ml of methanol and 47.5 µl of formaldehyde. The final volume was topped up with deionized water.

Washing solution in 100 ml: 35 ml of ethanol was added into 65 ml of deionized water.

Sensitizing solution in 100 ml: 0.025 g of sodium thiosulfate was added to a small volume of deionized water and mixed well. The solution was brought to the final volume of 100 ml.

Staining solution in 100 ml: 0.2 g of silver nitrate was added into a small amount of deionized water and 72 µl of formaldehyde was added. The solution was dissolved and made up to final volume with deionized water.

Developing solution in 100 ml: 6 g of sodium carbonate was added into a small amount of deionized water and dissolved. 2 ml of the sensitizing solution (sodium thiosulfate) and 47.75 µl of formaldehyde were then added and made up to the final volume with deionized water.

Terminating solution in 100 ml: 12 ml of acetic acid was added into 50 ml methanol. Both were mixed well and were topped up to the final volume with deionized water.

APPENDIX F – Substrate Preparation and Enzyme Assay Condition

1-Chloro-2,4-dinitrobenzene (CDNB)

2.85 ml Buffer A, 0.05 ml of sample, 0.05 ml 60 mM (0.0553 g in 3 ml Buffer A) GSH and 0.05 ml 60 mM (0.2430 g in 20 ml ethanol) CDNB were mixed. Change of absorbance at 340 nm was recorded for 6 minutes. Molar absorption coefficient, ξ_m is 9600 $L.mol^{-1}.cm^{-1}$.

1,2-Dichloro-4-nitrobenzene (DCNB)

2.80 ml Buffer B, 0.10 ml sample, 0.05 ml 240 mM (0.2212 g in 3 ml Buffer A) GSH and 0.05 ml 24 mM (0.092g in 20 ml ethanol) DCNB were mixed. Change of absorbance at 344 nm was recorded for 30 minutes. Molar absorption coefficient, ξ_m is 8400 $L.mol^{-1}.cm^{-1}$.

p-Nitrobenzyl chloride (NBC)

2.60 ml Buffer A, 0.1 ml sample, 0.25 ml 60 mM GSH and 0.05 ml 60 mM (0.2058 g in 20 ml ethanol) NBC were mixed. Change of absorbance at 310 nm was recorded for 10 minutes. Molar absorption coefficient, ξ_m is 1900 $L.mol^{-1}.cm^{-1}$.

Sulfobromophthalein (BSP)

2.60 ml Buffer C, 0.1 ml sample, 0.25 ml 60 mM GSH and 0.05 ml 2 mM (0.0334 g in 20 ml ethanol) BSP were mixed. Change of absorbance at 330 nm was recorded for 10 minutes. Molar absorption coefficient, ξ_m is 4500 $L.mol^{-1}.cm^{-1}$.

Ethacrynic Acid (EA)

2.8 ml Buffer A, 0.1 ml sample, 0.05 ml 15 mM (0.0138 g in 3 ml Buffer A) GSH and 0.05 ml 12 mM (0.0727 g in 20 ml ethanol) EA were mixed. Change of absorbance at 270 nm was recorded for 10 minutes. Molar absorption coefficient, ξ_m is 5000 $L.mol^{-1}.cm^{-1}$.

Trans-4-phenyl-3-butene-2-one (PBO)

2.8 ml Buffer A, 0.1 ml sample, 0.05 ml 15 mM GSH and 0.05 ml 3 mM (0.0876 g in 20 ml ethanol) PBO were mixed. Change of absorbance at 290 nm was recorded for 10 minutes. Molar absorption coefficient, ξ_m is - 24800 $L.mol^{-1}.cm^{-1}$.

Nitrocinnamaldehyde (NCA)

2.85 ml Buffer A, 0.05 ml of sample, 0.05 ml 60 mM (0.0553 g in 3 ml Buffer A) GSH and 0.05 ml 24 mM NCA were mixed. Change of absorbance at 340 nm was recorded for 6 minutes. Molar absorption coefficient, ξ_m is - 3200 $L.mol^{-1}.cm^{-1}$.

APPENDIX F – Enzyme Assay Condition and Parameters for Substrate Specificity

Substrates	Concentration		Buffer	Molar extinction coefficient ($M^{-1}cm^{-1}$)	Absorbance at wavelength (nm)	Reference
	Substrate (mM)	GSH (mM)				
1-chloro-2,4-nitrobenzene	1	1	A	9600	340	Habig et al., 1974
1,2-Dichloro-4-nitrobenzene	0.4	4	B	8400	344	Motoyama and Dauterman, 1977
p-nitrobenzyl chloride	1	5	A	1900	310	Habig et al., 1974
Ethacryanic acid	0.2	0.25	A	5000	270	Habig et al., 1974
Trans-4-phenyl-3-butene-2-one	0.05	0.25	A	-24800	290	Habig et al., 1974
Nitrocinnamaldehyde	0.4	1	A	-3200	360	Widersten et al., 1996
Sulfobromophthalein	0.03	5	C	4500	330	Zazali Alias, 2006

Buffer A = 0.1 M Phosphate, pH 6.5

Buffer B = 0.1 M Tris, pH 9.0

Buffer C = 0.1 M Phosphate, pH 7.

APPENDIX G – Standard Curve for Protein Content

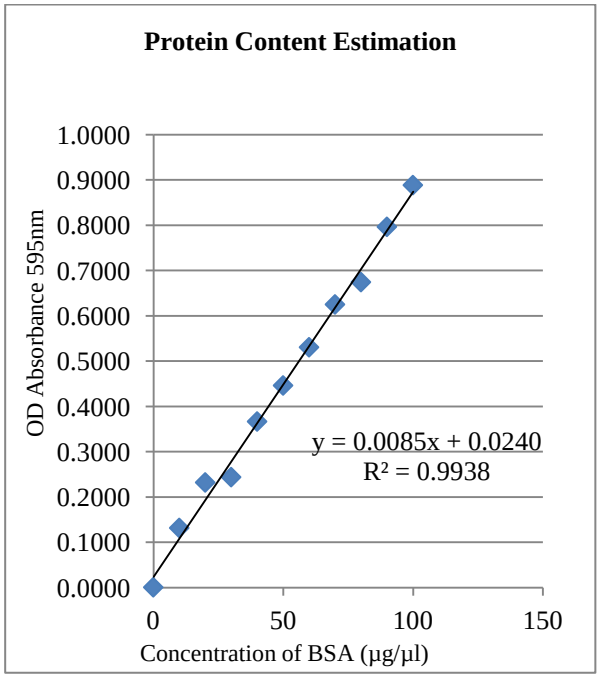

concentration BSA (µg/µl)	abs 1	abs 2	Average abs
0	0.0012	0.0008	0.0010
10	0.1282	0.1357	0.1320
20	0.2301	0.2347	0.2324
30	0.2242	0.2640	0.2441
40	0.3513	0.3825	0.3669
50	0.4299	0.4628	0.4464
60	0.5225	0.5390	0.5308
70	0.5949	0.6556	0.6253
80	0.6732	0.6760	0.6746
90	0.8133	0.7799	0.7966
100	0.8945	0.8828	0.8887

APPENDIX H - Molecular Weight Determination

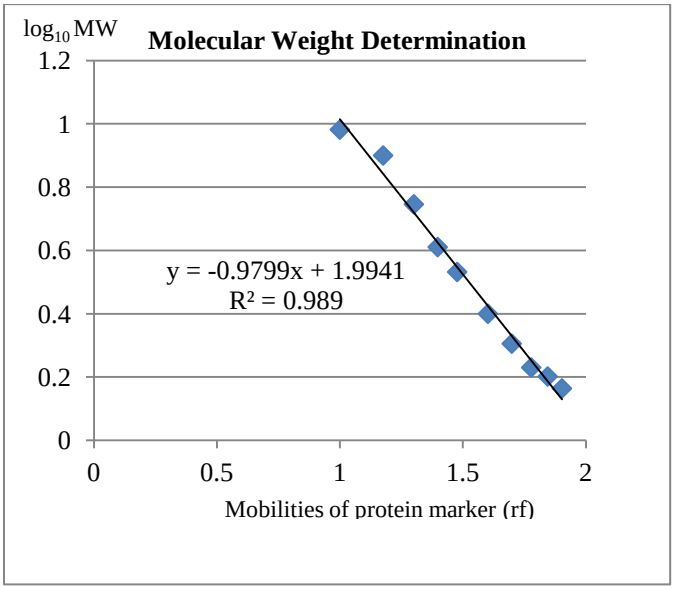

MW protein marker	$\log_{10}$ MW	Mobilities of protein marker (rf)
10	1	0.981130667
15	1.17609	0.89934
20	1.30103	0.745266667
25	1.39794	0.610036667
30	1.4771	0.531446667
40	1.60206	0.399363333
50	1.69897	0.30502
60	1.77815	0.22954
70	1.84509	0.20126
80	1.90309	0.1635

Calculation of bands:-

Band	Curve 1	Curve 2	Curve 3	Average	Rounded
band 1	27.2	26.95	26.71	26.95	27
band 2	26.6	26.39	26.16	26.38	26

APPENDIX I – PROTEIN IDENTIFICATION (MALDI-TOFF ANALYSIS)

Spot 1 as illustrated in Figure 5.3.3

COM=Project: Proteomics, Spot Set: Proteomics\110117, Label: #1, Spot Id: 37877, Peak List Id: 84820, MS Job Run Id: 11316

805.46814	4004.6643
806.14087	3276.2229
855.08563	4930.5483
856.07831	3780.1448
860.55615	4004.8
873.08746	3485.7451
906.5575	5493.2197
988.64166	3090.7368
1044.1198	7750.7383
1118.5844	8084.9658
1179.6782	5715.834
1235.6077	3837.2405
1300.116	8593.0273
1308.7468	6605.5874
1320.6775	5425.9038
1353.7322	3704.9019
1475.874	3660.7932
1493.8378	4971.0786
1791.8469	3390.1963
2163.2268	3921.0784

BEGIN IONS
PEPMASS=805.46814
CHARGE=1+

TITLE=Label: #1, Spot_Id: 37877, Peak_List_Id: 85581, MSMS Job_Run_Id: 11317, Comment:

112.11627	351.48401
129.14021	181.43748
157.13719	129.99394
158.1384	242.53285
159.12151	147.58638
175.15791	1578.4945
202.12419	131.06055
230.16769	381.22318
244.20799	131.16745
245.18378	356.276
258.18555	173.86446
262.2038	717.77704
269.19937	392.62805
299.19888	631.55408
317.21021	1240.9691
322.25381	1004.0972
359.24603	1518.4559
376.27499	416.41534
402.31769	386.19308
412.30292	739.4967
415.30017	397.22662
437.30579	445.76291
472.34598	553.01019
489.39499	330.68332
526.37384	350.08829
573.18146	521.52814
576.43616	344.32434
614.28369	573.78369
615.19659	431.32938
617.17664	5163.7632
628.51172	558.86371
647.46802	341.60718
656.51648	447.28851
673.56476	799.73376
674.54407	2420.9307
760.5304	405.87036
764.39606	649.87097
765.42621	258.85748
775.53809	1043.1473
784.60577	388.19559

END IONS

BEGIN IONS
PEPMASS=855.08563
CHARGE=1+

TITLE=Label: #1, Spot_Id: 37877, Peak_List_Id: 85583, MSMS Job_Run_Id: 11317, Comment:

322.24326	158.66661
477.04071	101.83389
621.11041	242.25026
622.11041	320.68903
623.09418	1116.2751
664.1911	266.58481
665.16443	389.94122
666.10895	2600.5598
667.09857	1234.6578
668.09607	536.53418
792.55725	352.05667
809.23303	334.49762
810.20764	454.7832
811.16046	2742.2588
812.13721	1514.9734
814.09833	335.55383

END IONS
BEGIN IONS
PEPMASS=860.55615
CHARGE=1+

TITLE=Label: #1, Spot_Id: 37877, Peak_List_Id: 85582, MSMS Job_Run_Id: 11317, Comment:

175.15413	206.96268
244.22099	532.2627
416.28619	155.82947
433.31781	287.55356
442.33838	126.67823
445.2988	126.4271
459.30545	163.19945
487.32544	493.8053
504.35724	168.29254
572.43933	227.56291
581.11365	335.4805
582.09729	107.88824
589.4447	355.65125
600.42737	395.72006
617.45453	558.91663

623.14746 770.88031
624.1701 356.97778
626.11127 255.12643
666.17773 704.69495
667.17505 976.00006
668.15857 1127.8743
670.12311 561.5412
732.53973 2295.2849
798.58594 533.11682
811.23663 1283.981
812.25311 1626.1001
813.22552 740.44135
814.20856 1589.6631
816.17279 598.74365
END IONS

BEGIN IONS
PEPMASS=873.08746
CHARGE=1+

TITLE=Label: #1, Spot_Id: 37877, Peak_List_Id: 85577, MSMS Job_Run_Id: 11317, Comment:
175.15994 163.40845
400.30664 180.19041
432.2966 161.28313
433.28687 263.63
442.33319 1169.7804
460.34671 137.81267
571.40344 354.8508
588.43567 212.25046
589.41431 445.36523
638.14331 452.24774
640.12079 719.98828
682.13934 2480.2744
684.1153 2259.0105
686.11243 425.6922
717.50165 520.31464
718.47748 520.12109
727.51898 901.30438
811.16913 1036.4485
827.22528 1420.0874
829.1629 942.41119
831.56805 613.02502
832.56018 885.57532
END IONS

BEGIN IONS
PEPMASS=982.49933
CHARGE=1+

TITLE=Label: #1, Spot_Id: 37877, Peak_List_Id: 85571, MSMS Job_Run_Id: 11317, Comment:
112.11108 386.41083
129.14021 197.23116
157.13422 101.65405
158.12292 185.99352
175.14795 690.44421
272.18832 211.93869
289.2056 101.54356
329.21329 234.40358
343.2077 125.11557
346.24316 172.63298
386.24295 259.31107
403.2652 308.16507
443.27176 412.69519
500.28253 493.31299
517.31927 279.05667
557.33252 582.25562
574.34357 374.21088
661.40283 389.52832
835.4892 363.13055
938.49939 512.85083
952.53784 646.1532
END IONS

BEGIN IONS
PEPMASS=988.64166
CHARGE=1+
TITLE=Label: #1, Spot_Id: 37877, Peak_List_Id: 85575, MSMS Job_Run_Id: 11317, Comment:
86.115547 230.14706
101.09101 155.38965
112.11472 449.40442
129.13477 165.91701
157.13512 102.17963
158.13217 192.57384
175.14821 2960.8142
215.18098 187.75104
216.14699 112.74232
230.15283 147.43423
271.22559 498.06891
272.19553 276.61731
288.24255 498.23065
325.23892 435.0155
343.26202 288.03271
359.24469 364.96707
384.31616 390.54456
386.24362 214.82484
401.34882 350.55353
430.30768 497.27292
457.28336 345.64886
472.38037 592.76184
475.30069 438.92807
487.33542 207.3996
499.33127 399.47134
517.3584 410.01077
559.4397 510.01489
570.38464 1129.1875
588.39081 1250.0638
646.50153 276.60199
701.48846 448.06366
943.65442 316.52634
944.68689 1660.5076
947.61743 420.92099
958.68115 491.80234
964.67206 582.76727
END IONS

BEGIN IONS
PEPMASS=1044.1198
CHARGE=1+

TITLE=Label: #1, Spot_Id: 37877, Peak_List_Id: 85588, MSMS Job_Run_Id: 11317, Comment:
175.15588 201.37256
811.16882 516.78589
812.1684 147.51183
827.64136 192.34677
854.22339 269.11972
855.16742 848.07031
856.17065 2685.7246
858.15833 369.86255
1000.252 102.42664
END IONS

BEGIN IONS
PEPMASS=1065.5798
CHARGE=1+

TITLE=Label: #1, Spot_Id: 37877, Peak_List_Id: 85574, MSMS Job_Run_Id: 11317, Comment:
86.124054 147.02776
112.12109 289.66641
129.1386 282.09692
175.15956 1655.8429
200.14508 132.35638
215.18666 214.80309
244.18594 159.81619
258.18225 127.99968
262.19043 281.1091
272.21152 226.09932
346.27393 707.46307
359.23788 292.42865
385.3172 356.33197
390.29663 1148.7925
402.35959 2042.627
435.30652 251.92088
443.35046 345.32208
448.25305 256.39063
459.3772 379.35596
489.36255 486.18301
500.38962 448.92908
517.37585 271.71182
574.42981 391.33527
577.34412 523.83832
607.34918 768.75537
618.46014 1520.3257
659.49585 389.47443
692.44714 223.60014
703.47021 275.94049
720.45325 594.70911
791.50751 443.6745
866.60059 335.9866
873.21539 882.06903
877.1709 588.60004
1016.7837 590.36786
1021.6437 963.18134
1023.6306 368.70926
END IONS
BEGIN IONS
PEPMASS=1107.6094
CHARGE=1+

TITLE=Label: #1, Spot_Id: 37877, Peak_List_Id: 85572, MSMS Job_Run_Id: 11317, Comment:
112.10123 160.79916
129.13219 118.01694
175.144 1512.5405
200.13083 617.70013
286.18576 309.96854
293.16647 142.67033
303.21732 307.20609
331.27411 151.21609
340.20264 174.44547
357.24167 356.15515
363.21106 306.56842
374.2608 455.13083
387.20621 119.31187
390.25903 327.77008
422.21707 714.61694
470.34644 176.91083
487.37079 1032.2078
492.29456 440.74777
533.26105 305.59964
537.34558 322.02133
550.30652 228.71048
616.43774 758.91718
621.35059 1290.0618
661.40076 515.00159
692.46869 405.35849
706.44244 301.85074
723.44617 243.09015
734.45569 439.86154
774.45801 454.00214
918.1156 418.0415
920.06384 219.14944
1042.6809 5097.0303
END IONS

BEGIN IONS
PEPMASS=1118.5844
CHARGE=1+

TITLE=Label: #1, Spot_Id: 37877, Peak_List_Id: 85589, MSMS Job_Run_Id: 11317, Comment:
272.21741 653.61395
437.31235 169.72893
458.31372 145.60748
586.396 127.50912
661.3584 152.46913
681.38586 386.647
723.45911 208.18782
810.50549 1073.8293
818.47345 139.4353
819.47278 182.98584
847.45178 909.45251
925.53284 366.11307
1070.1642 264.11288
1076.6274 178.45572
END IONS

BEGIN IONS
PEPMASS=1179.6782
CHARGE=1+

TITLE=Label: #1, Spot_Id: 37877, Peak_List_Id: 85586, MSMS Job_Run_Id: 11317, Comment:

112.12241	124.47714
175.15134	368.2843
232.17923	111.36675
286.19363	106.0063
293.15564	162.12427
303.22845	215.09409
371.2471	123.28239
387.27829	122.84453
404.29245	254.69409
422.23221	591.04333
500.36023	161.29001
517.3656	182.34213
535.32434	397.5
552.36646	132.53816
614.4566	154.94484
645.46057	166.98552
663.40149	349.53195
758.57446	482.17133
887.62878	448.29236
1135.7201	435.86023
1136.7198	259.92096

END IONS

BEGIN IONS
PEPMASS=1235.6077
CHARGE=1+

TITLE=Label: #1, Spot_Id: 37877, Peak_List_Id: 85580, MSMS Job_Run_Id: 11317, Comment:

112.10715	336.82877
129.12843	202.10468
175.14841	1690.4266
262.20349	117.90209
288.24786	227.9794
359.2897	215.85301
373.20053	125.80206
406.24988	124.41633
458.36365	500.4288
489.35376	201.4743
503.29352	367.21268
520.32184	215.79298
572.36084	125.56172
587.43488	259.19162
616.3916	186.21539
664.38641	158.36812
666.38043	267.15289
684.45361	205.12282
701.49695	578.08331
723.42987	332.65848
740.41473	160.82953
827.47876	229.40611
914.54901	170.84924
1190.7542	223.80957
1191.6544	656.54675
1193.6652	364.59824
1199.6962	190.42975
1202.7776	332.38345
1205.6335	610.0661
1214.736	329.87344

END IONS

BEGIN IONS
PEPMASS=1300.116
CHARGE=1+

TITLE=Label: #1, Spot_Id: 37877, Peak_List_Id: 85590, MSMS Job_Run_Id: 11317, Comment:

175.15144	308.67648
288.24753	106.66667
338.22943	1501.4237
453.27014	141.86276
489.24652	200.89754
692.45227	228.7972
706.46637	167.62994
812.48553	730.02832
1212.2408	701.15082
1233.8403	556.96802
1254.2402	1872.7667
1256.1932	14874.214

END IONS

BEGIN IONS
PEPMASS=1308.7468
CHARGE=1+

TITLE=Label: #1, Spot_Id: 37877, Peak_List_Id: 85587, MSMS Job_Run_Id: 11317, Comment:

175.16054	494.95099
243.19209	143.02582
303.26025	280.50372
338.25381	248.75648
400.30508	233.43384
417.33832	214.7757
530.41895	623.0141
535.32495	106.68107
659.49152	1853.7977
757.53961	187.36842
774.52856	485.75311
779.47107	172.57571
790.53094	189.71671
1256.3026	1798.8571
1258.3141	479.15094
1259.3452	520.71747

END IONS

BEGIN IONS
PEPMASS=1320.6775
CHARGE=1+

TITLE=Label: #1, Spot_Id: 37877, Peak_List_Id: 85585, MSMS Job_Run_Id: 11317, Comment:

175.15851	179.37442
338.24173	303.59134
627.37897	117.99779
1164.6697	265.62283
1252.8323	3369.2366
1256.7322	271.03668
1259.8573	2244.887
1300.3049	605.42468

END IONS

BEGIN IONS
PEPMASS=1353.7322
CHARGE=1+

TITLE=Label: #1, Spot_Id: 37877,
Peak_List_Id: 85579, MSMS Job_Run_Id:
11317, Comment:
112.1087 103.91589
175.15125 975.75427
278.14282 122.05882
288.25217 403.82297
360.23022 123.34441
385.27158 396.98642
402.31287 2904.0779
474.29889 121.92664
475.263 356.45184
478.32202 238.52713
499.34174 123.48512
500.32614 176.55423
517.37524 344.29315
589.32343 265.32492
664.45294 3823.72
702.42957 213.61671
762.47754 260.47595
779.48511 165.47156
859.54309 763.04926
876.56738 873.98248
973.62048 478.6571
990.62543 234.16522
1183.8025 326.80795
1309.7964 333.90048
END IONS

BEGIN IONS
PEPMASS=1475.874
CHARGE=1+

TITLE=Label: #1, Spot_Id: 37877,
Peak_List_Id: 85578, MSMS Job_Run_Id:
11317, Comment:
175.14424 256.7157
429.27408 145.41573
464.32666 810.16309
489.38251 285.4166
588.46234 311.67825
716.52716 304.76434
830.61249 436
871.5304 159.55081
888.57684 500.27341
958.71344 172.09715
959.65137 145.42688
987.65186 592.21228
1086.7739 215.07664
1100.7474 184.76712
1215.8226 217.96092
1319.8528 326.42905
1431.8875 431.50659
1433.8752 206.85486
END IONS

BEGIN IONS
PEPMASS=1493.8378
CHARGE=1+
TITLE=Label: #1, Spot_Id: 37877,
Peak_List_Id: 85584, MSMS Job_Run_Id:
11317, Comment:
400.29736 146.10281
545.39429 243.45967
657.43127 118.88477
728.52234 117.88682
986.71106 212.66043
1365.8706 2039.6951
END IONS

BEGIN IONS
PEPMASS=1791.8469
CHARGE=1+

TITLE=Label: #1, Spot_Id: 37877,
Peak_List_Id: 85576, MSMS Job_Run_Id:
11317, Comment:
112.11716 148.72549
175.14949 290.4902
319.215 123.74479
560.3407 169.23755
577.3407 225.89056
797.47137 180.53265
854.48694 152.42882
894.52075 148.62209
911.52911 228.02261
1038.5719 100.17605
1226.7302 213.39572
1743.9532 352.51315
1749.0031 235.58145
1761.8972 566.6499
END IONS

BEGIN IONS
PEPMASS=2384.1035
CHARGE=1+

TITLE=Label: #1, Spot_Id: 37877,
Peak_List_Id: 85573, MSMS Job_Run_Id:
11317, Comment:
112.11206 256.41241
175.15002 240.04903
346.22327 137.37671
403.23706 226.42157
460.26657 224.75137
517.32367 300.9541
557.3045 112.41428
574.3407 409.01001
661.375 221.24854
701.3869 248.38101
718.39954 455.38101
881.50842 483.45154
968.57764 279.87671
1025.5869 200.61383
1082.6039 326.09131
1122.5873 200.76791
1139.6809 597.93384
1226.6998 288.64572
1266.733 240.59653
1283.7352 426.51498

1446.8191 399.25266
1533.8965 297.93442
1677.932 247.20995
1734.941 258.63107
2335.2844 239.15067
2336.2241 218.59018
2348.1909 201.3521
2354.1636 817.9126
END IONS

Spot 2 as illustrated in Figure 5.3.3

COM=Project: Proteomics, Spot Set: Proteomics\110117, Label: #2, Spot Id: 37878, Peak List Id: 84821, MS Job Run Id: 11316
805.46027 1509.1096
856.56335 1695.9904
860.54858 1933.2865
864.50671 1506.7313
906.55139 2327.7412
935.57697 1362.0927
988.63153 2182.8525
1016.6258 1326.7332
1043.6031 1294.554
1107.6069 1553.4851
1155.6292 1337.0773
1300.1041 1724.183
1317.6979 1620.123
1353.7228 3314.2634
1379.6743 1376.4329
1464.8512 1906.3726
1590.7437 1383.8236
1663.9406 1334.2786
1791.8297 1467.653
2163.198 3827.9409

BEGIN IONS
PEPMASS=805.46027
CHARGE=1+

TITLE=Label: #2, Spot_Id: 37878, Peak_List_Id: 85603, MSMS Job_Run_Id: 11317, Comment:
112.12069 113.18542
175.1636 437.10226
262.21399 249.89067
299.21167 179.06279
315.22452 118.36441
317.20728 268.194
359.25031 452.90201
412.31076 171.00092
430.31879 109.45824
526.37567 152.98811
573.18182 218.27011
615.21478 184.52776
616.1983 221.0242
617.17999 2209.97
651.3443 196.44067
674.54321 810.24585
760.61847 225.51598
761.54382 180.71149
765.43188 342.16656
775.53662 351.48721
END IONS

BEGIN IONS
PEPMASS=860.54858
CHARGE=1+

TITLE=Label: #2, Spot_Id: 37878, Peak_List_Id: 85608, MSMS Job_Run_Id: 11317, Comment:
244.21298 234.03909
433.31424 130.25954
487.33676 242.81764
563.46704 242.97583
617.46631 218.05994
650.15125 158.35263
666.16614 321.70703
668.19275 336.21991
670.11926 331.27426
672.1488 348.22336
732.54694 888.56091
798.61292 309.79068
811.27985 320.06714
812.26349 336.51965
814.23535 328.66684
814.66602 369.12405
839.66791 419.21832
END IONS

BEGIN IONS
PEPMASS=935.57697
CHARGE=1+
TITLE=Label: #2, Spot_Id: 37878, Peak_List_Id: 85599, MSMS Job_Run_Id: 11317, Comment:
175.15662 348.18564
579.42212 308.48166
775.49707 262.29199
894.51337 253.20348
END IONS

BEGIN IONS
PEPMASS=982.49426
CHARGE=1+

TITLE=Label: #2, Spot_Id: 37878, Peak_List_Id: 85591, MSMS Job_Run_Id: 11317, Comment:
175.15923 122.36975
272.21606 225.63953
835.49048 1732.8676
940.57092 344.64008
952.5224 388.94168
END IONS

BEGIN IONS
PEPMASS=988.63153
CHARGE=1+

TITLE=Label: #2, Spot_Id: 37878, Peak_List_Id: 85609, MSMS Job_Run_Id: 11317, Comment:
175.14932 671.17798
271.22366 168.49258
288.25272 131.02563
384.33005 144.50121

472.39407 132.45107
570.3692 318.82169
588.42316 230.83661
944.67731 723.70172
958.65839 158.94394
END IONS

BEGIN IONS
PEPMASS=1016.6258
CHARGE=1+

TITLE=Label: #2, Spot_Id: 37878,
Peak_List_Id: 85596, MSMS Job_Run_Id:
11317, Comment:
242.20206 331.68408
269.18109 115.30709
325.21729 124.00537
398.23962 141.75896
430.36096 164.66411
497.32941 143.95091
514.33624 159.80148
526.28607 228.38879
544.41705 894.50104
811.5686 323.22034
886.66516 212.47237
887.66278 382.93613
888.59027 164.50415
903.65033 867.83423
942.71631 261.03091
971.64111 256.63629
END IONS

BEGIN IONS
PEPMASS=1043.6031
CHARGE=1+

TITLE=Label: #2, Spot_Id: 37878,
Peak_List_Id: 85595, MSMS Job_Run_Id:
11317, Comment:
175.15717 424.78983
369.21338 192.34843
370.28818 112.60648
387.23596 372.58789
399.31467 132.5231
416.34412 110.15327
480.34183 139.95514
500.32504 176.60472
556.4292 130.72385
785.59149 504.77917
811.17334 587.0835
854.19379 379.7525
855.17072 1218.5166
856.17529 3840.6216
914.66522 315.28265
917.62958 494.47659
995.70245 145.84093
998.68982 286.09625
999.69257 160.83215
1000.2126 194.40488
1003.6948 885.44391
END IONS

BEGIN IONS
PEPMASS=1107.6069
CHARGE=1+

TITLE=Label: #2, Spot_Id: 37878,
Peak_List_Id: 85604, MSMS Job_Run_Id:
11317, Comment:
175.14297 170
487.38126 130.39244
621.33038 209.3494
917.1358 141.24881
1064.656 258.09042
END IONS

BEGIN IONS
PEPMASS=1155.6292
CHARGE=1+

TITLE=Label: #2, Spot_Id: 37878,
Peak_List_Id: 85598, MSMS Job_Run_Id:
11317, Comment:
547.31311 101.41483
562.38623 240.87524
565.30994 151.24638
571.43359 1792.0817
583.35236 106.23678
594.37354 254.85236
734.51843 229.64888
1008.6335 238.72469
1113.6851 1242.9908
END IONS

BEGIN IONS
PEPMASS=1272.6598
CHARGE=1+

TITLE=Label: #2, Spot_Id: 37878,
Peak_List_Id: 85592, MSMS Job_Run_Id:
11317, Comment:
380.28397 103.33526
509.32639 206.34705
638.40363 292.3891
767.46448 532.89423
898.5365 495.99445
1026.6486 614.64172
1030.6248 276.99136
1141.6528 704.87262
1229.7686 263.65002
END IONS

BEGIN IONS
PEPMASS=1300.1041
CHARGE=1+

TITLE=Label: #2, Spot_Id: 37878,
Peak_List_Id: 85606, MSMS Job_Run_Id:
11317, Comment:
692.44464 183.46786
706.45398 131.30257
1212.2075 204.41966
1233.8243 309.41473
1254.2628 634.14227
1256.1895 4909.5142
END IONS

BEGIN IONS
PEPMASS=1317.6979
CHARGE=1+

TITLE=Label: #2, Spot_Id: 37878,
Peak_List_Id: 85605, MSMS Job_Run_Id:
11317, Comment:
727.52649 147.45055
842.53766 444.92139
1042.6687 164.94951
1131.7325 565.32233
END IONS

BEGIN IONS
PEPMASS=1325.674
CHARGE=1+

TITLE=Label: #2, Spot_Id: 37878,
Peak_List_Id: 85593, MSMS Job_Run_Id:
11317, Comment:
517.29633 201.44781
599.41779 152.40457
774.42694 116.49458
842.6347 476.50266
1096.6604 1917.0282
1131.7828 489.00967
1212.6526 980.95721
1263.8192 703.1004
1283.7534 387.47958
END IONS

BEGIN IONS
PEPMASS=1353.7228
CHARGE=1+

TITLE=Label: #2, Spot_Id: 37878,
Peak_List_Id: 85610, MSMS Job_Run_Id:
11317, Comment:
175.1479 211.86275
288.25497 105.98039
402.31369 573.23535
664.44897 705.11407
859.53595 171.89439
876.57458 141.4086
END IONS

BEGIN IONS
PEPMASS=1379.6743
CHARGE=1+

TITLE=Label: #2, Spot_Id: 37878,
Peak_List_Id: 85600, MSMS Job_Run_Id:
11317, Comment:
1292.7595 225.77203
END IONS

BEGIN IONS
PEPMASS=1464.8512
CHARGE=1+

TITLE=Label: #2, Spot_Id: 37878,
Peak_List_Id: 85607, MSMS Job_Run_Id:
11317, Comment:
806.50787 152.68298
1308.8602 345.78946
1422.9321 203.6855
END IONS

BEGIN IONS
PEPMASS=1537.8142
CHARGE=1+

TITLE=Label: #2, Spot_Id: 37878,
Peak_List_Id: 85594, MSMS Job_Run_Id:
11317, Comment:
514.35767 247.9091
756.55566 123.35104
1409.9052 225.3186
1493.842 161.11925
END IONS

BEGIN IONS
PEPMASS=1590.7437
CHARGE=1+

TITLE=Label: #2, Spot_Id: 37878,
Peak_List_Id: 85601, MSMS Job_Run_Id:
11317, Comment:
1427.7809 401.70529
END IONS

BEGIN IONS
PEPMASS=1663.9406
CHARGE=1+

TITLE=Label: #2, Spot_Id: 37878,
Peak_List_Id: 85597, MSMS Job_Run_Id:
11317, Comment:
1508.0009 818.45978
1603.0262 583.20563
1621.9939 650.13336
END IONS

BEGIN IONS
PEPMASS=1791.8297
CHARGE=1+

TITLE=Label: #2, Spot_Id: 37878,
Peak_List_Id: 85602, MSMS Job_Run_Id:
11317, Comment:
1628.8853 445.56451
1749.9554 124.7194
1761.8889 109.29909
END IONS

Spot 3 as illustrated in Figure 5.3.3

COM=Project: Proteomics, Spot Set:
Proteomics\110117, Label: #3, Spot Id: 37879,
Peak List Id: 84822, MS Job Run Id: 11316
805.4649 4122.1021
806.14594 5675.3608
832.3689 3817.4077
855.0899 8351.5586
856.08191 4584.5273
860.55542 25547.039

864.51318 4673.7036
873.0863 4737.6553
906.55835 5590.8633
935.5885 19694.613
988.63837 30377.242
1044.1311 9853.7617
1300.119 9096.4111
1353.7389 46082.355
1424.8251 6818.2544
1456.8236 7990.7842
1609.9104 7746.5688
1724.0248 5696.0781
1995.1688 3393.6272
2163.2544 7071.5688

BEGIN IONS
PEPMASS=806.14594
CHARGE=1+

TITLE=Label: #3, Spot_Id: 37879, Peak_List_Id: 85618, MSMS Job_Run_Id: 11317, Comment:
112.11248 120.49789
175.14977 672.81836
230.15208 245.99908
245.1666 210.60493
262.19708 400.84506
299.1944 388.1167
315.23651 173.6992
317.20386 640.56232
342.20728 159.94193
359.2341 752.23621
376.25018 216.81232
384.29095 158.75473
402.30435 261.62546
412.29578 442.25296
430.31839 184.34637
472.32718 288.88593
489.35034 183.36526
559.38153 149.70464
573.15417 642.67743
576.41559 212.14314
615.21191 495.35004
616.17065 284.37347
617.15729 5420.2021
760.54608 313.96185
762.24567 629.54364
763.52008 232.24188
775.52185 519.69867
END IONS

BEGIN IONS
PEPMASS=855.0899
CHARGE=1+

TITLE=Label: #3, Spot_Id: 37879, Peak_List_Id: 85624, MSMS Job_Run_Id: 11317, Comment:
322.25226 112.69043
622.10986 264.90317
623.0885 865.33612
664.1875 379.14771
665.20752 259.36707
666.10364 2370.6382
667.11188 730.51672
668.07837 464.06808
809.19373 346.83713
810.16766 495.57324
811.15326 1503.7113
812.14642 1596.4863
END IONS

BEGIN IONS
PEPMASS=860.55542
CHARGE=1+
TITLE=Label: #3, Spot_Id: 37879, Peak_List_Id: 85628, MSMS Job_Run_Id: 11317, Comment:
244.21794 1013.3854
348.23746 140.41614
357.31015 255.14932
416.2933 210.58441
433.30582 607.34503
445.28494 154.36826
487.32999 1008.9297
504.37088 344.02158
532.38672 154.41862
572.42719 378.24411
589.45325 555.13519
600.42389 628.16541
617.45404 911.20056
623.16144 214.83963
624.19348 114.89825
635.44727 183.9884
666.17358 281.18915
667.18005 429.00842
668.20111 504.7171
670.1781 329.44321
714.52759 316.6174
732.53613 4355.7832
811.2406 550.76459
812.26807 479.33994
813.25751 445.88464
814.2085 448.07828
816.16846 307.86786
END IONS

BEGIN IONS
PEPMASS=873.0863
CHARGE=1+

TITLE=Label: #3, Spot_Id: 37879, Peak_List_Id: 85617, MSMS Job_Run_Id: 11317, Comment:
175.16463 105.85068
638.13269 173.3857
640.11682 497.10672
682.14178 1248.1929
684.11383 1524.0078
811.17877 629.45502
827.20624 857.81445
829.17096 645.0954
END IONS

BEGIN IONS
PEPMASS=896.51422

CHARGE=1+
TITLE=Label: #3, Spot_Id: 37879, Peak_List_Id: 85614, MSMS Job_Run_Id: 11317, Comment:
175.15794 125.96097
365.25098 316.66922
504.37839 211.79359
528.35461 306.24246
532.37946 282.04956
585.37006 635.58508
698.48291 558.46863
704.19299 489.30396
706.1283 586.49548
799.5498 425.61838
831.63855 579.51776
851.17719 305.12006
END IONS

BEGIN IONS
PEPMASS=921.54126
CHARGE=1+

TITLE=Label: #3, Spot_Id: 37879, Peak_List_Id: 85616, MSMS Job_Run_Id: 11317, Comment:
127.11756 450.68628
175.16039 114.20242
256.17844 243.33737
333.25977 350.29413
351.2851 205.34315
369.28851 145.46698
426.3215 900.87427
495.25992 188.44829
496.34488 349.43784
553.38763 931.34387
561.41498 456.66385
566.29852 427.60297
589.41498 954.78705
662.39954 144.66577
666.4906 638.4184
679.39056 550.73468
730.06195 600.32294
732.09808 307.18738
775.51544 376.09921
874.13147 168.79628
875.15283 544.43439
876.65552 287.4505
877.1272 179.90401
880.08899 163.81757
END IONS

BEGIN IONS
PEPMASS=935.5885
CHARGE=1+

TITLE=Label: #3, Spot_Id: 37879, Peak_List_Id: 85627, MSMS Job_Run_Id: 11317, Comment:
84.107895 188.66177
112.11856 198.21803
129.13733 285.78433
175.15973 1586.5557
228.21431 150.64471
242.20345 156.74254
268.20374 111.4696
286.20599 718.91583
293.17883 231.99719
303.2392 326.80774
339.26865 121.86801
357.2836 459.13098
382.28308 140.31435
399.31442 378.97153
406.27405 128.72267
416.34091 302.41785
449.28891 479.91827
492.37775 251.26486
520.37451 423.41629
534.38367 331.64954
562.40002 451.45386
579.44537 1828.9183
605.46539 318.50354
633.47882 310.13565
708.48071 218.33081
779.59119 161.59523
819.57318 162.40175
891.6424 152.7442
893.62146 190.07176
END IONS

BEGIN IONS
PEPMASS=969.68445
CHARGE=1+

TITLE=Label: #3, Spot_Id: 37879, Peak_List_Id: 85613, MSMS Job_Run_Id: 11317, Comment:
175.14973 688.43079
271.20782 177.15686
288.25214 117.01825
305.11365 179.96652
322.23837 208.62721
359.29288 173.04805
370.29706 131.49776
384.31769 162.26228
682.53638 155.66168
721.36688 278.46088
726.41534 1472.736
728.4021 573.73785
800.55292 484.81583
926.53827 345.64142
END IONS

BEGIN IONS
PEPMASS=988.63837
CHARGE=1+

TITLE=Label: #3, Spot_Id: 37879, Peak_List_Id: 85629, MSMS Job_Run_Id: 11317, Comment:
86.114868 144.21568
101.09467 204.55882
112.11345 207.68423
129.14616 125.31805
158.12418 118.48052
175.14967 2696.1262
227.23149 126.60364

230.15906 126.478
246.16208 196.37256
271.2229 657.85791
288.25052 567.87878
325.23428 353.34879
343.2576 235.66339
359.24216 359.83545
374.21948 256.25275
384.32965 443.34521
401.35352 268.51776
430.29593 326.1633
457.2735 331.24576
459.32529 145.78613
472.3869 620.24066
475.28412 389.49292
487.33365 197.78992
499.34793 390.01886
517.35681 245.77052
542.40607 268.62238
559.43622 439.46552
560.42676 305.77505
570.37604 946.7616
588.39746 1243.9811
646.4906 438.90451
683.51239 191.57585
701.50635 237.0453
774.56836 252.02353
944.68842 1849.2957
958.67773 526.08411
END IONS

BEGIN IONS
PEPMASS=1044.1311
CHARGE=1+

TITLE=Label: #3, Spot_Id: 37879, Peak_List_Id: 85626, MSMS Job_Run_Id: 11317, Comment:
811.18811 305.63483
854.28278 331.02533
855.20349 635.52771
856.17926 2244.8635
858.16583 429.4826
1000.2467 206.88957
END IONS

BEGIN IONS
PEPMASS=1225.6987
CHARGE=1+

TITLE=Label: #3, Spot_Id: 37879, Peak_List_Id: 85612, MSMS Job_Run_Id: 11317, Comment:
266.20758 204.60675
379.29626 173.66876
494.36212 383.92615
551.42053 102.68147
604.40326 313.97363
622.43427 564.76154
732.47913 1741.7738
736.49139 531.67291
847.51837 909.29578
851.54437 1237.0277
922.61926 279.50385
950.63318 1325.4248
960.62305 1647.464
1079.6824 1263.6372
1088.7441 867.40057
1097.6982 608.96216
1161.7642 583.01141
END IONS

BEGIN IONS
PEPMASS=1300.119
CHARGE=1+

TITLE=Label: #3, Spot_Id: 37879, Peak_List_Id: 85625, MSMS Job_Run_Id: 11317, Comment:
692.4624 195.14569
1067.1521 299.47253
1111.1661 274.85641
1112.142 171.32265
1212.2203 771.10815
1216.7823 405.58524
1254.2522 2594.9072
1256.2134 17005.393
END IONS

BEGIN IONS
PEPMASS=1353.7389
CHARGE=1+

TITLE=Label: #3, Spot_Id: 37879, Peak_List_Id: 85630, MSMS Job_Run_Id: 11317, Comment:
70.086014 104.70589
112.11288 266.43726
129.1349 120.14706
136.10501 164.709
158.1234 150.18814
175.1443 2541.2197
201.14932 118.89912
213.11475 148.23328
271.20807 121.05755
278.1489 243.13773
288.24292 1116.9119
346.22116 193.04387
360.20792 248.36238
364.22003 191.29022
365.19598 259.46317
377.22003 207.59178
385.27576 987.15686
402.30002 8985
433.28363 145.57092
474.27216 174.17436
475.24911 1205.4795
478.30194 722.95502
490.28415 274.9429
499.3429 290.69095
500.31155 573.84259
517.34039 863.80383
544.28198 203.64499
572.27869 229.41658
589.30597 902.8172
647.40088 329.70065

664.43542 12218.266
673.39221 328.67307
674.41931 343.22241
690.42889 277.79095
702.42664 578.88947
761.45154 258.87497
762.4563 611.56421
779.4928 441.0098
816.4801 286.664
841.51373 264.93463
859.51788 2245.7825
876.55438 2670.2529
973.58398 1326.8813
990.60046 559.54382
1153.679 446.65106
1179.7253 304.38055
1240.7227 206.76003
1311.7804 334.9697
1323.7638 336.32654
END IONS

BEGIN IONS
PEPMASS=1424.8251
CHARGE=1+

TITLE=Label: #3, Spot_Id: 37879,
Peak_List_Id: 85620, MSMS Job_Run_Id:
11317, Comment:
329.19855 168.26422
591.3949 908.42194
607.34698 520.30585
678.42688 140.99716
706.41968 310.9733
719.51471 737.80615
818.59143 303.98868
933.64014 191.08681
1278.7552 138.38719
END IONS

BEGIN IONS
PEPMASS=1456.8236
CHARGE=1+

TITLE=Label: #3, Spot_Id: 37879,
Peak_List_Id: 85623, MSMS Job_Run_Id:
11317, Comment:
591.41809 157.80202
719.5235 110.07407
END IONS

BEGIN IONS
PEPMASS=1545.9001
CHARGE=1+

TITLE=Label: #3, Spot_Id: 37879,
Peak_List_Id: 85611, MSMS Job_Run_Id:
11317, Comment:
175.14491 246.41971
322.22522 1375.3097
402.29346 114.39682
437.26642 116.45103
468.30554 127.43826
636.44 119.59443
737.4635 1153.1791
1144.7316 219.17346
1161.7455 786.55725
1362.1351 808.53479
END IONS

BEGIN IONS
PEPMASS=1609.9104
CHARGE=1+

TITLE=Label: #3, Spot_Id: 37879,
Peak_List_Id: 85622, MSMS Job_Run_Id:
11317, Comment:
322.22595 1472.0588
720.43732 105.59163
737.46002 1127.3691
852.51508 101.57839
1161.7434 253.84331
1225.7579 523.90375
1475.8907 427.19577
1501.9559 140.80878
1503.9384 191.83293
1518.9733 331.28235
1545.0768 120.85025
1545.9915 15967.226
END IONS

BEGIN IONS
PEPMASS=1724.0248
CHARGE=1+

TITLE=Label: #3, Spot_Id: 37879,
Peak_List_Id: 85619, MSMS Job_Run_Id:
11317, Comment:
865.63184 229.38287
1033.7297 1177.7355
1104.7607 207.1171
1191.8136 255.51616
END IONS

BEGIN IONS
PEPMASS=1995.1688
CHARGE=1+

TITLE=Label: #3, Spot_Id: 37879,
Peak_List_Id: 85615, MSMS Job_Run_Id:
11317, Comment:
886.61493 262.65839
933.58185 100.9801
950.59424 1179.4115
1113.6602 122.05873
1200.7721 455.35806
1315.7452 200.87509
1542.0105 179.58817
1690.1036 177.22394
1754.0873 504.9314
1931.254 2544.7234
END IONS

BEGIN IONS
PEPMASS=2163.2544
CHARGE=1+

TITLE=Label: #3, Spot_Id: 37879, Peak_List_Id: 85621, MSMS Job_Run_Id: 11317, Comment:

780.53381	235.37477
855.52698	280.31604
909.59631	284.84702
954.69208	167.78941
1023.6644	232.68179
1080.6965	889.23907
1083.7034	165.17302
1209.7756	947.44904
1291.8638	127.06745
1308.8308	731.87964
1407.9607	178.48856
1521.9741	536.61285
1635.1174	184.27141
1749.1425	228.78786

END IONS

Spot 4 as illustrated in Figure 5.3.3

COM=Project: Proteomics, Spot Set: Proteomics\110117, Label: #4, Spot Id: 38022, Peak List Id: 84893, MS Job Run Id: 11316

805.47925	4731.2129
906.5777	4331.4717
987.66071	4440.0493
1058.6506	4024.3164
1154.7393	4770.4326
1190.7169	5167.3438
1191.6971	4327.8833
1220.7303	5516.8267
1269.7871	3722.5491
1319.783	5820.3374
1557.9313	6129.9106
1621.9379	13712.255
1963.1873	5261.4766
2027.2057	16258.824
2163.2678	11819.117
2273.365	6168.1978
2289.4021	6014.8101
2868.5608	12097.715
2882.5901	26898.922
2896.5999	3583.9072

BEGIN IONS
PEPMASS=805.47925
CHARGE=1+

TITLE=Label: #4, Spot_Id: 38022, Peak_List_Id: 86854, MSMS Job_Run_Id: 11317, Comment:

112.11397	184.56233
129.14351	116.31546
158.12149	108.16402
175.15108	722.33319
230.14928	212.88573
245.16589	160.45929
262.20013	583.61737
299.18872	391.11581
315.22354	205.94949
317.20474	699.09918
341.23151	129.97701
342.20575	192.66766
359.23285	843.84747
376.26392	238.78235
402.31195	284.37802
412.28979	356.70218
430.31039	264.31534
472.3324	288.93002
489.37247	151.65045
542.36334	144.26622
559.3783	189.40727
573.17352	127.45363
617.15399	1271.6309
619.16534	143.92104
647.43958	168.9268
763.4978	322.29169
775.52655	416.86539

END IONS

BEGIN IONS
PEPMASS=987.66071
CHARGE=1+

TITLE=Label: #4, Spot_Id: 38022, Peak_List_Id: 86853, MSMS Job_Run_Id: 11317, Comment:

260.25085	107.9902
325.26276	103.1293
343.26846	101.76471
373.3486	523.09344
386.28735	278.02008
401.25488	198.89482
412.32025	114.97057
430.3208	174.06363
444.40286	801.5686
499.38257	246.6601
502.3194	444.67188
514.35687	121.8074
526.3653	194.00154
544.39081	279.20633
558.46515	648.63788
587.42291	404.34186
597.43848	429.16629
598.41974	351.13928
615.43323	3351.7207
645.51642	978.94824
683.48547	274.08398
700.54321	413.70407
710.52948	440.95569
711.50592	311.61288
728.53949	1735.5842
773.59399	574.73511
826.70184	482.2045
841.64459	309.11349
857.63776	190.68356
874.64868	499.01776
940.84326	450.96408
965.82526	423.12582

END IONS

BEGIN IONS
PEPMASS=1026.64
CHARGE=1+

TITLE=Label: #4, Spot_Id: 38022, Peak_List_Id: 86847, MSMS Job_Run_Id: 11317, Comment:

266.19974	274.22797
288.24844	143.14893
379.30634	277.31644
476.34879	109.78394
494.35028	732.00195
533.39856	1024.5679
551.38647	159.52852
648.42365	1048.5187
652.45459	165.25769
680.44934	1115.8953
722.49042	214.87297
761.52814	2210.3909
781.51245	819.70416
852.59088	553.13916
862.55859	388.1481
880.59607	1467.6483
889.65259	1012.1033
898.62415	375.94739
982.69183	277.62125

END IONS

BEGIN IONS
PEPMASS=1058.6506
CHARGE=1+

TITLE=Label: #4, Spot_Id: 38022, Peak_List_Id: 86852, MSMS Job_Run_Id: 11317, Comment:

228.22485	101.74182
301.20773	176.34883
372.33182	1237.5743
387.24893	181.16023
471.42609	258.38486
483.30554	159.47491
501.31638	313.39944
552.33954	120.10827
558.47418	305.39005
570.35492	572.77185
588.35352	735.49146
659.44617	225.84772
669.43079	570.47314
672.54285	321.90845
687.44476	211.17532
858.6424	172.6929
873.16168	109.51491
912.65424	183.57913
929.67285	213.1564

END IONS

BEGIN IONS
PEPMASS=1107.671
CHARGE=1+

TITLE=Label: #4, Spot_Id: 38022, Peak_List_Id: 86850, MSMS Job_Run_Id: 11317, Comment:

129.12578	203.36519
175.15852	102.78338
372.3237	1032.7847
387.22891	593.07971
471.40689	249.19598
478.34946	115.52362
522.31628	105.72455
532.32819	149.18819
550.32764	384.74649
555.33734	122.0827
558.4613	319.68375
619.36896	586.69128
637.34674	510.57019
718.45062	469.08041
721.54047	225.19702
919.12573	273.45914
1042.691	859.09167
1066.1953	207.90756

END IONS

BEGIN IONS
PEPMASS=1154.7393
CHARGE=1+

TITLE=Label: #4, Spot_Id: 38022, Peak_List_Id: 86855, MSMS Job_Run_Id: 11317, Comment:

266.2041	108.9019
312.22089	100.44118
359.33328	102.23683
394.32825	109.52934
425.32181	142.7215
507.44577	348.76169
517.39984	120.76515
533.39148	608.7251
565.33838	234.59045
571.45844	2469.1101
583.34784	188.84477
622.49524	1092.1001
648.44684	690.97693
679.49658	240.48448
734.55267	321.14932
761.54907	1019.8089
808.57996	739.49988
821.60681	292.97495
889.66602	1482.4115
894.54022	349.08258
909.6546	522.85089
979.68622	219.04008
980.70129	196.81941
990.71381	207.85123
1008.7224	1204.6486
1026.7489	1275.4075
1117.7317	173.00116

END IONS

BEGIN IONS
PEPMASS=1190.7169
CHARGE=1+
TITLE=Label: #4, Spot_Id: 38022, Peak_List_Id: 86856, MSMS Job_Run_Id: 11317, Comment:

400.25098	110.41262
509.36017	641.63678
525.36005	149.60884
553.36334	262.44363
638.45551	187.62231

666.47198 396.79053
683.41571 142.8107
695.46161 205.64171
792.54498 939.02759
830.52295 374.15765
858.54761 194.40085
892.60559 1447.2054
896.57538 162.53197
901.55884 245.78105
906.58899 341.81265
1063.6329 111.29156
1077.7523 307.71838
END IONS

BEGIN IONS
PEPMASS=1220.7303
CHARGE=1+

TITLE=Label: #4, Spot_Id: 38022, Peak_List_Id: 86858, MSMS Job_Run_Id: 11317, Comment:
553.37274 327.23593
555.38086 189.79044
560.36646 134.77055
640.43713 106.83189
666.46619 375.64661
668.44916 214.52289
725.47559 141.73235
888.57831 309.30908
892.59491 1922.6937
924.57172 245.1467
1020.731 162.74741
1046.7358 158.58318
1074.7303 120.62621
1107.7355 274.58197
END IONS

BEGIN IONS
PEPMASS=1269.7871
CHARGE=1+

TITLE=Label: #4, Spot_Id: 38022, Peak_List_Id: 86851, MSMS Job_Run_Id: 11317, Comment:
266.20514 121.72808
390.29608 184.37502
494.3591 396.97263
590.44781 270.79782
680.43628 660.04755
763.51385 248.72287
776.53503 1460.0011
781.50848 514.37195
852.58997 329.75183
862.56537 191.07671
880.60468 1421.1807
891.58942 698.38843
1004.689 1264.0146
1008.7109 744.07056
1123.7621 1377.8546
1132.8021 737.82239
1141.7568 915.17487
1225.8462 200.9901
END IONS

BEGIN IONS
PEPMASS=1319.783
CHARGE=1+

TITLE=Label: #4, Spot_Id: 38022, Peak_List_Id: 86859, MSMS Job_Run_Id: 11317, Comment:
792.5517 715.20258
811.53247 222.55489
906.58929 292.86752
958.64728 314.42099
1029.7126 299.3595
1078.6938 166.60118
1191.7909 262.84488
1259.8496 129.26408
END IONS

BEGIN IONS
PEPMASS=1397.8999
CHARGE=1+

TITLE=Label: #4, Spot_Id: 38022, Peak_List_Id: 86848, MSMS Job_Run_Id: 11317, Comment:
507.42682 119.11822
526.37012 290.39377
616.4093 246.73909
622.48151 349.48407
639.45062 120.45686
776.55463 853.47217
808.56323 383.3071
850.55804 533.87769
889.5921 364.12057
891.6087 622.33478
909.63489 287.57861
1004.7068 376.03088
1008.7279 579.99121
1132.8093 520.5152
1136.8229 431.29919
1251.8866 954.11346
1269.9022 1091.7502
1330.9432 338.90741
1331.9583 106.57333
1336.8676 268.9122
END IONS

BEGIN IONS
PEPMASS=1557.9313
CHARGE=1+

TITLE=Label: #4, Spot_Id: 38022, Peak_List_Id: 86861, MSMS Job_Run_Id: 11317, Comment:
288.24323 306.76471
685.46802 191.24269
1173.842 131.09726
1423.9586 124.22653
1494.0271 3665.4617
1497.8456 293.52957
END IONS

BEGIN IONS
PEPMASS=1605.9407

CHARGE=1+

TITLE=Label: #4, Spot_Id: 38022, Peak_List_Id: 86849, MSMS Job_Run_Id: 11317, Comment:

175.14966	128.11658
288.23691	876.17651
685.49097	124.48622
733.45087	445.56088
749.45502	231.18996
1157.8508	161.17029
1221.7679	373.72571
1471.9645	240.78053
1515.0206	107.25012
1540.0197	1693.9922
1542.0181	12758.968
1546.9541	376.40079
1558.0314	109.73318
1563.9766	150.68297

END IONS

BEGIN IONS
PEPMASS=1621.9379
CHARGE=1+

TITLE=Label: #4, Spot_Id: 38022, Peak_List_Id: 86864, MSMS Job_Run_Id: 11317, Comment:

288.24951	516.83264
685.49774	133.10287
749.48108	424.95233
1237.786	254.84181
1487.9708	265.95001
1494.0693	2414.7017
1499.4166	910.85028
1515.9988	114.17338
1521.1798	220.62546
1531.0056	318.33417
1532.0076	138.6033
1540.0499	265.87225
1543.0718	228.19855
1558.0453	12782.766

END IONS

BEGIN IONS
PEPMASS=1963.1873
CHARGE=1+

TITLE=Label: #4, Spot_Id: 38022, Peak_List_Id: 86857, MSMS Job_Run_Id: 11317, Comment:

517.38513	416.71817
1330.921	101.62265
1478.0146	673.13831

END IONS

BEGIN IONS
PEPMASS=2027.2057
CHARGE=1+

TITLE=Label: #4, Spot_Id: 38022, Peak_List_Id: 86865, MSMS Job_Run_Id: 11317, Comment:

517.36304	707.23328
858.60028	127.38733
912.62524	111.82097
1302.8381	114.3364
1478.0015	319.85721
1541.9609	316.08371
1878.2374	132.12123
1962.308	104.35634
1963.3037	9177.6807
1968.1843	228.83243

END IONS

BEGIN IONS
PEPMASS=2163.2678
CHARGE=1+

TITLE=Label: #4, Spot_Id: 38022, Peak_List_Id: 86863, MSMS Job_Run_Id: 11317, Comment:

780.53528	243.28934
909.57422	155.17323
954.63428	112.99281
1023.6393	162.09059
1080.6887	753.82092
1209.7729	554.55725
1308.8492	467.17313
1407.9238	177.52971
1521.9834	309.74576
1749.1204	152.85545

END IONS

BEGIN IONS
PEPMASS=2273.365
CHARGE=1+

TITLE=Label: #4, Spot_Id: 38022, Peak_List_Id: 86862, MSMS Job_Run_Id: 11317, Comment:

722.40643	286.56781
1837.2451	281.39539
1838.078	221.64862
2225.439	116.74886

END IONS

BEGIN IONS
PEPMASS=2289.4021
CHARGE=1+

TITLE=Label: #4, Spot_Id: 38022, Peak_List_Id: 86860, MSMS Job_Run_Id: 11317, Comment:

1083.6797	135.3161
1853.3326	133.53636
1854.1493	143.45918
2225.499	1704.3879

END IONS

BEGIN IONS
PEPMASS=2882.5901
CHARGE=1+
TITLE=Label: #4, Spot_Id: 38022, Peak_List_Id: 86866, MSMS Job_Run_Id: 11317, Comment:

722.42303 965.25977
1022.5505 145.58807
1543.8904 476.43457
1907.139 237.4292
END IONS

Spot 5 as illustrated in Figure 5.3.3

COM=Project: Proteomics, Spot Set: Proteomics\110117, Label: #5, Spot Id: 37883, Peak List Id: 84826, MS Job Run Id: 11316
805.47461 7861.4126
832.3725 18705.863
834.37335 1996.7931
860.56842 5426.1353
906.57159 8879.0859
935.60504 3035.7842
1029.6816 7361.2744
1044.1177 1748.028
1069.599 1830.3494
1153.6589 4126.9468
1216.7964 1789.2157
1426.8484 7609.6519
1432.8325 1733.9745
1433.8334 6305.8354
1464.798 2039.9862
1501.8749 2462.7927
1624.9154 3307.2085
2163.2344 13229.412
2273.3491 2267.4644
2289.3247 2097.9988

BEGIN IONS
PEPMASS=805.47461
CHARGE=1+

TITLE=Label: #5, Spot_Id: 37883, Peak_List_Id: 85710, MSMS Job_Run_Id: 11317, Comment:
112.10772 101.68259
175.14905 508.84888
230.16 126.23785
245.17245 158.89766
262.19504 272.10785
299.17853 212.74989
317.20389 496.48438
342.21527 115.58224
359.23193 522.61444
376.23987 104.16878
402.30334 147.09999
412.2778 146.72025
430.3129 148.29164
472.33221 199.15413
489.36737 115.8951
614.24805 372.20996
617.15747 445.58157
757.48657 242.06372
775.50897 343.97009
END IONS

BEGIN IONS
PEPMASS=834.37335
CHARGE=1+

TITLE=Label: #5, Spot_Id: 37883, Peak_List_Id: 85703, MSMS Job_Run_Id: 11317, Comment:
398.27325 230.10771
575.43671 167.0533
608.46057 820.01373
632.42767 249.24478
643.22742 214.48001
644.17255 449.82236
645.13464 172.69009
646.40363 1023.8607
660.45197 351.76822
661.42023 136.48164
662.43274 728.21167
689.41101 155.02219
788.40527 222.03027
789.42291 215.60226
802.41022 253.32271
END IONS

BEGIN IONS
PEPMASS=855.11731
CHARGE=1+

TITLE=Label: #5, Spot_Id: 37883, Peak_List_Id: 85699, MSMS Job_Run_Id: 11317, Comment:
622.14801 221.14227
623.10852 280.56775
666.11975 1556.7957
667.15039 446.3703
811.16827 1077.1133
812.15405 398.47821
END IONS

BEGIN IONS
PEPMASS=860.56842
CHARGE=1+
TITLE=Label: #5, Spot_Id: 37883, Peak_List_Id: 85707, MSMS Job_Run_Id: 11317, Comment:
172.07549 103.04977
244.20419 313.09293
433.28671 179.71277
487.32004 193.42453
589.435 166.39525
617.453 232.25111
666.17029 1818.3365
667.20349 694.82404
668.20343 937.64392
669.22058 689.30475
670.20258 261.87183
672.12384 476.54755
676.05389 226.34497
732.51563 1218.0453
811.2533 1013.2021
813.23267 556.52936
814.29626 361.84543
END IONS

BEGIN IONS
PEPMASS=935.60504
CHARGE=1+

TITLE=Label: #5, Spot_Id: 37883, Peak_List_Id: 85705, MSMS Job_Run_Id: 11317, Comment:
175.14427 205.26956
579.42462 203.02185
END IONS

BEGIN IONS
PEPMASS=968.48602
CHARGE=1+

TITLE=Label: #5, Spot_Id: 37883, Peak_List_Id: 85693, MSMS Job_Run_Id: 11317, Comment:
305.11728 106.35769
721.38062 177.41899
726.39929 973.40771
728.39099 282.25443
END IONS

BEGIN IONS
PEPMASS=1029.6816
CHARGE=1+
TITLE=Label: #5, Spot_Id: 37883, Peak_List_Id: 85708, MSMS Job_Run_Id: 11317, Comment:
175.15875 459.95099
271.22464 110.93138
472.39832 213.57788
569.41949 159.2429
586.47089 143.71327
629.45398 362.47797
985.7605 563.64227
END IONS

BEGIN IONS
PEPMASS=1044.1177
CHARGE=1+

TITLE=Label: #5, Spot_Id: 37883, Peak_List_Id: 85700, MSMS Job_Run_Id: 11317, Comment:
855.19659 402.28339
856.1908 435.53378
857.21191 126.2579
END IONS

BEGIN IONS
PEPMASS=1069.599
CHARGE=1+

TITLE=Label: #5, Spot_Id: 37883, Peak_List_Id: 85702, MSMS Job_Run_Id: 11317, Comment:
494.34515 144.87517
595.41089 160.23083
776.4646 128.6394
877.22729 435.49423
879.18817 197.52658
END IONS

BEGIN IONS
PEPMASS=1095.6039
CHARGE=1+

TITLE=Label: #5, Spot_Id: 37883, Peak_List_Id: 85695, MSMS Job_Run_Id: 11317, Comment:
175.14238 170.21909
909.10089 319.35855
END IONS

BEGIN IONS
PEPMASS=1216.7964
CHARGE=1+
TITLE=Label: #5, Spot_Id: 37883, Peak_List_Id: 85701, MSMS Job_Run_Id: 11317, Comment:
1088.7814 908.034
END IONS
BEGIN IONS
PEPMASS=1301.8575
CHARGE=1+
TITLE=Label: #5, Spot_Id: 37883, Peak_List_Id: 85694, MSMS Job_Run_Id: 11317, Comment:
175.15184 158.77451
303.25208 219.95099
338.22818 147.62785
1254.2548 602.40894
1256.222 5283.7319
END IONS

BEGIN IONS
PEPMASS=1308.7518
CHARGE=1+

TITLE=Label: #5, Spot_Id: 37883, Peak_List_Id: 85692, MSMS Job_Run_Id: 11317, Comment:
175.15092 277.12842
303.2547 282.16183
659.47485 394.50436
774.52783 111.54783
1256.2729 1278.2411
1257.2814 966.01672
1263.7611 306.57187
END IONS

BEGIN IONS
PEPMASS=1399.8165
CHARGE=1+

TITLE=Label: #5, Spot_Id: 37883, Peak_List_Id: 85697, MSMS Job_Run_Id: 11317, Comment:
616.4068 198.73438
657.42609 303.01495
768.51959 212.23717
889.54633 186.41354
1334.8478 196.85614
1336.7603 137.55905
END IONS

BEGIN IONS
PEPMASS=1426.8484

CHARGE=1+
TITLE=Label: #5, Spot_Id: 37883, Peak_List_Id: 85709, MSMS Job_Run_Id: 11317, Comment:
175.15059 116.02941
368.26434 174.8609
506.25006 302.24011
515.36414 134.26146
619.3468 428.80145
732.42499 229.69498
1212.8444 503.43842
1366.8296 140.20979
END IONS

BEGIN IONS
PEPMASS=1501.8749
CHARGE=1+
TITLE=Label: #5, Spot_Id: 37883, Peak_List_Id: 85704, MSMS Job_Run_Id: 11317, Comment:
687.46771 606.0791
END IONS

BEGIN IONS
PEPMASS=1509.8472
CHARGE=1+
TITLE=Label: #5, Spot_Id: 37883, Peak_List_Id: 85696, MSMS Job_Run_Id: 11317, Comment:
669.3808 149.11636
687.49878 789.56708
END IONS

BEGIN IONS
PEPMASS=1624.9154
CHARGE=1+
TITLE=Label: #5, Spot_Id: 37883, Peak_List_Id: 85706, MSMS Job_Run_Id: 11317, Comment:
1337.9381 337.02893
1510.0203 384.54971
1563.0673 299.91125
END IONS

BEGIN IONS
PEPMASS=2225.1414
CHARGE=1+
TITLE=Label: #5, Spot_Id: 37883, Peak_List_Id: 85698, MSMS Job_Run_Id: 11317, Comment:
1142.6078 131.16101
END IONS

BEGIN IONS
PEPMASS=2274.3496
CHARGE=1+
TITLE=Label: #5, Spot_Id: 37883, Peak_List_Id: 85691, MSMS Job_Run_Id: 11317, Comment:
1186.6295 168.67824
1427.9116 277.0672
1657.019 414.55222
1837.1696 1037.3845
2225.4607 477.70871
END IONS

Spot 6 as illustrated in Figure 5.3.3

COM=Project: Proteomics, Spot Set: Proteomics\110117, Label: #6, Spot Id: 37884, Peak List Id: 84827, MS Job Run Id: 11316
805.44537 17883.271
832.34143 3770.0283
835.50983 3332.7375
860.52936 12948.169
906.53302 8892.4922
921.50201 1530.1835
935.56342 7903.5859
1029.641 18272.473
1046.6335 2119.5498
1145.6992 2616.8594
1153.6155 5715.459
1179.6415 1589.8945
1301.8054 5287.2725
1432.7982 3594.989
1450.833 1739.4526
1464.7719 2539.8894
1882.0326 1932.6251
2163.1387 9224.0205
2273.1997 2519.6079
2289.2498 1704.7816

BEGIN IONS
PEPMASS=805.44537
CHARGE=1+

TITLE=Label: #6, Spot_Id: 37884, Peak_List_Id: 85729, MSMS Job_Run_Id: 11317, Comment:
175.14694 156.18871
262.1882 115.73627
299.18393 130.73509
317.20764 218.80545
359.22168 256.55524
412.27402 142.8425
617.14331 282.07751
END IONS

BEGIN IONS
PEPMASS=835.50983
CHARGE=1+
TITLE=Label: #6, Spot_Id: 37884, Peak_List_Id: 85724, MSMS Job_Run_Id: 11317, Comment:
398.29269 503.42334
575.42889 358.39594
608.45648 1822.0308
643.33636 246.35715
644.19427 901.16882
646.38824 828.6344
662.43408 581.51996
664.414 134.88744
689.50659 227.07582
721.53033 231.62096
END IONS

BEGIN IONS
PEPMASS=856.05176
CHARGE=1+
TITLE=Label: #6, Spot_Id: 37884, Peak_List_Id: 85712, MSMS Job_Run_Id: 11317, Comment:
175.15518 126.08153
622.1369 375.09338
623.09155 602.24213
665.14307 343.20197
666.12103 2543.8438
667.10785 932.42566
668.10382 463.16949
732.47815 482.28821
811.18365 2160.4929
812.15167 987.45648
END IONS

BEGIN IONS
PEPMASS=860.52936
CHARGE=1+
TITLE=Label: #6, Spot_Id: 37884, Peak_List_Id: 85728, MSMS Job_Run_Id: 11317, Comment:
244.2003 333.6521
416.27106 107.03661
433.30536 279.26236
480.24271 112.15961
487.298 323.64346
504.3486 144.28828
572.43402 244.21704
589.43231 295.15152
600.42853 251.14163
617.43604 459.79803
666.31561 487.69205
667.29956 470.43985
668.24603 403.82404
669.32074 277.44107
670.2243 437.05212
672.11731 449.86353
674.11115 242.51735
676.06049 247.15765
732.52466 1994.8319
812.3111 325.01059
813.30444 424.07648
END IONS

BEGIN IONS
PEPMASS=921.50201
CHARGE=1+
TITLE=Label: #6, Spot_Id: 37884, Peak_List_Id: 85717, MSMS Job_Run_Id: 11317, Comment:
127.11185 111.54265
333.26163 108.34563
390.25726 163.35765
426.30612 255.44537
496.32437 138.51129
553.36829 344.67139
561.38562 116.47845
589.40515 269.15768
662.35815 231.41548
666.47278 236.56998
730.02612 929.93256
731.03998 276.87076
733.00287 305.67603
875.12158 707.50714
882.39886 299.12558
END IONS

BEGIN IONS
PEPMASS=935.56342
CHARGE=1+
TITLE=Label: #6, Spot_Id: 37884, Peak_List_Id: 85727, MSMS Job_Run_Id: 11317, Comment:
175.15903 272.59805
286.2048 124.02753
579.43567 285.72275
END IONS
BEGIN IONS
PEPMASS=1029.641
CHARGE=1+
TITLE=Label: #6, Spot_Id: 37884, Peak_List_Id: 85730, MSMS Job_Run_Id: 11317, Comment:
175.15295 1079.2021
271.22525 226.66667
287.17545 156.86082
288.255 198.57948
325.24713 134.30179
343.26465 111.4158
384.33908 104.25083
400.27341 138.57701
401.34814 126.42435
415.26535 155.18436
444.29614 169.69505
472.40576 462.10767
513.39392 125.70704
516.31836 228.89165
558.37085 165.16844
569.42889 136.53131
586.47827 279.86145
611.40527 190.60837
629.43921 677.01154
687.50092 176.58577
742.55023 150.86697
985.72968 1283.7356
END IONS

BEGIN IONS
PEPMASS=1046.6335
CHARGE=1+
TITLE=Label: #6, Spot_Id: 37884, Peak_List_Id: 85721, MSMS Job_Run_Id: 11317, Comment:
855.26093 440.18863
857.24689 322.008
END IONS

BEGIN IONS
PEPMASS=1135.5697
CHARGE=1+
TITLE=Label: #6, Spot_Id: 37884, Peak_List_Id: 85715, MSMS Job_Run_Id: 11317, Comment:

175.15448 104.01961
691.43909 132.1407
692.44141 130.69049
1077.7142 215.0806
END IONS

BEGIN IONS
PEPMASS=1145.6992
CHARGE=1+
TITLE=Label: #6, Spot_Id: 37884,
Peak_List_Id: 85723, MSMS Job_Run_Id:
11317, Comment:
610.46765 186.39853
664.47375 152.90219
723.5484 114.56869
1046.7493 170.08192
1078.8132 139.74054
END IONS

BEGIN IONS
PEPMASS=1239.672
CHARGE=1+
TITLE=Label: #6, Spot_Id: 37884,
Peak_List_Id: 85716, MSMS Job_Run_Id:
11317, Comment:
175.15337 141.42157
592.38568 132.35754
720.4566 207.33229
END IONS

BEGIN IONS
PEPMASS=1262.7124
CHARGE=1+
TITLE=Label: #6, Spot_Id: 37884,
Peak_List_Id: 85714, MSMS Job_Run_Id:
11317, Comment:
505.34256 176.26367
618.46796 128.7065
758.59546 113.614
1198.8469 1579.5186
END IONS

BEGIN IONS
PEPMASS=1301.8054
CHARGE=1+
TITLE=Label: #6, Spot_Id: 37884,
Peak_List_Id: 85726, MSMS Job_Run_Id:
11317, Comment:
303.24954 119.01961
1256.1985 153.37485
END IONS

BEGIN IONS
PEPMASS=1308.7153
CHARGE=1+
TITLE=Label: #6, Spot_Id: 37884,
Peak_List_Id: 85713, MSMS Job_Run_Id:
11317, Comment:
175.13974 360.39215
303.2709 423.64832
511.38409 103.07214
530.43048 121.58058
610.43555 137.42368
659.47003 300.21912
1256.2501 499.49527
1258.2408 300.84961
END IONS

BEGIN IONS
PEPMASS=1432.7982
CHARGE=1+
TITLE=Label: #6, Spot_Id: 37884,
Peak_List_Id: 85725, MSMS Job_Run_Id:
11317, Comment:
591.40326 401.54633
615.35706 233.28976
650.38403 204.89153
719.52826 376.50629
818.60443 167.44994
836.4801 138.94302
923.5589 158.16603
END IONS

BEGIN IONS
PEPMASS=1450.833
CHARGE=1+
TITLE=Label: #6, Spot_Id: 37884,
Peak_List_Id: 85719, MSMS Job_Run_Id:
11317, Comment:
591.38202 155.4886
719.5058 119.34256
1386.8539 274.83813
END IONS

BEGIN IONS
PEPMASS=1464.7719
CHARGE=1+
TITLE=Label: #6, Spot_Id: 37884,
Peak_List_Id: 85722, MSMS Job_Run_Id:
11317, Comment:
383.25345 128.30264
END IONS

BEGIN IONS
PEPMASS=1882.0326
CHARGE=1+
TITLE=Label: #6, Spot_Id: 37884,
Peak_List_Id: 85720, MSMS Job_Run_Id:
11317, Comment:
813.57861 142.4501
1069.6879 873.94788
1182.804 104.17822
1393.9154 266.50015
1541.0029 263.23157
END IONS

BEGIN IONS
PEPMASS=2290.2554
CHARGE=1+
TITLE=Label: #6, Spot_Id: 37884,
Peak_List_Id: 85711, MSMS Job_Run_Id:
11317, Comment:
437.28784 108.19585
1190.8179 153.07292
1200.8379 190.71794
1313.8593 361.01147

1427.9033 330.70316
1428.8901 283.77225
1657.0028 880.59448
1789.1642 355.1716
1853.1727 1270.3662
2225.4468 7535.6318
END IONS

Spot 7 as illustrated in Figure 5.3.3

COM=Project: Proteomics, Spot Set: Proteomics\110117, Label: #7, Spot Id: 38019, Peak List Id: 84890, MS Job Run Id: 11316
804.50732 4483.0991
805.49115 8613.3027
832.39111 2644.7205
878.58606 3557.7368
906.58362 7536.9204
929.62274 2077.9219
971.62213 2184.7021
1020.588 2634.2766
1041.5583 2082.6611
1046.6764 4296.7803
1107.6678 2128.9121
1153.6774 4865.3838
1295.8259 6224.5098
1306.7802 2077.5942
1621.954 4374.3564
2027.2162 3788.7024
2163.27 19654.9
2273.3887 8049.4707
2289.3816 9998.6416
2882.5652 4945.3843

BEGIN IONS
PEPMASS=805.49115
CHARGE=1+
TITLE=Label: #7, Spot_Id: 38019, Peak_List_Id: 86804, MSMS Job_Run_Id: 11317, Comment:
112.12175 143.17499
175.16069 889.54047
186.13945 210.81972
230.17018 116.23168
245.1873 132.33353
262.2084 382.64706
285.21802 163.45186
299.19473 253.6366
317.22287 552.48126
322.26355 204.76474
342.22437 183.42374
359.24384 603.36469
376.27048 136.67842
402.30667 195.0106
412.30707 288.57306
430.33517 138.57021
472.35129 193.60118
489.38174 184.48369
503.38263 1269.9283
520.39972 364.54654
602.47864 185.5607
617.18292 153.92175
618.18158 145.56593
760.5816 383.35968
761.13965 103.0801
763.52899 130.41393
775.5506 385.44586
END IONS

BEGIN IONS
PEPMASS=878.58606
CHARGE=1+
TITLE=Label: #7, Spot_Id: 38019, Peak_List_Id: 86797, MSMS Job_Run_Id: 11317, Comment:
175.1595 544.85254
357.26584 171.2742
449.29282 176.75462
520.37384 123.25552
522.40497 440.655
605.4538 114.0177
688.13782 208.6019
END IONS

BEGIN IONS
PEPMASS=929.62274
CHARGE=1+
TITLE=Label: #7, Spot_Id: 38019, Peak_List_Id: 86794, MSMS Job_Run_Id: 11317, Comment:
444.38242 394.83624
486.36508 673.47278
600.49615 240.64725
664.49005 246.93468
736.08844 218.39473
800.56329 456.82983
801.59485 944.65259
END IONS

BEGIN IONS
PEPMASS=971.62213
CHARGE=1+
TITLE=Label: #7, Spot_Id: 38019, Peak_List_Id: 86796, MSMS Job_Run_Id: 11317, Comment:
175.14891 161.37256
277.215 168.91177
368.28442 364.7059
440.28561 128.44757
515.37402 131.96678
END IONS

BEGIN IONS
PEPMASS=987.65894
CHARGE=1+
TITLE=Label: #7, Spot_Id: 38019, Peak_List_Id: 86792, MSMS Job_Run_Id: 11317, Comment:
175.15479 115.88235
373.33899 237.00208
386.29352 100.52259
444.40118 322.54901
502.32776 211.41452
558.4776 191.12234
587.4245 203.24219
597.42505 134.08511

598.40894 183.3159
615.42004 1403.7654
645.5127 312.71033
700.52655 268.5293
711.49512 168.82074
728.5401 465.11923
773.58325 253.60709
943.62866 257.28003
END IONS

BEGIN IONS
PEPMASS=1026.6456
CHARGE=1+
TITLE=Label: #7, Spot_Id: 38019,
Peak_List_Id: 86791, MSMS Job_Run_Id:
11317, Comment:
175.15825 110.44115
402.31604 213.12425
494.35449 195.26738
533.39825 279.31668
648.42322 315.50546
680.4458 375.23611
761.51886 519.0882
781.51294 293.45242
880.61865 429.03641
889.6178 264.58118
899.62848 123.97477
936.664 299.24963
963.72601 1610.2931
981.69482 254.5428
END IONS

BEGIN IONS
PEPMASS=1046.6764
CHARGE=1+
TITLE=Label: #7, Spot_Id: 38019,
Peak_List_Id: 86799, MSMS Job_Run_Id:
11317, Comment:
175.1611 219.90196
262.19598 140.7861
769.54858 155.63974
856.20129 405.49316
950.71082 188.59108
977.69818 1067.3356
END IONS

BEGIN IONS
PEPMASS=1107.6678
CHARGE=1+
TITLE=Label: #7, Spot_Id: 38019,
Peak_List_Id: 86795, MSMS Job_Run_Id:
11317, Comment:
175.14246 101.91177
372.31915 158.78259
619.38202 115.07333
863.54132 143.72488
1042.6957 705.97083
END IONS

BEGIN IONS
PEPMASS=1191.7015
CHARGE=1+
TITLE=Label: #7, Spot_Id: 38019,
Peak_List_Id: 86789, MSMS Job_Run_Id:
11317, Comment:
509.36282 294.08252
792.55109 441.28021
830.52087 191.63788
892.61914 228.40698
906.62604 168.08725
1127.777 238.75209
1147.7657 260.66571
END IONS

BEGIN IONS
PEPMASS=1220.7368
CHARGE=1+
TITLE=Label: #7, Spot_Id: 38019,
Peak_List_Id: 86788, MSMS Job_Run_Id:
11317, Comment:
553.36743 140.1842
666.47955 255.80075
892.59833 964.97607
1107.7612 149.21704
1157.7095 148.58998
END IONS

BEGIN IONS
PEPMASS=1295.8259
CHARGE=1+
TITLE=Label: #7, Spot_Id: 38019,
Peak_List_Id: 86802, MSMS Job_Run_Id:
11317, Comment:
175.14784 207.20589
310.24963 130.34314
501.29865 106.08438
583.40564 130.11046
793.56842 105.13652
810.5788 873.37311
1251.8702 326.49628
1256.1847 276.13806
END IONS

BEGIN IONS
PEPMASS=1306.7802
CHARGE=1+
TITLE=Label: #7, Spot_Id: 38019,
Peak_List_Id: 86793, MSMS Job_Run_Id:
11317, Comment:
659.47772 164.86256
1031.7039 251.52924
1063.6676 538.04095
1239.8622 471.91098
1242.8606 1842.1278
1257.3033 165.77872
END IONS

BEGIN IONS
PEPMASS=1350.7831
CHARGE=1+
TITLE=Label: #7, Spot_Id: 38019,
Peak_List_Id: 86787, MSMS Job_Run_Id:
11317, Comment:
750.526 104.04931
863.60608 129.2525

944.61658 234.19312
1075.7295 353.51196
1107.6521 379.37625
1259.8618 277.97772
1286.89 2126.4612
END IONS

BEGIN IONS
PEPMASS=1557.9391
CHARGE=1+
TITLE=Label: #7, Spot_Id: 38019,
Peak_List_Id: 86790, MSMS Job_Run_Id:
11317, Comment:
288.24561 335.79483
685.4837 209.95908
1173.7642 163.55115
1494.0095 4437.4932
END IONS

BEGIN IONS
PEPMASS=1621.954
CHARGE=1+
TITLE=Label: #7, Spot_Id: 38019,
Peak_List_Id: 86800, MSMS Job_Run_Id:
11317, Comment:
288.2493 231.66667
749.48053 231.75963
1494.0615 934.95129
1499.3915 436.87332
1557.0389 110.32544
1558.043 4515.4463
END IONS

BEGIN IONS
PEPMASS=2027.2162
CHARGE=1+
TITLE=Label: #7, Spot_Id: 38019,
Peak_List_Id: 86798, MSMS Job_Run_Id:
11317, Comment:
517.36426 297.38776
1478.0261 205.85428
1542.0524 233.78981
1962.2051 136.87631
1963.3038 4827.0513
1968.1162 104.98882
END IONS

BEGIN IONS
PEPMASS=2163.27
CHARGE=1+
TITLE=Label: #7, Spot_Id: 38019,
Peak_List_Id: 86806, MSMS Job_Run_Id:
11317, Comment:
652.46985 122.56855
780.51855 277.64862
855.55511 307.64142
909.61053 355.793
954.63123 215.20891
1023.6545 212.86517
1080.6816 1169.8107
1083.6528 122.15726
1209.748 991.75873
1308.8435 786.01349
1407.8741 251.54211
1521.995 578.82391
1658.9952 124.64498
1749.1553 341.39441
END IONS

BEGIN IONS
PEPMASS=2273.3887
CHARGE=1+
TITLE=Label: #7, Spot_Id: 38019,
Peak_List_Id: 86803, MSMS Job_Run_Id:
11317, Comment:
1837.1213 222.20471
1839.0992 102.4811
2225.356 206.78169
END IONS

BEGIN IONS
PEPMASS=2289.3816
CHARGE=1+
TITLE=Label: #7, Spot_Id: 38019,
Peak_List_Id: 86805, MSMS Job_Run_Id:
11317, Comment:
1427.9287 180.31241
1657.0452 228.62048
1789.2235 131.86916
1853.1545 317.01773
2225.4756 2140.834
2230.3599 124.96968
END IONS

BEGIN IONS
PEPMASS=2882.5652
CHARGE=1+
TITLE=Label: #7, Spot_Id: 38019,
Peak_List_Id: 86801, MSMS Job_Run_Id:
11317, Comment:
651.39636 174.43147
722.42133 1141.0876
1543.8473 519.67328
1907.0815 289.98874
END IONS

Spot 8 as illustrated in Figure 5.3.3

COM=Project: Proteomics, Spot Set:
Proteomics\110117, Label: #8, Spot Id: 37880,
Peak List Id: 84823, MS Job Run Id: 11316
805.46313 10340.202
832.36224 4364.9819
906.55823 24635.465
912.61676 43048.785
1017.5974 37218.816
1031.6125 8768.7578
1044.127 3865.123
1097.6638 10000.036
1153.6439 7829.9019
1155.7164 14409.699
1173.7147 3146.178
1174.7168 7951.7842
1200.6771 30386.492
1214.689 3986.4001
1234.7513 3659.3201

1262.6014 6330.8921
1433.8108 10842.58
1491.8807 5903.7554
2163.2148 38686.273
2225.1287 6091.7246

BEGIN IONS
PEPMASS=805.46313
CHARGE=1+

TITLE=Label: #8, Spot_Id: 37880,
Peak_List_Id: 85646, MSMS Job_Run_Id:
11317, Comment:
175.15259 186.81226
262.19699 105.03655
317.20261 223.30829
359.22342 259.23596
617.19086 373.80942
775.52045 193.98062
END IONS

BEGIN IONS
PEPMASS=862.49841
CHARGE=1+
TITLE=Label: #8, Spot_Id: 37880,
Peak_List_Id: 85636, MSMS Job_Run_Id:
11317, Comment:
175.14772 120.41715
419.3013 187.38853
620.45319 383.80484
650.18097 229.42407
662.42853 165.79301
668.19196 541.83447
670.26892 443.15259
672.15015 428.53958
674.07532 557.75531
676.07019 685.14764
811.27063 573.79059
812.23419 157.93829
813.19928 198.09955
814.3175 626.88757
816.23297 372.80646
END IONS

BEGIN IONS
PEPMASS=912.61676
CHARGE=1+
TITLE=Label: #8, Spot_Id: 37880,
Peak_List_Id: 85650, MSMS Job_Run_Id:
11317, Comment:
268.18933 162.40024
313.23489 121.17658
441.38263 129.37517
444.35754 892.40186
452.36237 149.54243
469.37555 1284.9526
583.45758 280.29773
600.4624 143.55881
664.55469 203.21638
720.11084 402.54865
722.08203 212.27061
738.60516 157.57861
766.5498 310.6167
784.61536 2281.0208
END IONS

BEGIN IONS
PEPMASS=968.48352
CHARGE=1+
TITLE=Label: #8, Spot_Id: 37880,
Peak_List_Id: 85634, MSMS Job_Run_Id:
11317, Comment:
721.38837 253.73219
726.39575 865.67902
728.40106 225.23848
936.60022 276.19937
END IONS

BEGIN IONS
PEPMASS=974.54547
CHARGE=1+
TITLE=Label: #8, Spot_Id: 37880,
Peak_List_Id: 85632, MSMS Job_Run_Id:
11317, Comment:
175.15009 186.26855
438.35165 181.34834
531.28564 446.56625
697.38416 168.81363
726.44647 372.14261
728.43756 648.94006
731.54218 232.76501
846.50574 248.86362
END IONS

BEGIN IONS
PEPMASS=1017.5974
CHARGE=1+
TITLE=Label: #8, Spot_Id: 37880,
Peak_List_Id: 85649, MSMS Job_Run_Id:
11317, Comment:
175.15816 742.79413
212.14861 155.12952
243.18092 152.81223
288.25635 278.97043
325.24771 224.7088
372.24939 524.79718
385.29889 270.40875
465.33145 229.8376
482.37015 2158.0613
491.34622 135.99023
499.3934 663.42102
519.35571 144.21738
629.45868 403.95798
646.48901 1635.0667
775.5545 742.74823
END IONS

BEGIN IONS
PEPMASS=1031.6125
CHARGE=1+
TITLE=Label: #8, Spot_Id: 37880,
Peak_List_Id: 85644, MSMS Job_Run_Id:
11317, Comment:
175.15222 265.86105
288.26819 113.37986
385.27191 120.33371

386.25476 243.68442
482.36096 747.25171
499.38803 218.10933
629.44598 194.71948
646.47614 387.67615
789.56042 240.87518
END IONS

BEGIN IONS
PEPMASS=1044.127
CHARGE=1+
TITLE=Label: #8, Spot_Id: 37880, Peak_List_Id: 85638, MSMS Job_Run_Id: 11317, Comment:
175.16144 104.97625
855.16968 729.72229
856.17383 668.50317
END IONS

BEGIN IONS
PEPMASS=1097.6638
CHARGE=1+
TITLE=Label: #8, Spot_Id: 37880, Peak_List_Id: 85645, MSMS Job_Run_Id: 11317, Comment:
255.18935 313.05124
272.22174 378.03925
316.17548 152.59805
369.25137 275.99707
386.26547 145.68765
429.27219 252.7451
542.38214 248.79782
613.43018 287.25919
669.52295 126.98836
782.61804 952.87335
897.68329 274.09534
909.12817 542.00385
910.17822 140.01259
END IONS

BEGIN IONS
PEPMASS=1118.5834
CHARGE=1+
TITLE=Label: #8, Spot_Id: 37880, Peak_List_Id: 85635, MSMS Job_Run_Id: 11317, Comment:
272.21814 478.26172
369.28839 119.6619
437.31818 250.81546
443.27652 113.52149
518.31512 155.17996
633.36957 162.30031
681.40997 527.08899
760.48108 229.36945
761.50024 196.21063
810.50464 514.15356
818.47119 344.41815
847.46979 486.10355
925.17761 477.19595
926.1167 236.00946
END IONS

BEGIN IONS
PEPMASS=1155.7164
CHARGE=1+
TITLE=Label: #8, Spot_Id: 37880, Peak_List_Id: 85647, MSMS Job_Run_Id: 11317, Comment:
570.42377 192.76538
571.45575 538.56091
586.41052 110.10809
683.52234 203.88806
734.52802 113.3595
796.5863 402.99457
846.62402 137.40703
909.69153 130.48955
963.20074 229.89197
1091.8268 1053.0236
END IONS

BEGIN IONS
PEPMASS=1165.6537
CHARGE=1+
TITLE=Label: #8, Spot_Id: 37880, Peak_List_Id: 85633, MSMS Job_Run_Id: 11317, Comment:
175.15863 163.07054
486.32306 165.16113
680.48334 139.76761
1119.7499 267.65863
END IONS

BEGIN IONS
PEPMASS=1174.7168
CHARGE=1+
TITLE=Label: #8, Spot_Id: 37880, Peak_List_Id: 85643, MSMS Job_Run_Id: 11317, Comment:
175.15114 237.93741
416.35486 115
545.4035 143.07956
802.57867 193.84532
809.51117 424.09875
999.67993 740.8761
1017.6968 1029.2999
1113.7732 424.60364
1130.7825 269.35046
1131.7721 328.19702
END IONS

BEGIN IONS
PEPMASS=1200.6771
CHARGE=1+
TITLE=Label: #8, Spot_Id: 37880, Peak_List_Id: 85648, MSMS Job_Run_Id: 11317, Comment:
412.29279 1562.0544
525.3996 233.11754
639.47125 409.52103
676.39246 260.36157
754.4967 242.58932
789.49524 252.5836
825.52655 265.13907
898.61786 161.79994
926.59076 811.49561
954.59595 106.51501

1054.6418 750.09717
1072.6593 177.3793
END IONS

BEGIN IONS
PEPMASS=1214.689
CHARGE=1+
TITLE=Label: #8, Spot_Id: 37880,
Peak_List_Id: 85639, MSMS Job_Run_Id:
11317, Comment:
412.29236 616.58484
525.39325 144.20685
639.44843 201.35228
754.4621 175.8378
940.60461 350.09918
1068.6517 398.13153
1086.6532 279.71188
1153.7095 424.5488
END IONS

BEGIN IONS
PEPMASS=1234.7513
CHARGE=1+
TITLE=Label: #8, Spot_Id: 37880,
Peak_List_Id: 85637, MSMS Job_Run_Id:
11317, Comment:
175.15031 195.29411
458.34613 106.70499
701.5329 237.45355
END IONS

BEGIN IONS
PEPMASS=1262.6014
CHARGE=1+
TITLE=Label: #8, Spot_Id: 37880,
Peak_List_Id: 85642, MSMS Job_Run_Id:
11317, Comment:
701.4021 216.25189
887.46136 210.93945
988.51593 165.22043
1197.7385 319.42502
END IONS

BEGIN IONS
PEPMASS=1491.8807
CHARGE=1+
TITLE=Label: #8, Spot_Id: 37880,
Peak_List_Id: 85640, MSMS Job_Run_Id:
11317, Comment:
272.2037 259.99988
369.23917 181.08775
556.39624 129.31288
669.51422 160.13837
710.44214 195.11644
782.61176 1533.0226
823.52234 167.37897
897.62512 289.75607
1007.6448 224.81082
1106.7278 145.75488
1362.9146 431.59064
1365.8496 235.84348
END IONS

BEGIN IONS
PEPMASS=1504.8298
CHARGE=1+
TITLE=Label: #8, Spot_Id: 37880,
Peak_List_Id: 85631, MSMS Job_Run_Id:
11317, Comment:
703.50555 167.69121
782.64496 226.14998
817.573 365.71564
917.54486 384.20831
932.59863 172.21782
1030.6211 215.11823
1143.7279 350.4097
END IONS

BEGIN IONS
PEPMASS=2225.1287
CHARGE=1+
TITLE=Label: #8, Spot_Id: 37880,
Peak_List_Id: 85641, MSMS Job_Run_Id:
11317, Comment:
1142.6541 165.25845
1445.7372 155.77113
1811.0338 158.68913
END IONS

Spot 9 as illustrated in Figure 5.3.3

COM=Project: Proteomics, Spot Set:
Proteomics\110117, Label: #9, Spot Id: 37881,
Peak List Id: 84824, MS Job Run Id: 11316
802.48578 5917.2515
805.46222 7706.8398
806.13367 9156.4688
832.35748 11244.778
855.0874 9465.6455
856.07013 8699.8711
873.07556 7034.5508
906.54999 7590.5405
912.61389 16173.699
923.50989 5271.1489
954.50818 5306.0107
1017.5925 7847.563
1044.1193 16554.623
1153.6453 4605.6812
1155.6389 7332.1484
1200.6733 7075.6919
1259.6194 5661.8462
1300.1069 14686.016
1464.8475 9192.6064
2163.21 4551.1709

BEGIN IONS
PEPMASS=806.13367
CHARGE=1+

TITLE=Label: #9, Spot_Id: 37881,
Peak_List_Id: 85665, MSMS Job_Run_Id:
11317, Comment:
112.1062 147.32422
158.12679 124.35581
175.15237 762.79724
230.15865 256.31754

245.17149 220.77592
262.19693 371.25488
269.18863 211.37534
286.21613 176.44655
299.18079 328.41342
317.2001 644.61743
341.22769 168.15063
342.19598 237.96925
359.23514 1000.735
402.30753 254.37891
412.29678 319.55444
430.31232 254.95422
472.33347 217.09552
489.37744 187.99405
526.30634 250.9799
544.39355 220.40881
573.1618 252.51788
615.20691 408.38187
617.15997 2959.231
619.14874 462.03351
674.54126 1201.7725
675.51038 370.22488
763.50806 276.16138
775.52124 583.31158
785.59314 247.84441
END IONS

BEGIN IONS
PEPMASS=847.46753
CHARGE=1+
TITLE=Label: #9, Spot_Id: 37881,
Peak_List_Id: 85657, MSMS Job_Run_Id:
11317, Comment:
234.07234 123.23527
339.24506 132.48192
362.31619 104.82899
550.36707 140.64185
634.21381 1524.2151
636.20392 284.53665
654.27545 247.46062
656.20825 1548.8641
658.15228 329.46463
659.15314 281.26794
660.1748 445.19699
662.12616 803.64996
685.45624 311.61823
805.51453 1465.4105
808.49817 203.28885
811.51306 277.8306
812.5141 187.79373
817.50714 394.38055
END IONS

BEGIN IONS
PEPMASS=855.0874
CHARGE=1+
TITLE=Label: #9, Spot_Id: 37881,
Peak_List_Id: 85667, MSMS Job_Run_Id:
11317, Comment:
302.15897 101.8204
477.0488 208.74295
495.07394 227.84605
622.13312 843.21484
623.11877 588.25372
663.22662 342.14691
664.14117 286.73389
665.1499 446.9642
666.1261 2782.4375
669.12891 182.14969
691.43195 483.68411
767.16187 327.47623
811.16168 1364.3771
812.15265 1228.0562
814.13043 208.63971
814.57446 107.43631
END IONS

BEGIN IONS
PEPMASS=864.51025
CHARGE=1+
TITLE=Label: #9, Spot_Id: 37881,
Peak_List_Id: 85655, MSMS Job_Run_Id:
11317, Comment:
250.04865 152.14894
275.23935 162.16177
287.20944 134.3992
302.16235 192.4825
346.27176 157.79106
348.15826 117.09969
356.25766 174.44359
362.30576 166.63914
385.31686 160.59605
399.34125 165.869
416.35846 174.84407
419.32327 178.44366
509.40823 244.55554
550.37024 639.37811
563.48444 3852.5916
605.38147 767.82239
623.14709 362.09628
650.23596 948.29694
666.14856 670.81995
668.13715 676.45081
672.22424 1415.3285
678.51929 1648.9963
736.495 1702.0245
748.56171 712.66815
811.29285 1341.0873
812.23798 1281.6206
813.23291 702.78088
814.19867 960.59491
816.20752 822.84064
END IONS

BEGIN IONS
PEPMASS=873.07556
CHARGE=1+
TITLE=Label: #9, Spot_Id: 37881,
Peak_List_Id: 85661, MSMS Job_Run_Id:
11317, Comment:
254.18265 194.24532
260.2131 136.24069
353.26468 178.85889
400.31335 135.14815
442.33932 186.33603
466.33801 218.31

478.33566 128.98409
496.35916 518.23236
513.36749 414.93954
595.41821 1444.3909
612.47504 210.70108
638.14502 214.75363
640.12372 511.01718
666.1424 626.89484
682.14709 1648.6792
684.12122 1840.5933
686.11676 333.71939
688.12085 1054.4548
725.55005 423.05878
742.58533 363.38812
743.5932 675.90094
811.18091 680.13568
827.25293 727.66998
829.1723 471.53513
END IONS

BEGIN IONS
PEPMASS=912.61389
CHARGE=1+
TITLE=Label: #9, Spot_Id: 37881,
Peak_List_Id: 85669, MSMS Job_Run_Id:
11317, Comment:
101.09057 212.84314
112.11362 142.88246
175.16656 123.5718
185.15167 139.94539
243.19312 100.61789
268.19669 294.57281
298.25381 114.07934
313.24393 240.50064
339.23715 193.83163
422.27399 226.98901
441.36395 317.73099
444.36176 1791.8538
452.34885 364.65143
469.37256 3071.8445
487.41141 145.26262
583.4577 560.21875
600.5011 371.53473
636.45221 201.73335
664.54865 430.69037
720.11169 1117.1177
723.06744 384.62637
738.59357 767.45313
766.57751 420.14374
782.58917 228.96368
783.59711 235.40794
784.59473 4809.0283
865.17865 496.55179
882.67462 315.14774
END IONS

BEGIN IONS
PEPMASS=923.50989
CHARGE=1+
TITLE=Label: #9, Spot_Id: 37881,
Peak_List_Id: 85658, MSMS Job_Run_Id:
11317, Comment:
157.14188 103.05231
390.27332 159.83261
647.37854 177.43845
662.39893 275.06738
664.43494 525.56384
736.02686 370.4473
810.49988 2198.9565
880.08173 261.62656
END IONS

BEGIN IONS
PEPMASS=938.4729
CHARGE=1+
TITLE=Label: #9, Spot_Id: 37881,
Peak_List_Id: 85651, MSMS Job_Run_Id:
11317, Comment:
172.09645 110.87746
175.14928 139.89438
286.19275 183.61162
341.2168 142.22836
398.26367 175.11702
415.28317 565.69104
524.328 367.61697
663.40192 362.01038
775.4718 2618.0229
806.56848 621.92426
891.14642 564.56659
894.61432 700.22345
895.58765 1506.0544
903.53778 296.54953
END IONS

BEGIN IONS
PEPMASS=954.50818
CHARGE=1+
TITLE=Label: #9, Spot_Id: 37881,
Peak_List_Id: 85659, MSMS Job_Run_Id:
11317, Comment:
175.15146 111.22999
272.19012 196.02902
585.54022 202.50967
594.39594 590.04706
675.39514 269.95987
676.33649 158.78296
692.42963 158.6006
767.08008 356.13092
795.51025 358.49042
798.52191 821.56458
823.53827 906.77979
888.61151 579.6153
911.56421 223.72015
912.58893 922.61609
END IONS

BEGIN IONS
PEPMASS=982.492
CHARGE=1+
TITLE=Label: #9, Spot_Id: 37881,
Peak_List_Id: 85656, MSMS Job_Run_Id:
11317, Comment:
175.15077 119.29855
272.21411 1073.5714
305.20911 162.33777
368.24286 219.00259

396.2254 145.24429
458.30258 136.49924
476.28922 162.55357
524.3009 280.36862
533.33612 259.00232
590.37518 237.88928
710.3913 467.07822
810.51074 1007.9271
817.5011 372.04922
835.49841 3071.4058
940.55878 438.82602
952.54199 454.53079
END IONS

BEGIN IONS
PEPMASS=993.55164
CHARGE=1+
TITLE=Label: #9, Spot_Id: 37881, Peak_List_Id: 85653, MSMS Job_Run_Id: 11317, Comment:
175.15593 983.2547
244.13481 128.15068
271.21829 103.85714
288.25766 104.27151
293.16595 103.17769
342.26151 204.36302
343.22656 173.04842
359.29263 157.31253
407.22882 308.28452
414.29327 129.18195
458.39859 571.21063
472.31659 127.41789
508.28586 176.4418
536.29968 823.57715
587.44763 208.68867
607.36603 259.8194
635.36725 218.65778
684.45978 177.75943
701.51477 677.43658
706.43524 122.52843
929.6355 332.11218
947.62372 473.40643
951.60516 169.22466
END IONS

BEGIN IONS
PEPMASS=1017.5925
CHARGE=1+
TITLE=Label: #9, Spot_Id: 37881, Peak_List_Id: 85664, MSMS Job_Run_Id: 11317, Comment:
112.12166 105.40849
175.15901 666.89777
212.15111 208.37381
243.18604 145.41376
271.2301 107.65881
288.25818 221.70076
325.25528 211.9498
372.25397 490.18509
385.29175 281.02872
465.32178 152.54723
482.3595 1691.8237
499.39261 574.72473
514.38013 191.87776
519.31738 166.98505
629.45404 302.02734
646.48572 1394.2416
775.55121 680.83453
888.66217 410.32013
903.68805 215.91228
904.65051 147.20021
973.60138 262.87708
975.60101 144.32388
END IONS

BEGIN IONS
PEPMASS=1044.1193
CHARGE=1+
TITLE=Label: #9, Spot_Id: 37881, Peak_List_Id: 85670, MSMS Job_Run_Id: 11317, Comment:
811.20264 216.8941
854.22931 207.4697
855.18695 421.77109
856.17499 839.60565
858.14545 173.10989
859.15973 113.15846
917.64038 220.35632
1003.6914 402.30261
END IONS

BEGIN IONS
PEPMASS=1097.651
CHARGE=1+
TITLE=Label: #9, Spot_Id: 37881, Peak_List_Id: 85654, MSMS Job_Run_Id: 11317, Comment:
112.11366 180.71861
129.13171 115.60093
175.15224 205.99782
255.18579 646.40253
272.21716 1091.5818
316.1622 422.44812
369.25305 907.66882
386.28711 468.84009
398.31082 114.60065
401.26465 266.3775
413.31778 173.5587
429.26135 718.11871
485.37122 276.27356
500.3201 310.22113
514.37109 323.45459
542.37592 722.10065
556.41211 257.01959
613.43622 913.81006
669.5412 366.37912
712.49841 244.48048
782.62384 3083.1514
897.66376 722.24158
907.12085 374.51273
909.1264 1559.6467
934.57428 333.25433
1053.1727 292.68271
1055.6617 1532.2808
END IONS

BEGIN IONS
PEPMASS=1155.6389
CHARGE=1+
TITLE=Label: #9, Spot_Id: 37881,
Peak_List_Id: 85663, MSMS Job_Run_Id:
11317, Comment:
562.40167 274.71448
571.44965 1310.1202
594.36053 431.21368
683.53998 158.87967
734.51843 289.07858
796.58655 225.13718
894.57751 246.10793
1068.7124 239.10829
1091.814 854.62292
1113.7003 1009.631
END IONS

BEGIN IONS
PEPMASS=1200.6733
CHARGE=1+
TITLE=Label: #9, Spot_Id: 37881,
Peak_List_Id: 85662, MSMS Job_Run_Id:
11317, Comment:
412.29236 1807.3181
525.41376 315.14896
639.45941 594.4964
676.40973 353.84274
754.50281 274.47275
789.49438 338.36816
825.54944 439.99847
926.57007 751.4649
943.58398 321.97693
954.64264 183.47731
1054.6626 746.49585
1072.688 184.52563
1153.7848 293.59665
END IONS

BEGIN IONS
PEPMASS=1259.6194
CHARGE=1+
TITLE=Label: #9, Spot_Id: 37881,
Peak_List_Id: 85660, MSMS Job_Run_Id:
11317, Comment:
396.21524 132.2674
413.2587 100.62388
524.30438 285.64359
533.32141 149.36383
550.35681 1897.3579
701.40887 200.24397
710.4068 479.55447
736.45221 160.71704
1001.5932 242.74017
1067.2345 337.94788
1068.1609 385.28162
1078.6248 406.36813
1088.6548 777.75366
1096.6483 1209.624
1212.3022 291.44592
1218.696 206.33539
END IONS

BEGIN IONS
PEPMASS=1300.1069
CHARGE=1+
TITLE=Label: #9, Spot_Id: 37881,
Peak_List_Id: 85668, MSMS Job_Run_Id:
11317, Comment:
1212.2488 325.38138
1254.2709 1127.5619
1256.2079 7267.9849
END IONS

BEGIN IONS
PEPMASS=1464.8475
CHARGE=1+
TITLE=Label: #9, Spot_Id: 37881,
Peak_List_Id: 85666, MSMS Job_Run_Id:
11317, Comment:
659.49561 539.6087
774.55408 231.43118
806.51331 432.05078
1162.7585 147.60547
1290.8431 567.27063
1308.8604 1771.7271
1404.9539 460.90506
1422.9415 1068.9683
END IONS

BEGIN IONS
PEPMASS=1491.8806
CHARGE=1+
TITLE=Label: #9, Spot_Id: 37881,
Peak_List_Id: 85652, MSMS Job_Run_Id:
11317, Comment:
255.18405 110.24632
267.16098 107.33526
272.20929 582.02081
369.2294 401.95987
386.24847 292.27133
466.30612 148.15698
485.34955 252.3783
556.40466 269.74091
669.5105 339.51517
709.42035 219.16815
710.42285 359.02365
782.61053 3236.8938
822.48004 218.58395
823.51288 262.99911
880.61096 172.04114
897.66321 683.10162
936.66089 410.47708
1007.6627 391.09271
1106.7535 372.17758
1300.238 1000.1144
1301.2632 449.29828
1362.9294 800.68158
1424.9926 561.18933
END IONS

Spot 10 as illustrated in Figure 5.3.3

COM=Project: Proteomics, Spot Set:
Proteomics\110117, Label: #10, Spot Id: 37882,
Peak List Id: 84825, MS Job Run Id: 11316

805.45398 3114.3696
906.54865 3733.6948
912.60504 13625.023
974.53131 1746.7339
1017.5842 8169.2554
1031.603 2195.6506
1044.1112 1372.1067
1097.6503 3700.4902
1153.6307 1970.8528
1155.6998 2653.1362
1173.6962 1558.4402
1174.7007 4485.9604
1200.661 7056.0889
1235.5992 2196.4275
1262.5859 3514.9297
1264.5798 1623.8463
1300.0892 2763.5598
1491.8687 3192.2764
2163.1716 3993.1372
2225.1257 1860.0001

BEGIN IONS
PEPMASS=805.45398
CHARGE=1+

TITLE=Label: #10, Spot_Id: 37882,
Peak_List_Id: 85683, MSMS Job_Run_Id:
11317, Comment:
175.149 384.86905
262.18887 186.02985
299.18274 145.81624
317.19272 318.52145
322.24609 105.65135
359.23816 354.06653
402.28836 144.34859
412.29654 137.14619
612.27325 188.92714
614.18463 357.06607
615.15039 310.75043
617.15405 1251.1473
775.5083 337.2338
END IONS

BEGIN IONS
PEPMASS=820.33954
CHARGE=1+

TITLE=Label: #10, Spot_Id: 37882,
Peak_List_Id: 85672, MSMS Job_Run_Id:
11317, Comment:
172.09708 141.20004
354.16553 155.23479
382.14694 213.7619
545.25195 357.63544
624.19849 222.93231
628.21289 366.61853
629.07074 690.79877
630.14819 300.23926
631.22504 314.45078
632.177 255.97421
674.3031 566.80127
692.32513 340.07697
759.48798 246.22801
770.34253 357.52536
773.41595 242.84808
774.50665 336.50565
776.47723 243.04994
799.44171 329.86008
END IONS

BEGIN IONS
PEPMASS=912.60504
CHARGE=1+
TITLE=Label: #10, Spot_Id: 37882,
Peak_List_Id: 85690, MSMS Job_Run_Id:
11317, Comment:
101.09897 136.7673
112.1074 155.07085
157.14786 114.16667
185.14012 135.79126
243.19487 126.437
268.19495 315.48749
298.24023 107.81061
313.23318 204.7836
339.23215 177.27173
426.34714 137.08971
441.35287 216.76244
444.36188 2262.6143
452.33951 325.88858
469.37354 3437.0034
583.4657 628.81531
600.47974 464.3399
664.61322 279.58521
665.52057 197.6082
720.09808 574.10181
721.12024 204.85805
738.5755 743.7738
766.59961 410.29602
782.59595 252.73254
783.60956 316.67346
784.60205 5108.2593
849.54919 244.55002
882.66736 191.6718
END IONS

BEGIN IONS
PEPMASS=968.47925
CHARGE=1+
TITLE=Label: #10, Spot_Id: 37882,
Peak_List_Id: 85673, MSMS Job_Run_Id:
11317, Comment:
305.11337 221.09532
558.29767 145.34082
721.38666 426.82413
726.39685 2388.3975
728.39038 470.81073
776.97314 334.7533
END IONS

BEGIN IONS
PEPMASS=974.53131
CHARGE=1+
TITLE=Label: #10, Spot_Id: 37882,
Peak_List_Id: 85677, MSMS Job_Run_Id:
11317, Comment:
489.23639 109.92802

531.30194 448.70654
533.29138 122.97346
846.50049 172.42734
END IONS

BEGIN IONS
PEPMASS=1017.5842
CHARGE=1+
TITLE=Label: #10, Spot_Id: 37882, Peak_List_Id: 85689, MSMS Job_Run_Id: 11317, Comment:
175.14369 669.26471
212.14131 203.4628
243.16411 115.62424
288.24414 185.08058
325.23944 159.65236
372.22525 442.16183
385.27795 141.46234
465.31552 167.63184
482.34433 1573.2583
499.37119 551.05365
519.32269 154.04297
629.4278 261.85693
646.47107 1309.9957
775.53558 772.88928
982.62512 132.93773
END IONS

BEGIN IONS
PEPMASS=1031.603
CHARGE=1+
TITLE=Label: #10, Spot_Id: 37882, Peak_List_Id: 85679, MSMS Job_Run_Id: 11317, Comment:
175.15451 508.4982
212.15546 126.76471
288.25946 149.85295
325.24368 122.05882
385.2785 218.65804
386.26913 295.88983
465.32968 117.55882
482.35458 1255.1051
499.38931 411.83908
629.46057 264.38461
646.48578 590.20087
789.56372 269.84174
END IONS

BEGIN IONS
PEPMASS=1044.1112
CHARGE=1+
TITLE=Label: #10, Spot_Id: 37882, Peak_List_Id: 85676, MSMS Job_Run_Id: 11317, Comment:
175.15271 144.62347
646.52997 298.24341
811.19244 476.37537
812.16461 174.70238
854.22089 410.26334
855.1615 1148.0862
856.17529 3267.6299
END IONS

BEGIN IONS
PEPMASS=1097.6503
CHARGE=1+
TITLE=Label: #10, Spot_Id: 37882, Peak_List_Id: 85686, MSMS Job_Run_Id: 11317, Comment:
255.19142 199.95746
272.21747 391.74835
316.17435 152.23914
369.26065 271.96078
429.27185 304.76083
542.38678 256.52322
556.40729 107.60102
613.43573 331.42517
782.62488 987.90015
897.6441 215.78984
907.0957 263.08835
909.11578 801.90027
1054.1765 132.46237
END IONS

BEGIN IONS
PEPMASS=1107.585
CHARGE=1+
TITLE=Label: #10, Spot_Id: 37882, Peak_List_Id: 85675, MSMS Job_Run_Id: 11317, Comment:
175.15114 277.32391
616.41919 124.63868
782.65375 182.62044
917.15985 357.50134
1042.6997 1080.6495
END IONS

BEGIN IONS
PEPMASS=1117.5848
CHARGE=1+
TITLE=Label: #10, Spot_Id: 37882, Peak_List_Id: 85671, MSMS Job_Run_Id: 11317, Comment:
175.16821 129.41206
255.20627 110.24658
272.22324 427.60904
437.32178 303.18704
443.31686 151.23399
518.3299 249.29094
633.37469 428.03485
681.40009 841.78558
760.47241 369.24725
761.46692 190.3432
810.52936 355.69299
818.51239 527.15973
847.48206 470.91611
881.14319 409.64413
925.13654 561.86334
1068.2509 634.96722
1070.1912 947.23505
END IONS

BEGIN IONS
PEPMASS=1155.6998
CHARGE=1+

TITLE=Label: #10, Spot_Id: 37882, Peak_List_Id: 85681, MSMS Job_Run_Id: 11317, Comment:
360.2522 102.09608
473.31042 250.06142
565.35376 156.98021
570.43646 202.00658
571.43958 1277.1024
586.41943 174.0627
683.52356 410.11777
734.55048 170.96155
796.59985 770.73755
846.61176 260.55573
909.71802 256.60648
1091.8087 2307.521
END IONS

BEGIN IONS
PEPMASS=1174.7007
CHARGE=1+
TITLE=Label: #10, Spot_Id: 37882, Peak_List_Id: 85687, MSMS Job_Run_Id: 11317, Comment:
129.13144 121.42157
175.15163 483.0708
416.35495 220.58823
545.42792 274.56674
630.41644 142.57578
802.61285 416.83701
809.50061 270.30811
873.63196 370.44769
999.68713 1034.8506
1017.6881 1597.6244
1113.7858 352.94803
1130.7874 453.37656
1131.7803 740.59821
END IONS

BEGIN IONS
PEPMASS=1200.661
CHARGE=1+
TITLE=Label: #10, Spot_Id: 37882, Peak_List_Id: 85688, MSMS Job_Run_Id: 11317, Comment:
412.29962 2129.9788
525.39178 350.2944
639.4649 481.38568
676.39337 330.45483
714.45856 127.28901
754.508 241.87073
789.49988 410.78806
825.56598 392.47235
898.58911 239.12558
926.58752 864.20691
943.61945 269.71674
954.59344 239.71892
1054.6646 991.65112
1072.6865 281.87723
END IONS

BEGIN IONS
PEPMASS=1235.5992
CHARGE=1+
TITLE=Label: #10, Spot_Id: 37882, Peak_List_Id: 85680, MSMS Job_Run_Id: 11317, Comment:
175.15123 133.33333
END IONS

BEGIN IONS
PEPMASS=1262.5859
CHARGE=1+
TITLE=Label: #10, Spot_Id: 37882, Peak_List_Id: 85685, MSMS Job_Run_Id: 11317, Comment:
587.3233 204.17094
701.38824 405.62939
816.4223 135.64194
887.48724 229.99599
988.49347 277.28967
END IONS

BEGIN IONS
PEPMASS=1300.0892
CHARGE=1+
TITLE=Label: #10, Spot_Id: 37882, Peak_List_Id: 85682, MSMS Job_Run_Id: 11317, Comment:
175.14168 107.83173
338.2319 313.05466
812.50208 117.10258
1112.121 246.90016
1212.2123 640.08087
1254.2509 1804.6636
1256.2158 10869.416
END IONS

BEGIN IONS
PEPMASS=1491.8687
CHARGE=1+
TITLE=Label: #10, Spot_Id: 37882, Peak_List_Id: 85684, MSMS Job_Run_Id: 11317, Comment:
272.21213 426.32336
369.22855 260.30893
386.26181 269.11765
485.33762 196.01456
556.40771 164.81552
669.4942 175.25873
710.41675 212.04472
782.60663 2167.751
823.50647 202.84052
897.65625 609.85358
936.63074 255.52361
1007.6384 178.2834
1225.8489 118.85957
1362.949 685.92993
1365.8163 492.92545
END IONS

BEGIN IONS
PEPMASS=1619.9646
CHARGE=1+
TITLE=Label: #10, Spot_Id: 37882, Peak_List_Id: 85674, MSMS Job_Run_Id: 11317, Comment:

272.20676 139.36273
386.2717 131.67761
556.40875 127.00661
669.50861 146.78259
782.60046 1113.8068
838.54266 133.83694
897.64294 291.33887
1135.7466 184.56509
1234.8783 196.89061
1362.9735 363.78534
1429.1426 262.65164
1557.9695 242.80209
1574.1283 450.92279
1576.084 480.08228
END IONS

BEGIN IONS
PEPMASS=2225.1257
CHARGE=1+
TITLE=Label: #10, Spot_Id: 37882,
Peak_List_Id: 85678, MSMS Job_Run_Id:
11317, Comment:
1142.5708 362.03445
END IONS

REFERENCES

Agianian, B., Tucker, P.A., Schouten, A., Leonard, K., Bullard, B. & Gros, P. (2003) Structure of a *Drosophila* sigma class glutathione S-transferase reveals a novel active site topography suited for lipid peroxidation products. *Journal of Molecular Biology* 326, 151-165.

Alias, Z. & Clark, A.G. (2007) Studies on the glutathione S-transferase proteome of adult *Drosophila melanogaster*: Responsiveness to chemical challenge. *Proteomics* 7, 3618-3628.

Alias, Z. (2006) The proteome of insect glutathione S-transferases: its response to toxic challenge. In *School of Biological Sciences*. Wellington: Victoria University of Wellington pp. 232.

Armstrong, R.N. (1997) Structure, catalytic mechanism and evolution of the glutathione transferases. *Chemistry Respiratory and Toxicology* 10, 2–18

Bayne, B.L. (1976) Marine Mussels: *Their Ecology and Physiology*. Cambridge University Press, Cambridge, UK.

Bernal-Hernández, Y.Y., Medina-Díaz, I.M., Robledo-Marenco, M.L., Velázquez-Fernández, J.B., Girón-Pérez, M.I. & Ortega-Cervantes, L. (2010) Acetylcholinesterase and metallothionein in oysters (*Crassostrea corteziensis*) from a subtropical Mexican Pacific estuary. *Ecotoxicology* 19, 819-825.

Blanchette, B., Feng, X., & Singh, B.R. (2007) Marine Glutathione S–Transferases: Reviews. *Marine Biotechnology* 9, 513–542.

Blanchette, B.N. & Singh, B.R. (1999) Purification and characterization of the glutathione-S-transferases from the Northern quahog *Mercinaria mercinaria. Marine Biotechnology* 1, 74–80.

Blanchette, B.N. & Singh, B.R. (2002) Isolation and characterization of glutathione-S-transferase isozyme Q3 from the Northern quahog, *Mercinaria mercinaria. Journal of Protein Chemistry* 21, 151–159.

Bolton, R.M. & Ahokas, J.T. (1997) Purification and characterization of hepatic glutathione transferase from an insectivorous marsupial, the brown antechinus, *Antechinus stuartii*. *Xenobiotica* 27, 573–586.

Bordini, E., Hamdan, M. & Righetti, P.G. (2000) Alkylation power of free immobiline chemicals towards proteins in isoelectric focusing and two-dimensional maps, as explored by matrix assisted laser desorption/ionization-time of flight-mass spectrometry. *Electrophoresis* 21, 2911-2918.

Bringans, S., Eriksen, S., Kendrick, T., Gopalakrishnakone, P., Livk, A., Lock, R. & Lipscombe, R. (2008) Proteomic analysis of the venom of the *Heterometrus longimanus* (Asian black scorpion). *Proteomics* 8(5), 1081-1096.

Cajaraville, M., Bebianno, M., Blasco, J., Porte, C., Sarasquete, C., & Viarengo, A. (2000) The use of biomarkers to assess the impact of pollution in coastal environments of the Iberian Peninsula: a pratical approach. *The Science of the Total Environment* 247, 295-311.

Chamrad, D.C., Korting, G., Stuhler, K., Meyer, H.E., Klose, J. & Bluggel, M. (2004) Evaluation of algorithms for protein identification from sequence databases using mass spectrometry data. *Proteomics* 4, 619-628.

Chronopoulou, G.E. & Labrou N.E (2009) Glutathione Transferases: Emerging Multidisciplinary Tools in Red and Green Biotechnology. *Recent Patents on Biotechnology* 3, 211-223.

Clark, A.G., Letoa, M. & Ting, W.S. (1977) Purification by affinity chromatography of glutathione S-transferase from larvae of *Galleria mellonella*. *Life Sciences* 20, 141-147.

Clark, A.G., Marshall, S.N. & Qureshi, A.R. (1990) Synthesis and use of an isoform-specific affinity matrix in the purification of glutathione S-transferases from the housefly, *Musca domestica* (L). *Protein Expression and Purification* 1, 121-126.

Clark, A.G., Smith, J.N. & Speir, T.W. (1973) Cross specificity in some vertebrate and insect glutathione-transferases with methyl parathion (dimethyl-p-nitrophenyl phosphorothionate), 1-chloro-2,4-dinitrobenzene and S-crotonyl-N-acetylcysteamine as substrates. *Biochemical Journal* 135, 385-392.

Cossu, C., Doyotte, A., Bubut, M., Exinger, A., & Vasseur, P. (2000) Antioxidant biomarkers in freshwater bivalves, *Unio tumidus*, in response to different contamination profiles of aquatic sediments. *Ecotoxicology and Environmental Safety* 45, 106-121.

Dirr, H., Reinemer, P. & Huber, R. (1994) X-ray crystal structures of cytosolic glutathione S-transferase: implications for protein architecture, substrate recognition and catalytic function. *European Journal Biochemistry* 220, 645–661.

Dixon, D.P., Lapthom, A. & Edwards, R. (2002) Plant glutathione transferases. *Genome Biology 3 Reviews* 3004.1–3004.10.

Dourado, D.F.A.R., Fernandes, P.A. & Joao Ramos, M. (2008) Mammalian Cytosolic Glutathione Transferases. *Current Protein and Peptide Science* 9, 325-337.

Doyen, P., Vasseur, P. & Rodius, F. (2005) cDNA cloning and expression pattern of pi-class glutathione S-transferase in the freshwater bivalves *Unio tumidus* and *Corbicula fluminea*. *Comparative Biochemistry and Physiology* 140, 300–308.

Enayati, A.A., Ranson, H. & Hemingway, J. (2005) Insect glutathione transferases and insecticide resistance. *Insect and Molecular Biology* 14, 3-8.

Fenn, J.B., Mann, M., Meng, C.K., Wong, S.F. & Whitehouse, C.M. (1990) Electrospray ionization - principles and practice. *Mass Spectrometry Review* 9, 37-70.

Fitzpatrick, P.J. & Sheehan, D. (1993) Separation of multiple forms of glutathione S-transferase from the blue mussel, *Mytilus edulis*. *Xenobiotica* 23, 851–861.

Fitzpatrick, P.J., Krag, T.O.B., Hojrup, P. & Sheehan, D. (1995a) Characterization of a glutathione S-transferase and a related glutathione-binding protein from gill of the blue mussel, *Mytilus edulis. Biochemical Journal* 305, 145–150.

Fitzpatrick, P.J., O'Halloran, J., Sheehan, D., & Walsh, A.R. (1997) Assessment of a glutathione *S*-transferase and related proteins in the gill and digestive gland of *Mytilus edulis* (L.) as potential organic pollution biomarkers. *Biomarkers* 2, 51–6.

Fitzpatrick, P.J., Sheehan, D. & Livingstone, D.R. (1995b) Studies on isoenzymes of glutathione S-transferase in the 538 Brian Blanchette et al.: Marine Gluthathione S-Transferases digestive gland of *Mytilus galloprovincialis* with exposure to pollution. *Marine Environment Respiratory* 39, 241–244.

Frova, C. (2006) Glutathione transferases in the genomics era: New insights and perspectives. *Biomolecular Engineering* 23, 149-169.

Gakuta, T. & Toshiro, A. (2000) Disruption of the microsomal glutathione S-transferase-like gene reduces life span *Drosophila melanogaster*. *Gene* 253, 179-187.

Gallagher, E.P., Sheehy, K.M., Lame, M.W., & Segall, H.J. (2000) In vitro kinetics of hepatic glutathione S-transferase conjugation in largemouth bass and brown bullheads. *Environmental Toxicology and Chemistry* 19, 319–326.

Galvani, M., Hamdan, M., Herbert, B. & Righetti, P.G. (2001a) Alkylation kinetics of proteins in preparation for two-dimensional maps: A matrix assisted laser desorption/ionization mass spectrometry investigation. *Electrophoresis* 22, 2058-2065.

Galvani, M., Rovatti, L., Hamdan, M., Herbert, B. & Righetti, P.G. (2001b) Protein alkylation in the presence/absence of thiourea in proteome analysis: A matrix assisted laser desorption/ionization-time of flight-mass spectrometry investigation. *Electrophoresis* 22, 2066-2074.

Görg, A., Weiss, W. & Dunn, M.J. (2004) Current two-dimensional electrophoresis technology for proteomics. *Proteomics* 4, 3665-3685.

Gromova, I. & Celis, J.E. (2006) Protein Detection in Gels by Silver Staining: A Procedure Compatible with Mass-Spectrometry Cell Biology: A Laboratory Handbook. 3rd Edition. *Elsevier Academic Press*.

Guthenberg, C. & Mannervik, B. (1979) Purification of glutathione S-transferases from rat lung by affinity chromatography- evidence for an enzyme form absent in rat liver. *Biochemical and Biophysical Research Communications* 86, 1304-1310.

Habig, W.H., Pabst, M.J. & Jakoby, W.B. (1974) Glutathione S-transferases the first enzymatic step in mercapturic acid formation. *Journal of Biological Chemistry* 249, 7130–7139.

Hamdan, M., Bordini, E., Galvani, M. & Righetti, P.G. (2001) Protein alkylation by acrylamide, its N-substituted derivatives and cross-linkers and its relevance to proteomics: A matrix assisted laser desorption/ionization-time of flight-mass spectrometry study. *Electrophoresis* 22, 1633-1644.

Handy, R.D., Galloway, T.S. & Depledge, M.H. (2003) A proposal for the use of biomarkers for the assessment of chronic pollution and regulatory toxicology. *Ecotoxicology* 12, 331–343.

Hayes, J.D., Flanagan, J.U. & Jowsey, I.R. (2005) Glutathione transferases. *Annual Review of Pharmacology and Toxicology* 45, 51–88.

Herbert, B., Galvani, M., Hamdan, M., Oliver, E., MacCarthy, J., Pedersen, S. & Righetti, P.G. (2001) Reduction and alkylation of proteins in preparation of two-dimensional map analysis: Why, when and how? *Electrophoresis* 22, 2046-2057.

Hoarau, P., Damiens, G., Romeo, M., Gnassia-Barelli, M. & Bebianno, M.J. (2006) Cloning and expression of a GSTpi gene in *Mytilus galloprovincialis*. Attempt to use the GST-pi transcript as a biomarker of pollution. *Comparative Biochemistry and Physiology Part C* 143, 196–203.

Hoarau, P., Garello, G., Gnassia-Barelli, M., Remeo, M. & Girard J.P. (2002) Purification and partial characterization of seven glutathione S-transferase isoforms from the clam *Ruditapes decussates*. *European Journal Biochemistry* 269, 4359–4366.

Jakoby, W.B., Habig, W.H., Keen, J.H., Ketley, J.N. & Pabst, M.J. (1976) Glutathione S-transferases: catalytic aspects. *In Glutathione: Metabolism and Function*, Arias IM, Jakoby WB, eds. (New York: Raven Press) p 189.

Johansson, A.S. & Mannervik, B. (2001) Human glutathione transferase A3-3, a highly efficient catalyst of double-bond isomerization in the biosynthetic pathway of steroid hormones. *Journal of Biological Chemistry* 276, 33061-33065.

Kaufman, R. (1995) Matrix-assisted laser desorption ionization (MALDI) mass spectrometry: A novel analytical tool in molecular biology and biotechnology. *Journal of Biotechnology* 41, 155-175.

Kim, J., Suh, H., Kim, S., Kim, K., Ahn, C. and Yim, J. (2006) Identification and characteristics of the structural gene for the *Drosophila* eye colour mutant sepia, encoding PDA synthase, a member of the Omega class glutathione S-transferases. *Biochemical Journal* 398, 451-460.

Kim, M., In-Young, A., Cheon, J. & Park, H. (2009) Molecular cloning and thermal stress-induced expression of a pi-class glutathione *S*-tranferase (GST) in the Antarctic bivalve *Laternula elliptica*. *Comparative Biochemistry and Physiol*ogy *Part A* 152, 207-213.

Laemmli, U.K. (1970) Cleavage of structural proteins during assembly of head of bacteriophage-T4. *Nature* 227, 680-685.

Lee, K.H. (2001) Proteomics: A technology-driven and technology-limited discovery science. *TRENDS Biotechnology* 19, 217-222.

Liebler, D.C. & Yates III, J.R. (2002) Introduction to proteomics: Tools for the new biology. *Humana Press Inc., New Jersey*. Pp 77-87.

Lo Bello, M., Nuccettelli, M., Caccuri, A.M., Stella, L., Parker, M.W., Rossjohn, J., McKinstry, W.J., Mozzi, A.F., Federici, G., Polizio, F., Pederson, J.Z. & Ricci, G. (2001) Human gluthathione transferases P1-1 and nitric oxide carriers. *Journal of Biological Chemistry* 276, 42138-42145.

Manduzio, H., Monsinjon, T., Galap, C., Leboulenger, F., & Rocher, B. (2004) Seasonal variations in antioxidant defences in blue mussels *Mytilus edulis* collected from a polluted area: major contributions in gills of an inducible isoform of Cu/Zn- superoxide dismutase and of glutathione S-transferase. *Aquatic Toxicology* 70, 83-93.

Mannervik, B. (1985) The isoenzymes of glutathione transferase. *Advance Enzymology Related Areas of Molecular Biology* 57, 357–417.

Merril, C. R. (1990) in Methods in Enzymology (Deutscher, M. P., 20. Wrana, J. L., Zhang, Q., and Sodek, J. (1989) *Nucleic Acids Research Education* 182, pp. 477–488, Academic Press, San Diego.

Myrnes, B. & Nilsen, I.W. (2007) Glutathione S-transferase from the Icelandic scallop *Chlamys islandica*: Isolation and partial characterization. *Comparative Biochemistry and Physiology, Part C* 144, 403-407.

Neuhoff, V., Arold, N., Taube, D. & Ehrhardt, W. (1988) Improved staining of proteins in polyacrylamide gels including isoelectric focusing gels with clear background at nanogram sensitivity using Coomassie Brilliant Blue G-250 and R-250. *Electrophoresis* 9, 255–262.

O'Farrell, P.H. (1975) High resolution two-dimensional electrophoresis of proteins. *Journal of Biological Chemistry* 250, 4007-4021.

Pal, R. (2010) Proteomic analysis of glutathione transferases from *Lucilia cuprina*. *Victoria University of Wellington* (Doctor of Philosophy in Cell and Molecular Bioscience)

Park, H., Ahn, I.Y., Kim, H., Lee, J. & Shin, S.C. (2009) Glutathione S-transferase as a biomarker in the Antarctic bivalve *Laternula elliptica* after exposure to the polychlorinated biphenyl mixture Aroclor 1254. *Comparative Biochemistry and Physiology, Part C* 150, 528–536.

Patterson, S.D. (2000) Proteomics: The industrialization of protein chemistry. *Current Opinion Biotechnology* 11, 413-418.

Pe´rez-Lo´pez, M., Anglade, P., & Bec-Ferte´, M.P. (2000) Characterization of hepatic and extrahepatic glutathione S-transferases in rainbow trout (*Oncorhynchus mykiss*) and their induction by 3, 39, 4, 49-tetrachlorobiphenyl. *Fish Physiology and Biochemistry* 22, 21–32.

Perez, E., Blasco, J. & Sol, M. (2004) Biomarker responses to pollution in two invertebrate species: *Scrobicularia plana* and *Nereis diversicolor* from the Cádiz bay (SW Spain*). Marine Environmental Research* 58 (2-5) 275-279.

Porte, C., Biosca, M., Sole, M. & Albaiges, J. (2001) The integrated use of chemical analysis, cytochrome P450 and stress proteins in mussels to assess pollution along the Galician coast (NW Spain). *Environment Pollution* 112, 26–268.

Robertson, E.F., Dannelly, H.K., Malloy, P.J. & Reeves H.C. (1987) Rapid isoelectric focusing in a vertical polyacrylamide minigel system. *Analytical Biochemistry* 167, 290–294.

Sa´enz, L.A., Seibert, E.L., Zanette, J., Fiedler, H.D., Curtius, A.J., Ferreira, J.F., Almeida, E.A., Marques, M.R.F. & Bainy, A.C.D. (2010) Biochemical biomarker sand metals in *Perna perna* mussels from mariculture zones of Santa Catarina, Brazil. *Ecotoxicology and Environmental Safety* 73, 796–804.

Salinas, A.E. & Wong, M.G. (1999) Glutathione S-transferases: A review. *Current Medicine Chemistry* 6, 279–309.

Shaw, M. & Reiderer, B.M. (2003) Sample preparation for two-dimensional gel electrophoresis. *Proteomics* 3, 1408-1417.

Sheehan, D. & McDonagh, B. (2008) Oxidative Stress and Bivalves: A proteomic Approach. *Invertebrate Survival Journal,* 110-123.

Sheehan, D., McIntosh, J., Power, A., Fitzpatrick, P.J. (1995) Environmental biochemistry. *Biochemistry of Society Translation* 23, 419–22.

Sheehan, D., Meade, G., Foley, V.M., & Dowd, C.A. (2001) Structure, function and evolution of glutathione transferases: implications for classification of nonmammalian members of an ancient enzyme superfamily. *Biochemical Journal* 360, 1–16.

Shevchenko, A., Wilm, M., Vorm, O. & Mann, M. (1996) Mass spectrometric sequencing of proteins from silver-stained polyacrylamide gel. *Analytical Chemistry* 68, 850-858.

Sies H. (1991) Oxidative stress: Introduction. In: Sies H (ed) Oxidative stress, oxidants and antioxidants, *Academic Press Publisher*, San Diego, pp 1-15.

Simons, P.C. & Vanderjagt, D.L. (1977) Purification of glutathione S-transferases from human liver using glutathione affinity chromatography. *Analytical Biochemistry* 82, 334-341.

Spector, T. (1978) Refinement of coomassie blue method of protein quantitation - simple and linear spectrophotometric assay for less than or equal to 0.5 to 50 mu-g of protein. *Analytical Biochemistry* 86, 142-146.

Stewart, N.A., Pham, V.T., Choma, C.T. & Kaplan, H. (2002) Improved peptide detection with matrix-assisted laser desortion/ionization mass spectrometry by trimethylation of amino groups. *Rapid Communication Mass Spectrometer* 16, 1448-1453.

Switzer, R.C., Merril, C.R. & Shifrin, S. (1979) A highly sensitive silver stain for detecting proteins and peptides in polyacrylamide gels. *Analytical Biochemistry* 98(1), 231-7.

Tang, A.H. & Tu, C.P.D. (1994) Biochemical characterization of *Drosophila* glutathione S-transferases D1 and D21. *Journal of Biological Chemistry* 269, 27876-27884.

Verlecar, X., Jena, K. & Chainy, G. (2007) Seasonal variation of oxidative biomarkers in the gills and digestive gland of green-lipped mussel *Perna viridis* from Arabian Sea. *Coastal and Shelf Science* 76(4), 745-752.

Vidal, M.L., Rouimi, P., Debrauwer, L. & Narbonne, J.F. (2002) Purification and characterization of glutathione S-transferases from the freshwater clam *Corbicula fluminea* (Mu¨ller). *Comparative Biochemistry and Physiology C* 131, 477-489.

Whalen, K.E., Morin, D., Lin, C.Y., Tjeerdema, R.S., Jared, V.G. & Hahn, M.E. (2008) Proteomic identification, cDNA cloning and enzymatic activity of gluthathione S-transferases from the generalist marine gastropod, *Cyphoma gibbosum*. Biology Department, Joint Program in Oceanography at the Massachusetts Institute of Technology and the Woods Hole Oceanographic Institution pp 362.

Wilce, M.C.J., Qakley, A.J., Rossjohn, J., Feil, S.C., LoBello, M., Ricci, G., Board, P.G., & Parker, M.W. (1996) Crystallographic studies of Pi- and Theta-class glutathione-S-transferases. *In Glutathione S-transferases: Structure, Function and Clinical Implications*, Vermeulen NPE, Mulder GJ, Nieuwenhuyse H, Peters WHM, van Bladeren PJ, eds. (London: Taylor and Francis) pp 39–56

Winterbourn, C.C. (2008) Reconciling the chemistry and biology of reactive oxygen species. *Nature Chemistry and Biology* 4, 278-286.

Wood, W. (1828) Asian marine biology *Marine Biological Association of Hong Kong*, Brian Morton, 1-3 pp 27-48.

Xu, C., Pan, L., Liu, N., Wang, L. & Miao, J. (2010) Cloning, characterization and tissue distribution of a pi-class glutathione S-transferase from clam (*Venerupis philippinarum*): Response to benzo[α]pyrene exposure. *Comparative Biochemistry and Physiology Part C* 152, 160–166.

Yan, J.X., Wait, R., Berkelman, T., Harry, R.A., Westbrook, J.A., Wheeler, C.H. & Dunn, M.J., (2000) A modified silver staining protocol for visualization of proteins compatible with matrix-assisted laser desorption/ionization and electrospray ionization-mass spectrometry. *Electrophoresis* 17, 3666-72.

Yan, X., Sanchez, J-N., Rouge, V., Williams, K.L. & Hochstrasser, D.F. (1999) Modified immobilized pH gradient gel strip equilibration procedure in SWISS-2DPAGE protocols. *Electrophoresis* 20, 723-726.

Yang, H., Nie, L., Zhu, S. & Zhou, X. (2002) Purification and characterization of a novel glutathione S-transferase from *Asaphis dichotoma*. *Archive of Biochemistry and Biophysiology* 403, 202–208.

Yang, H., Zeng, Q., Nie, L., Zhu, S., Zhou, X. (2003) Purification and characterization of a novel glutathione S-transferase from *Atactodea striata*. *Biochemistry and Biophysiology Respiratory Communication* 307, 626–631.

Yang, H.L., Zeng, Q.Y., Li, E.Q., Zhu, S.G., Zhou, X.W. (2004) Molecular cloning, expression and characterization of glutathione S-transferase from *Mytilus edulis. Comparative Biochemistry and Physiology B* 139, 175–182.

Yuen, W.K. & Ho, J.W. (2001) Purification and characterization of multiple glutathione S-transferase isozymes from *Chironomidae* larvae. *Comparative Biochemistry and Physiology* 129A, 631–640.

Zanette, J., José Maria Monserrat, J.M. & Adalto Bianchini, A. (2006) Biochemical biomarkers in gills of mangrove oyster *Crassostrea rhizophorae* from three Brazilian estuaries. *Comparative Biochemistry and Physiology, Part C* 143, 187–195.

Zhou, Q., Zhang, J., Fu, J., Shi, J., Jiang, G. (2008) Review Biomonitoring: An appealing tool for assessment of metal pollution in the aquatic ecosystem. *Analytical Chimica Acta* 606, 135–150.